ABOUT CSRC	中心简介	01 - 06
PEOPLE	人员情况	07 - 24
RESEARCH HIGHLIGHTS	科研亮点	25 - 60
RESEARCH PROJECTS	科研项目	61 - 67
<b>PUBLICATIONS</b>	发表论文	68 - 84
EVENTS	学术活动	85 - 90
COLLABORATIONS	合作交流	91 - 92
VISITORS	学术访问	93
CSRC HOME-BUILDING	科研大楼	94 - 96

本册所列所有信息为2017年1月至12月期间



### ABOUT CSRC



Beijing Computational Science Research Center (CSRC) is a multidisciplinary research organization under the auspices of the China Academy of Engineering Physics (CAEP). Established in August 2009, CSRC positions itself as a center of excellence in computational science research addressing current and critical issues in multidisciplinary of Mathematics, Mechanics, Physics, Chemistry, Materials Science, and Computational Science.

#### **Mission of CSRC:**

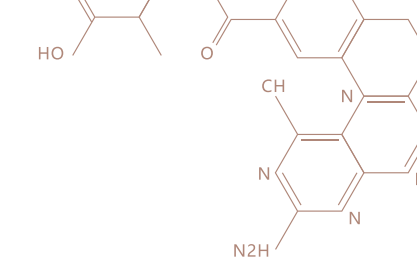
- © carry out fundamental, frontier, critical, and multidisciplinary research with advanced computational approaches, thereby attract talents worldwide and train highly qualified research personnel, to support grand scientific development and technology innovation in China;
- © develop and maintain collaboration with research institutes elsewhere by building a comprehensive and internationalized research platform, to support academic and technological exchange and advancement;
- © innovate and reform organizational structures, management policies and methods for enabling creative and effective scientific research, to raise our national competence in technology innovation and enhance our comprehensive strength in science and technology.

Specifically, CSRC supports the development and implementation of grand challenging projects in natural science and engineering where computational modeling and simulation play a key role. CSRC also encourages its members to engage in the development of computational algorithms and software.

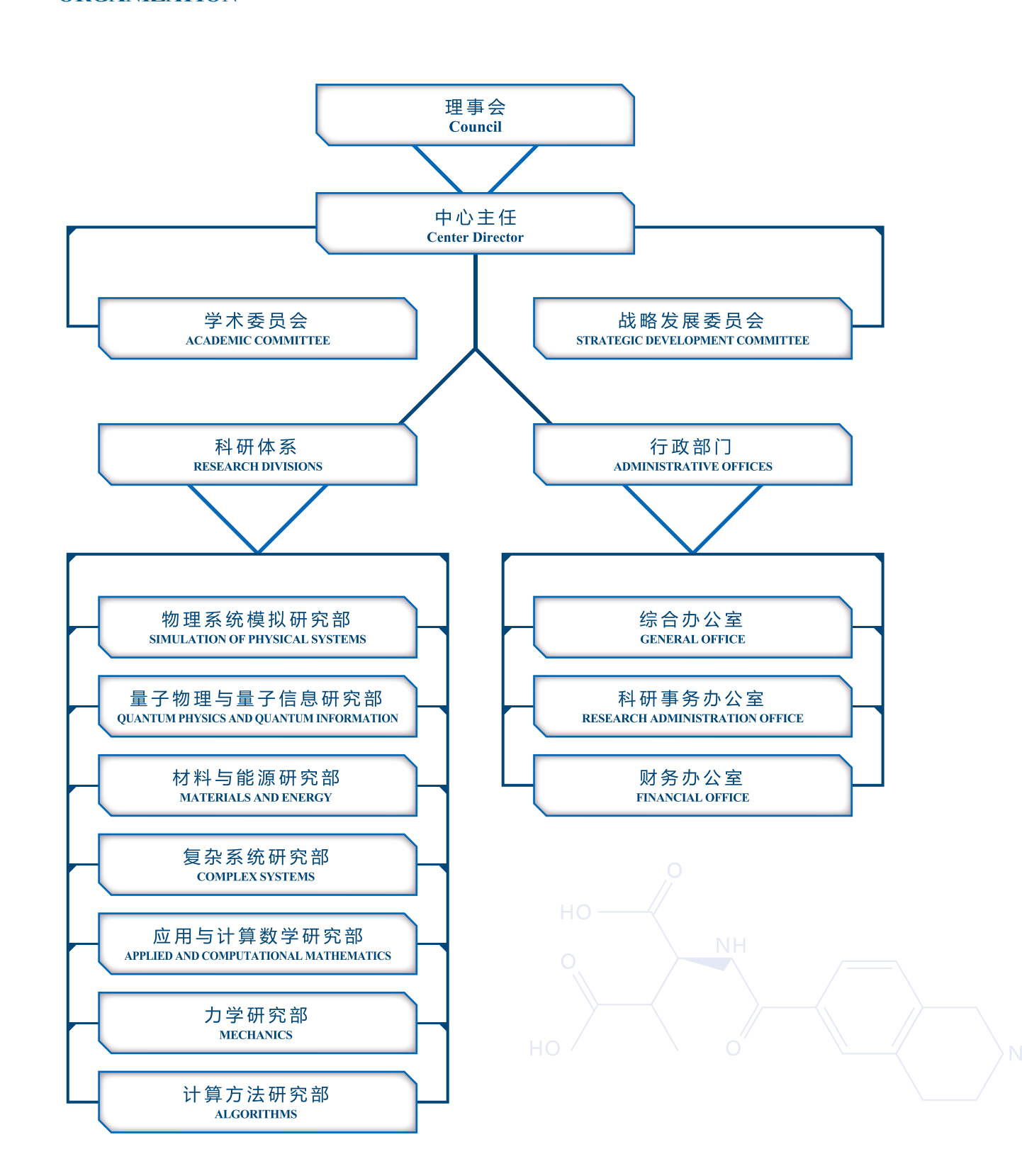
As of December 2017, CSRC has recruited 42 faculty members, 3 engineers, 42 associate members, 141 postdoctoral fellows and 119 students. With its talented research staff, CSRC has established the following seven divisions: Simulation of Physical Systems, Quantum Physics and Quantum Information, Materials and Energy, Complex Systems, Applied and Computational Mathematics, Mechanics, and Algorithms. In research performance, CSRC has published 426 papers, organized 10 academic conferences and workshops, 7 tutorials, 6 colloquiums on scientific frontiers, and 90 CSRC seminars. CSRC has also forged partnerships with many prestigious universities and research institutions around the world.







#### 中心组织构架 ORGANIZATION

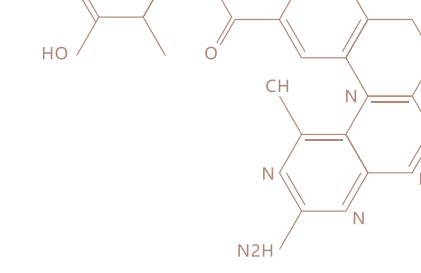


02 - 03 |



#### 学术委员会成员 MEMBERS OF ACADEMIC COMMITTEE

领域 Field	姓名 Name	单位 Institute
	孙昌璞 (主席)	北京计算科学研究中心
	Chang-Pu Sun (Chair)	Beijing Computational Science Research Center
	贺贤土	北京应用物理与计算数学研究所
	Xian-Tu He	Institute of Applied Physics and Computational Mathematics, CAEP
	王鼎盛	中国科学院物理研究所
	Ding-Sheng Wang	Institute of Physics, CAS
	陶瑞宝	复旦大学
	Rui-Bao Tao	Fudan University
	张肇西	中国科学院理论物理研究所
	Zhao-Xi Zhang	Institute of Theoretical Physics, CAS
	朱邦芬	清华大学
	Bang-Fen Zhu	Tsinghua University
	赵宪庚	中国工程院
	Xian-Geng Zhao Chinese Academy of Engineering	Chinese Academy of Engineering
物 理	赵光达	北京大学
Physics	Guang-Da Zhao	Peking University
	邢定钰	南京大学
	Ding-Yu Xing	Nanjing University
	郑 杭	上海交通大学
	Hang Zheng	Shanghai Jiao Tong University
	李树深	中国科学院半导体研究所
	Shu-Shen Li	Institute of Semiconductors, CAS
	向 涛 中国科学院物理所	中国科学院物理所
	Tao Xiang	Institute of Physics, CAS
	赵政国	中国科学技术大学
	Zheng-Guo Zhao	University Of Science And Technology Of China
	林海青	北京计算科学研究中心
	Hai-Qing Lin	Beijing Computational Science Research Center
	游建强	北京计算科学研究中心
	Jian-Qiang You	Beijing Computational Science Research Center



领域 Field	姓名 Name	单位 Institute
	来鲁华	北京大学
	Lu-Hua Lai	Peking University
	李 隽	清华大学
	Jun Li	Tsinghua University
化学与生物物理	陈润生	中国科学院生物物理研究所
Chemistry & Biophysics	Run-Sheng Chen	Institute of Biophysics, CAS
	汤雷翰	北京计算科学研究中心
	Lei-Han Tang	Beijing Computational Science Research Center
	欧阳颀	北京大学
	Qi Ouyang	Peking University
	魏苏淮	北京计算科学研究中心
	Su-Huai Wei	Beijing Computational Science Research Center 北京计算科学研究中心 Beijing Computational Science Research Center
材料科学	高世武	
Materials Science	Shiwu Gao	Beijing Computational Science Research Center
	祝世宁	南京大学
	Shi-Ning Zhu	Nanjing University
	邵久书	北京师范大学
	Jiu-Shu Shao	Beijing Normal University
化 学	张 希	清华大学
Chemistry	Yi-Long Bai	Tsinghua University
	杨学明	中国科学院大连化学物理所
	Xue-Ming Yang	Dalian Institute of Chemical Physics, CAS
	李家春	中国科学院力学研究所
	Jia-Chun Li	Institute of Mechanics, CAS
	白以龙	中国科学院力学研究所
力 学	Yi-Long Bai	Institute of Mechanics, CAS
Mechanics	符 松	清华大学
	Song Fu	Tsinghua University
	罗礼诗	北京计算科学研究中心
	Li-Shi Luo	Beijing Computational Science Research Center

#### 续表

领域 Field	姓名 Name	单位 Institute
	崔俊芝	中国科学院数学与系统科学研究院
	Jun-Zhi Cui	Academy of Mathematics and Systems Science, CAS
计算数学	张平文	北京大学
Computational Mathematics	Ping-Wen Zhang	Peking University
	江松	北京应用物理与计算数学研究所
	Song Jiang	Institute of Applied Physics and Computational Mathematics, CAEP
	李大潜	复旦大学
	Da-Qian Li	Fudan University
	袁亚湘	中国科学院数学与系统科学研究院
	Ya-Xiang Yuan	Academy of Mathematics and Systems Science, CAS
数 学	杜强	北京计算科学研究中心
Mathematics	Qiang Du	Beijing Computational Science Research Center
	张智民	北京计算科学研究中心
	Zhi-Min Zhang	Beijing Computational Science Research Center
	王奇	北京计算科学研究中心
	Qi Wang Beijing Computational Science Research Center	
计算科学	钱德沛	中山大学
Computational Science	De-Pei Qian	Sun Yat-sen University



### 科研亮点 HIGHLIGHTS

UNIVERSAL SCALING AND CRITICAL EXPONENTS OF THE ANISOTROPIC QUANTUM RABI MODEL	·
LOCALIZATION IN OUT-OF-EQUILIBRIUM DISORDERLESS SYSTEMS	/ 2
NEARLY DECONFINED SPINON EXCITATIONS IN THE SQUARE-LATTICE SPIN-1/2 HEISENBERG ANTIFERROMAGNET	/ 3
GENERAL GREEN'S FUNCTION FORMALISM FOR LAYERED SYSTEMS: WAVE FUNCTION APPROAC	ЭН З
THERMODYNAMIC PHASE DIAGRAM OF BERYLLIUM USING OUR PHONON QUASIPARTICLE APPROACH	
MEASURING OUT-OF-TIME-ORDER CORRELATORS ON A NUCLEAR MAGNETIC RESONANCE QUANTUM SIMULATOR	/ á
OBSERVATION OF THE EXCEPTIONAL POINT IN CAVITY MAGNON-POLARITONS	/ 3
OPTICAL LEVITATION OF NANODIAMONDS BY DOUGHNUT BEAMS IN VACUUM	// 3
A UNIVERSAL RULE FOR CONTROLLING SPIN CURRENTS IN QUANTUM SPIN HALL SYSTEMS	
PREDICTION OF IDEAL TOPOLOGICAL SEMIMETALS WITH TRIPLY DEGENERATE POINTS IN NACU3TE2 FAMILY	
SURFACE EVOLUTION OF A PT-PD-AU ELECTROCATALYST FOR STABLE OXYGEN REDUCTION	<i></i>
BAND STRUCTURE ENGINEERING OF $Cs_2AgBiBr_6$ PEROVSKITE THROUGH ORDER-DISORDERED TRANSITION	
A NEW ALGORITHM FOR XFEL SINGLE PARTICLE SCATTERING DATA ANALYSIS	<i></i>
RATCHETING OF A VIRAL TRANSCRIPTION PROTEIN MACHINE ALONG DNA WITHOUT BACKTRACKING	
A STABLE SCHEME FOR A 2D DYNAMICAL Q-TENSOR MODEL OF NEMATIC LIQUID CRYSTAL	<i>J</i> 4
CALCULATING CORNER SINGULARITIES BY BOUNDARY INTEGRAL EQUATIONS	4
ERROR ANALYSIS OF A FINITE DIFFERENCE METHOD ON GRADED MESHES FOR A TIME- FRACTIONAL DIFFUSION EQUATION	4
NUMERICAL SOLUTION OF THE NONLOCAL DIFFUSION EQUATION ON THE REAL LINE	And the second
FAST EVALUATION OF THE CAPUTO FRACTIONAL DERIVATIVE AND ITS APPLICATIONS TO FRACTIONAL DIFFUSION EQUATIONS	
MATHEMATICAL AND NUMERICAL ANALYSIS OF DYNAMIC GINZBURG-LANDAU EQUATIONS IN NONCONVEX POLYGONS BASED ON HODGE DECOMPOSITION	
HESSIAN RECOVERY FOR FINITE ELEMENT METHOD	
MODELING THE FORMATION OF TIO, ULTRA-SMALL NANOPARTICLES	
MULTISCALE STUDY OF PLASMONIC SCATTERING AND LIGHT TRAPPING EFFECT IN SILICON NANOWIRE ARRAY SOLAR CELLS	

## UNIVERSAL SCALING AND CRITICAL EXPONENTS OF THE ANISOTROPIC QUANTUM RABI MODEL

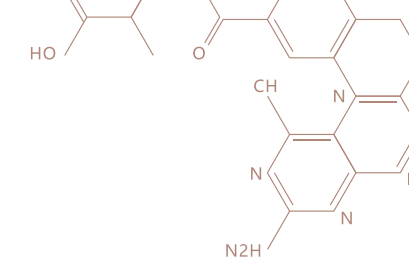
The quantum Rabi model (QRM), which describes a two-level system coupled to a single electromagnetic mode, provides a basic paradigm of light-matter interactions. Due to recent theoretical and experimental progress, the ORM attracted interest from researchers working on quantum optics, solid state physics, fundamental properties of quantum physics, and mathematical physics. The first analytical solution of the QRM, which is an important breakthrough on the mathematical and physical aspects of this model, was obtained by Braak only in 2011 [1]. While it is well known that at weak coupling the QRM can be approximated by the Jaynes-Cummings (JC) Hamiltonian, recent experimental progress in circuit QED has allowed to reach the ultrastrong and even deep-strong coupling regimes [2,3,4]. Very recently [5,6], it was proved that both the QRM and JC model can realize a new type of quantum phase transition (QPT) which, surprisingly, does not require the thermodynamic limit.

The QPT considered by Refs. [5,6] occurs as a function of coupling strength when the ratio η between the atomic and cavity frequency tends to infinity, and its properties are in fact very similar to the superradiant QPT of the Dicke model. In the latter case, a single cavity mode interacts with many two-level systems (large N), while the QRM corresponds to the N=1 case. The similarity to thermodynamic QPTs motivates investigating whether familiar concepts like universality classes are still generally applicable at N=1. More generally, the relationship of this new type of few-body QPTs and their thermodynamic counterparts has not been clearly understood.

To elucidate these issues, a recent investigation [7] involving Maoxin Liu, Stefano Chesi, Zu-Jian Ying and Hai-Qing Lin from CSRC, Hong-Gang Luo from Lanzhou University, and Xiaosong Chen from CAS-ITP & UCAS, has developed a general analytical approach valid in the limit of large n. The treatment not only derives a perturbative effective Hamiltonian applicable to the critical region (from a fourth-order Schrieffer-Wolff transformation), but extends the perturbative results obtaining a non-perturbative effective mass and mean-field potential. These quantities provide a full description of the low-energy properties at arbitrary coupling strengths (i.e., also away from the critical point). The treatment of Ref. [7] is not only applicable to the original QRM and JC model at N=1, but also allows to include a finite anisotropy and an arbitrary (but finite) value of N. As expected, a well-defined universality class is established at arbitrary values of the anisotropy parameter (except the JC model). It was also found that the low-energy description at given anisotropy is independent of N, after appropriately rescaling η. Therefore, the few-body QPTs at arbitrary N display identical nonuniversal features, like the critical coupling or the value of the order parameter away from the QPT.

The effective low-energy theory described in this work is in excellent agreement with numerical calculations of the phase diagram, critical exponents, and scaling functions, also presented in Ref. [7]. Other interesting features revealed by this work are a superradiance-induced freezing of the effective mass and discontinuous scaling functions in the Jaynes-Cummings limit. Besides these theoretical achievements, this work could be relevant for experimental platforms like circuit QED and trapped ion systems, where the appropriate regime might be realized soon [3,4,8,9]. Because of its great potential interest, the article was selected by Physical Review Letters as an "Editors' Suggestion".





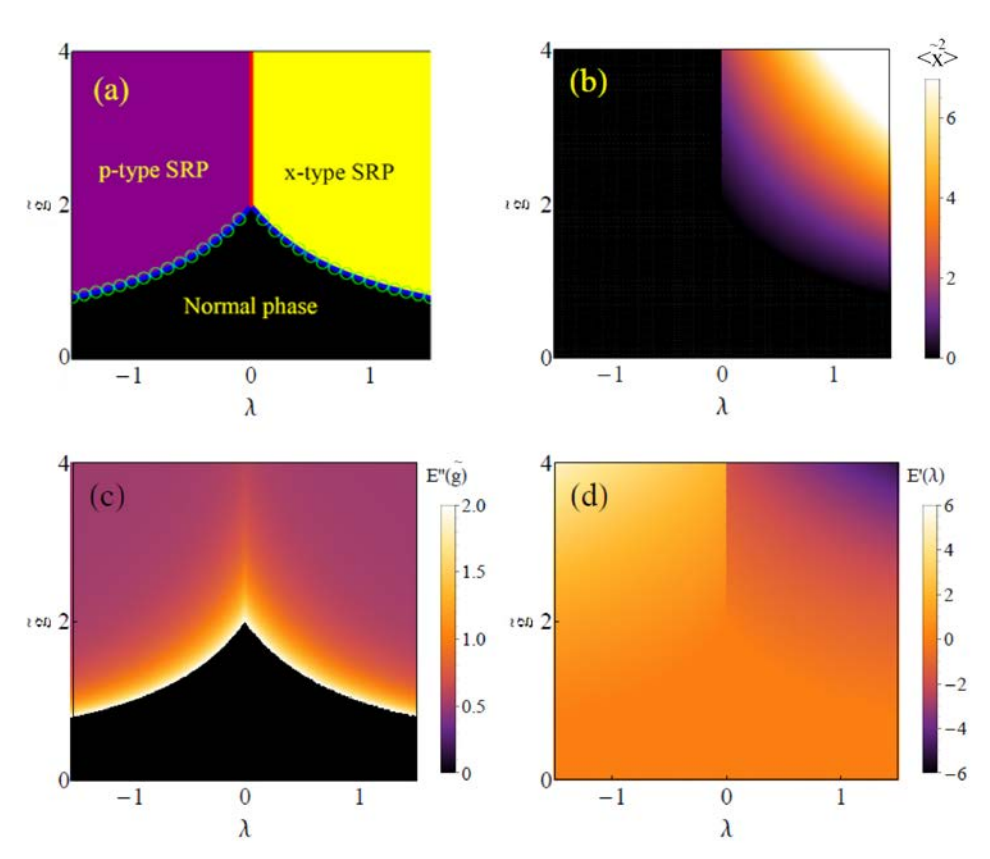


**Fig. 1.** Phase diagram (a) and order parameter (b) of the QRM with anisotropy. The red (blue) line in panel (a) indicates a first (second) order phase transition. The order of the transition is revealed by the first and second derivative of the ground state energy, respectively shown in panels (d) and (c).

#### **References:**

- [1] D. Braak, Phys. Rev. Lett. 107, 100401 (2011).
- [2] P. Forn-Diaz, et al., Phys. Rev. Lett. 105, 237001 (2010).
- [3] F. Yoshihara, T. Fuse, S. Ashhab, K. Kakuyanagi, S. Saito, and K. Semba, Nat. Phys. 13, 44 (2017).
- [4] P. Forn-Díaz, et al., Nat. Phys.13, 39 (2017).
- [5] M.-J. Hwang, R. Puebla, and M. B. Plenio, Phys. Rev. Lett. 115, 180404 (2015).
- [6] M.-J. Hwang and M. B. Plenio, Phys. Rev. Lett. 117,123602 (2016).
- [7] S. Maoxin Liu, Stefano Chesi, Zu-Jian Ying, Xiaosong Chen, Hong-Gang Luo, and Hai-Qing Lin Phys. Rev. Lett. 119, 220601 (2017) Editor's Suggestion. DOI: https://doi.org/10.1103/PhysRevLett.119.220601
- [8] R. Puebla, M.-J. Hwang, J. Casanova, and M. B. Plenio, Phys. Rev. Lett. 118, 073001 (2017).
- [9] Z. Chen, Y. Wang, T. Li, L. Tian, Y. Qiu, K. Inomata, F. Yoshihara, S. Han, F. Nori, J. S. Tsai, and J. Q. You, Phys. Rev. A 96, 012325 (2017).

### LOCALIZATION IN OUT-OF-EQUILIBRIUM DISORDERLESS SYSTEMS

When isolated quantum systems are taken out of equilibrium, its dynamics can be described by a time evolution which is unitary, unlike classically chaotic systems. The conditions that lead these systems to thermalize and the information regarding its initial preparations to be lost over the course of its evolution can be seen as result of the dephasing in the dynamics of the coherence between the eigenstates. Its mathematical basic grounds were based in what we call nowadays as the Eigenstate Thermalization Hypothesis (ETH) [1,2] and it became clear that interactions between the constituents of the system are essential in the thermalization mechanism. On the other hand, much attention has been also given to another aspect that may, in fact, prevent thermalization. When disorder comes into play an isolated quantum system can experience a halting of thermalization and, ultimately, localization takes place. This localization is manifest in the absence of mass transport and it can be seen as a generalization of the famous Anderson localization phenomenon when interactions are included.

Several numerical studies have shown this phenomenon in the presence of interactions [3], which we dub as many-body localization (MBL), and also a handful number of experiments [4] have also tackled it. In the latter, the analyzed quantum system is consisted of atoms trapped in a potential generated by laser beams in an optical lattice. By introducing disorder on the onsite energy levels, one can emulate the physics of the Anderson model with interactions which can be tuned in a controllable fashion. The most common way to identify this localization (and the associated lack of thermalization) is to follow the dynamical properties of a carefully prepared quantum system. Specifically, experiments in optical lattices employ high-fidelity preparation of initial states whose properties are well known, as for example, by confining the atoms in certain regions of the trapping environment. By measuring how the information of the initial prepared state is preserved for long-times after the release of this constraint one is able to identify the regimes where disorder is sufficient to lead to the MBL phenomenon.

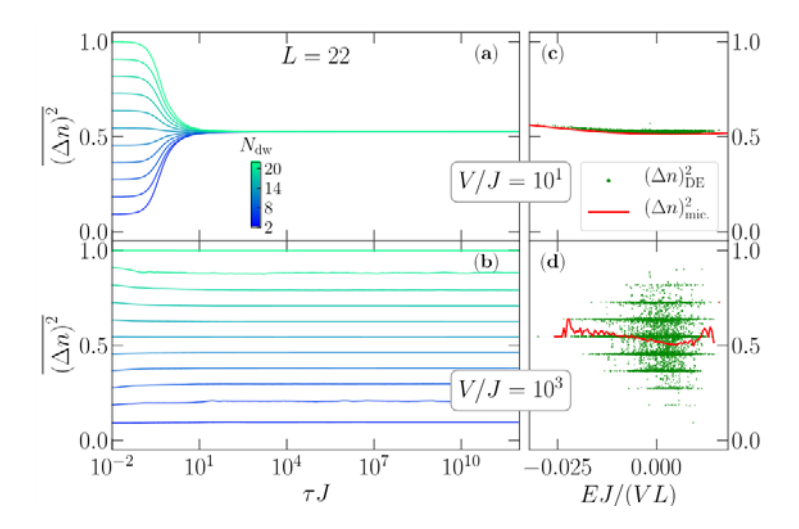
On the other hand, much recent theoretical work has been devoted to understanding whether disorder is a necessary ingredient to generate localization in interacting systems. Pioneering works by Kagan and Maksimov on Helium mixtures have laid the foundation of localization when there are two constituents in the system, a light and a heavy one. In these cases, the heavy particles generate an effective random quasistatic potential which blocks the diffusion of the light ones, thus localizing them. More recently, some proposals tried to tackle this problem and much to the surprise found that an initial transient localization ultimately leads to diffusion. In a recent publication [5], Rubem Mondaini from CSRC and Zi Cai (Shanghai Jiaotong University) have investigated one of the first evidences of many-body localization in a translation invariant Hamiltonian with a single species of particles. Specifically, they tackled the problem of (hardcore) bosons in a lattice which interact via a quasi-periodic infinite range interaction. Despite the model may sound rather artificial, it has been shown to be emulated experimentally for trapped atoms in a optical lattice embedded in a cavity [6]. The long (infinite)-range interaction is mediated by vacuum modes of the cavity and are independently controlled by tuning the cavity resonance. The Hamiltonian reads,

$$\hat{H} = -J \sum_{i} (\hat{\alpha}_{i}^{\dagger} \alpha_{i+1} + \text{h.c.}) - \sum_{i < j} V_{ij} \left( \hat{n}_{i} - \frac{1}{2} \right) \left( \hat{n}_{i} - \frac{1}{2} \right)$$
 (1)

where J is the nearest-neighbor tunneling amplitude, and the interactions  $V_{ij}$  have the functional form  $V_{ij} = (V/L) \cos[2\pi p_{i-j}]$ . By taking p as an irrational number, the long-range interactions are no longer commensurate with the lattice and glassy behavior emerges when the interactions are sufficiently large. We investigate this glass-



like regime at zero temperature and show it can also be obtained in an isolated quantum system at *infinite temperatures*. To make a closer connection with the experiments, they investigate the persistence of the information of initial preparations under a quench. In particular, they quantify the degree of inhomogeneity of an initial pure state, via  $(\Delta \hat{n}\,)^2 = (1/L\,) \sum_i (\hat{n}_{i+1} - \hat{n}_i)^2\,.$ 



Before the quench, this observable represents the number of domain walls are present in the initial state. Its time evolution is depicted in Fig. (1) for two values of interactions. If a system thermalizes, a time-evolved state can be thought as a featureless state that no longer preserves local information of the initial state. That is the case in Fig. 1(a) for small values of interactions. Surprisingly, if one increases its magnitude, the tine-evolved state no longer loses information and memory of the initial preparations can be retrieved for arbitrarily long times, as shown in Fig. 1(b). with this clear indication of many-body localization in a translation-invariant (disorderless) system, we expect that this work may sparkle interest in the experimental investigation of the ideas we present, ultimately settling the issue of whether disorder is a necessary mechanism to its observation. Further aspects of these problem, as the study of commensurate long-range interactions, are an ongoing research being currently investigated at CSRC.

**Fig. 1.** Time evolution of the integrated charge inhomogeneity averaged over states with similar number of domain walls in ergodic [nonergodic] regimes in panel (a) [panel (b)] with  $V/J=10^1\ [V/J=10]$ . Panels (c) and (d) are comparisons of the diagonal ensemble prediction (infinite-time limit) and the microcanonical (thermodynamic) result for the corresponding values of interactions

#### References:

- [1] Quantum statistical mechanics in a closed system, J. M. Deutsch, Phys. Rev. A 43 2046 (1991).
- [2] Chaos and quantum thermalization, M. Srednicki, Phys. Rev. E 50, 888 (1994).
- [3] Many-body localization and thermalization in disordered Hubbard chains, R. Mondaini and M. Rigol, Phys. Rev. A 92, 041601 (2015).
- [4] Observation of many-body localization of interacting fermions in a quasirandom optical lattice, M. Schreiber, S. S. Hodgman, P. Bordia, Henrik P. Lüschen, M. H Fischer, R. Vosk, E. Altman, U. Schneider, and I. Bloch, Science 349, 842–845 (2015).
- [5] Many-body self-localization in a translation-invariant Hamiltonian, R. Mondaini and Zi Cai, Phys. Rev. 96 94, 035153 (2017).
- [6] Quantum phases from competing shortand long-range interactions in an optical lattice, R. Landig, L. Hruby, N. Dogra, M. Landini, R. Mottl, T. Donner, and T. Esslinger, Nature 532, 476 (2016).

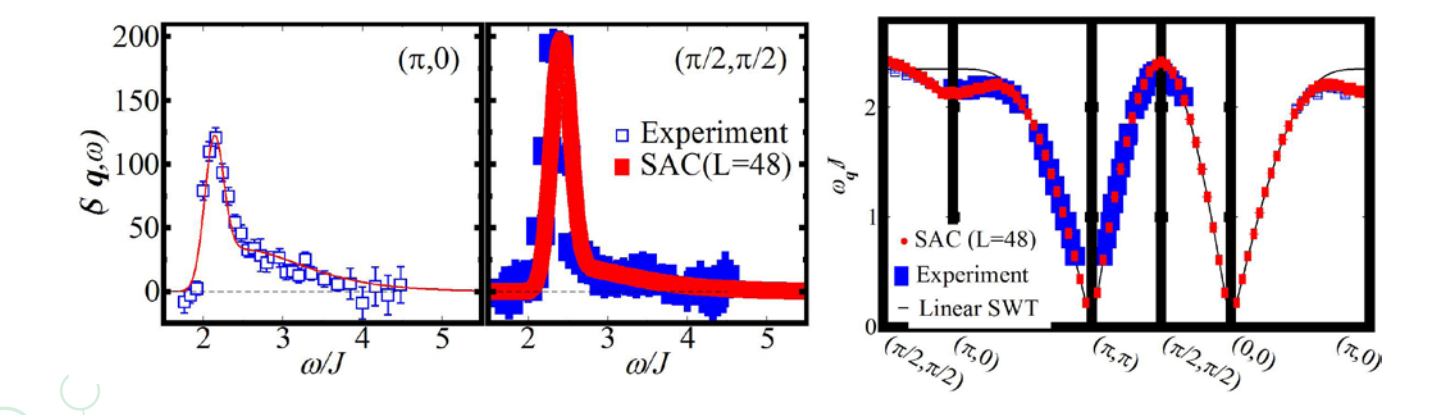
••••• 2017 ANNUAL REPORT RESEARCH HIGHLIGHTS

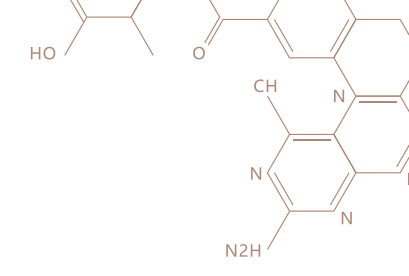
#### NEARLY DECONFINED SPINON EXCITATIONS IN THE SQUARE-LATTICE SPIN-1/2 HEISENBERG ANTIFERROMAGNET

The anomaly in the excitation spectrum around the wave-vector  $(\pi,0)$  in experimental realizations of the 2D spin-1/2 Heisenberg spin model, such as CFTD, is a long-standing issue, which is also reproduced in calculations with the Heisenberg model. It is manifested as a suppression of the excitation energy and an associated enhancement of spectral weight in the continuum above the spin-wave (magnon) peak. The physical reasons behind the anomaly have been debated over the past 20 years or so, and in the last few years the interest in the issue has heated up further as new high-resolution neutron scattering experiments have been carried out [1]. The main question is whether the anomaly is caused simply by more or less standard multi-magnon excitation processes [2], or whether there are more exotic reasons such as deconfinement of spinons [1]. On the other hand, the recently improved analytic continuation (SAC) method [3] enables people to study the spectral anomaly in greater details than previously. Most importantly, it provides an unbiased way to extract the energy and amplitude of the leading  $\delta$ -function (magnon pole) contribution to the dynamic spin structure factor.

Recently, Hui Shao and Stefano Chesi of CSRC, Yan Qi Qin and Zi Yang Meng from IOP, Sylvain Capponi from University of Toulouse, and Anders Sandvik from Boston University, have used the improved SAC method to investigate the spin excitation spectral functions of the spin-1/2 square-lattice Heisenberg antiferromagnet [4], and, as shown in Fig. 1, the results are in excellent agreement with recent neutron scattering experiment on CFTD. Moreover, the abnormal reduction of the excitation energy at  $(\pi,0)$  is found together with a reduction of the magnon weight. Upon turning on a competing four-spin interaction which brings the system to a critical point with deconfined spinon excitations, they observe a rapid reduction of the magnon weight to zero (see Fig. 2 left). This, along with an effective model of the excitations - one magnon or two spinons (see Fig.2 right), brings to the picture of

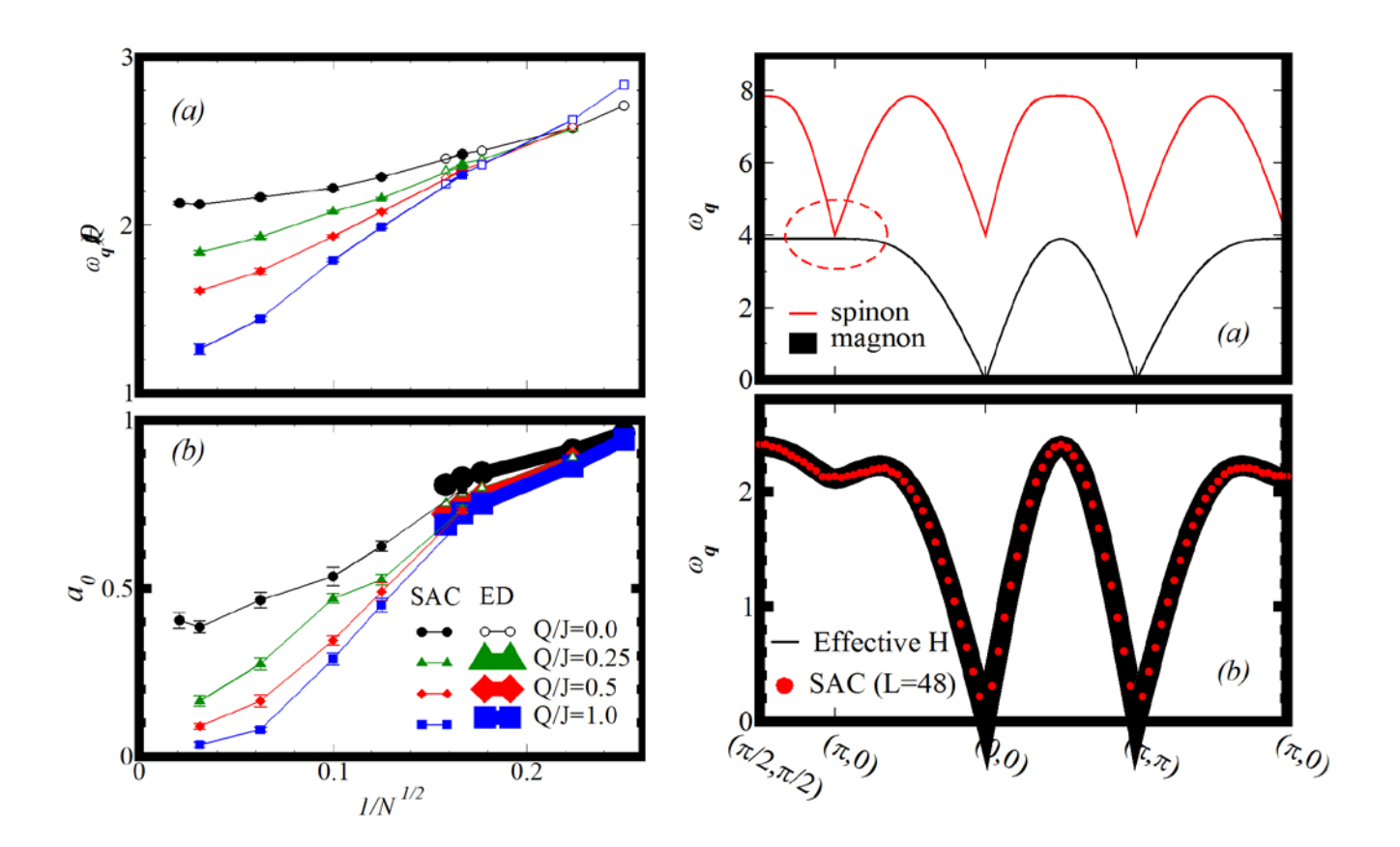
**Fig. 1.** Comparison of the SAC results on the spin-1/2 square-lattice Heisenberg antiferromagnet and the new neutron scattering experiments carried out on CFTD. Left panel: spectral functions at two wave vectors; Right panel: single-magnon dispersion along a representative path of the BZ.





nearly deconfined spinons at  $(\pi,0)$  - a precursor to deconfined quantum criticality. This work bridges the two interpretations (magnons versus spinons), by elucidating the so far neglected role of the interplay between the magnon pole and the continuum above it. Furthermore, it is the first study of the dynamics of the J-Q model and the evolution of its excitation spectrum upon approaching the deconfined quantum-critical point, where hitherto unknown aspects of the spinon deconfinement mechanism remains uncovered.

Fig. 2. Left panel: size dependence of the excitation energy (a) and the relative weight of the magnon pole (b) at  $q=(\pi,0)$  close to the Heisenberg limit of the J-Q model; Right panel: (a) dispersions of the bare excitations and (b) the lowest energy of the mixed spinon-magnon system obtained with the dispersions in (a).



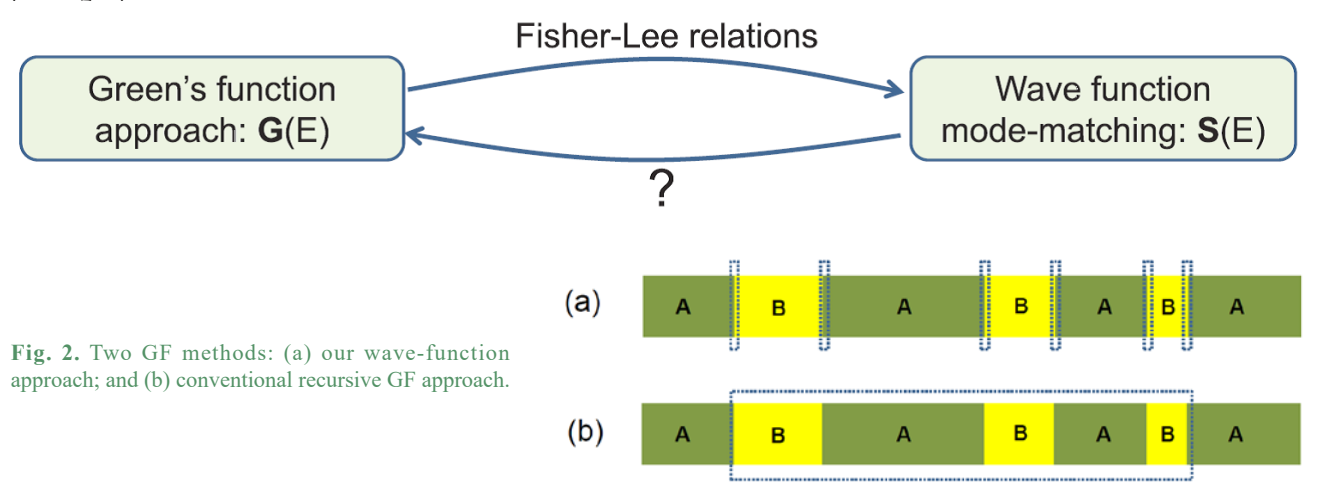
#### References

- [1] B. D. Piazza et al., Nat. Phys. 11, 62 (2015).
- [2] M. Powalski et al., arXiv:1701.04730 (2017).[5]
- [3] A.W. Sandvik, Phys. Rev. B 57, 10287 (1998); H. Shao and A. W. Sandvik, in progress.
- [4] H. Shao, Y. Qin, S. Capponi, S. Chesi, Z. Meng, and A. W. Sandvik, Phys. Rev. X 7, 041072 (2017).

#### GENERAL GREEN'S FUNCTION FORMALISM FOR LAYERED SYSTEMS: WAVE FUNCTION APPROACH

The single-particle Green's function (GF) of mesoscopic structures plays a central role in mesoscopic quantum transport. The recursive GF technique based on the Dyson equation is a standard tool to compute this quantity numerically, but it still suffers from two limitations. First, it is limited to relatively small systems. Second, its connection to another widely used approaches – the wave function mode matching approach -- remains incomplete (see Fig. 1).

Fig. 1. Two widely-used approaches in mesoscopic quantum transport and their connection



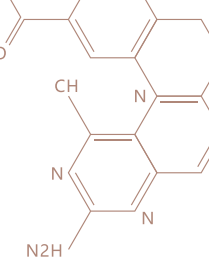
Recently, the research group of Prof. Wen Yang at CSRC together with Prof. Kai Chang at Institute of Semiconductors, CAS addressed both issues by developing a wave function approach to calculate the Green's function of a general layered system. This new method enjoys two distinguishing features. First, only the interfaces

between uniform regions need numerical treatment, so the time cost scales are determined by the number of interfaces [dashed boxes in Fig. 2(a)]. By contrast, the time cost of the recursive GF technique is determined by the length of the central region [dashed box in Fig. 2(b)]. Thus, it can speed up the calculation by 1-2 orders of magnitudes. Second, it establishes the reverse of the well-known Fisher-Lee relation (see Fig. 1) and hence connects the wave function mode-matching approach back to the GF approach, thus paving the way for extracting the scattering information of novel quasi-particles in the solid state by local transport measurements.

#### References

[1] Shu-Hui Zhang, Wen Yang, and Kai Chang, Phys. Rev. B 95, 075421 (2017).





#### THERMODYNAMIC PHASE DIAGRAM OF BERYLLIUM USING OUR PHONON QUASIPARTICLE APPROACH

Beryllium (Be) has been applied widely in various industry areas, especially for nuclear weapon design. It is also an important material for fundamental research such as plasmonics under high pressure. Therefore, it is important to understand the phase stability of Be under extreme conditions. However, there are controversy and debating about the existence of its bcc phase and the associated hcp  $\rightarrow$  bcc transition both experimentally and theoretically. The phase stability of Be has been extensively studied experimentally. However, in most of experiments, no sign of bcc symmetry was ever captured [PRB 86, 174118 (2012); PRB 72, 094113 (2005); J. Phys. F 14, L1 (1984); J. Phys. F 14, L65 (1984); JPCM 14, 10569 (2002); PRB 65, 172107 (2002); PRB 79, 064106 (2009).]. So far, only three experimental reports declared the observation of bcc phase. Martin and Moore captured bcc Be at 1500 K near the melting temperature (~ 1550 K) at ambient pressure [J. Less-Common Met. 1, 85 (1959)], Abey provided a positive hcp/bcc phase boundary, [NTRL NTIS 198506, 1984]. However, Francois and Contre reported a negative hcp/bcc phase boundary [Proceedings of the Conference Internationale sur la Metallurgie du Beryllium, Grenoble (Presses Universitaires de France, Paris, 1965)]. On the theoretical side, the investigation of bcc Be with traditional methods encounters difficulty. This is because that the stabilization of bcc Be is primarily driven by lattice anharmonicity. Unfortunately, widely used quasiharmonic approximation (QHA) and Debye model are not able to capture such effect. For this reason, theoretical transition is still missing for P < 11 GPa. When P > 11 GPa, bcc Be is stabilized by pressure and QHA has been extensively employed. Nonetheless, the QHA predicted hcp/bcc boundary shows significantly discrepancy from the experimental revelation. This presumably hints that the anharmonic effect is also pronounced at high pressure [J. Phys. IV France 134, 257 (2006); PRB 82, 104118 (2010); JAP 111, 053503 (2012); PRB 79, 064106 (2009); PRB 71, 214108 (2005); PRB 76, 235109 (2007); RB 75, 035132 (2007)].

Using a novel approach which characterizes phonon quasiparticles from first-principles calculations, the research group led by Dong-Bo Zhang at Beijing Computational Science Research Center carried out a systematic study of phase stability of Be under high pressure and

#### References

[1] Y. Lu, T. Sun, Ping Zhang, P. Zhang, **Dong-Bo Zhang\***, and R. M. Wentzcovitch, Pre-melting *hcp to bcc* Transition in Beryllium, Physical Review Letters **118**, 145702 (2017).

high temperature. The outcomes show that Be exhibits pronounced anharmonic effects in both the bcc and hcp phases. The bcc phase, however, is favorable only in a very narrow temperature range near the melting temperature with a positive Clapeyron slope of ~ 41K/GPa. The temperature range where the bcc phase exists shrinks with increasing pressure and eventually disappears at around 11 GPa. This result agrees well with experiments.

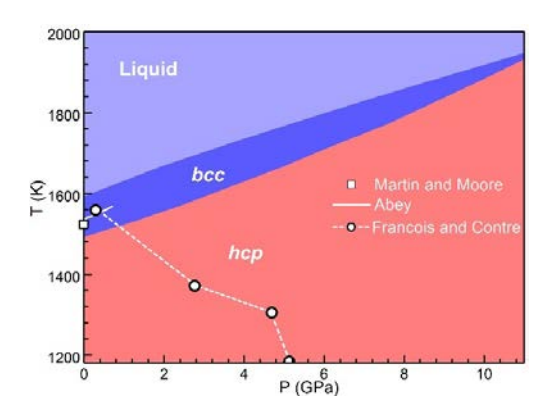
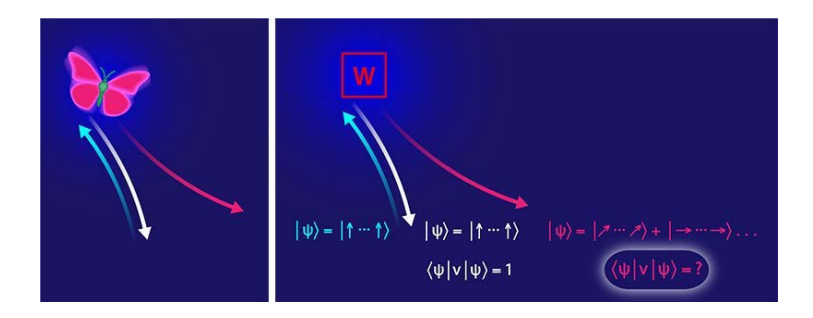


**Fig. 1.** Phase diagram of Be. The melting line is dopted from *PRB* **82**, 104118 (2010). The experimental results for the *hcp/bcc* phase

#### MEASURING OUT-OF-TIME-ORDER CORRELATORS ON A NUCLEAR MAGNETIC RESONANCE QUANTUM SIMULATOR



The idea of the out-of-time-order correlator (OTOC) has recently emerged in the study of a variety of research fields, e.g., condensed matter systems, quantum chaos and gravitational systems [1][2][3]. This quantity was suggested by Alexei Kitaev as a quantum generalization of a classical measure of chaotic behaviors [4], see Fig. 1. Despite of the significance of the OTOC revealed by recent theories, experimental measurement of the OTOC remains challenging. First of all, unlike the normal time-ordered correlators, the OTOC cannot be related to conventional spectroscopy measurements, such as ARPES, neutron scattering, through the linear response theory. Secondly, direct simulation of this correlator requires the backward evolution in time, that is, the ability of completely reverse the Hamiltonian, which is extremely challenging.

Fig. 1. A classical chaotic system can be diagnosed by the pres-ence of the butterfly effect, in which a small perturbation like the tiny flap of a butterfly's wing has a huge effect on the system at some later point in time. Analogously, in ex-periment with a quantum spin system, here described by a wave function. Quantum-control techniques are used to evolve the system forward in time (blue line), to apply a perturbation W, and to evolve the systems backward in time (red line). Then a measurement is performed to diag-nose the effect of the perturbation.

Recently, Jun Li, a postdoctoral fellow in Chang-pu Sun's group in CSRC and his collaborators Hui Zhai from Institute for advanced study, Tsinghua University, and Bei Zeng from Institute for quantum computing, University of Waterloo, and Xinhua Peng from University of Science and Technology of China, performed for the first time the measurements of OTOCs on a NMR quantum simulator. The system be simulated is an Ising spin chain model, whose Hamiltonian is written as

$$\hat{H} = \sum \left( -\hat{\sigma}_i^z \hat{\sigma}_{i+1}^z + g \hat{\sigma}_i^x + h \hat{\sigma}_i^z \right)$$

The parameter values g=1, h=0 correspond to the traverse field Ising model, where the system is integrable. The system is non-integrable whenever both g and h are non-zero. Experiment was done on a four nuclear spins in the iodotrifluroethylene molecule, see Fig. 2. The experiment simu-lates the dynamics governed by the system Hamiltonian H, and measures the OTOCs of operators that are initially acting on different local sites. The time dynamics of the OTOCs are observed, from which entanglement entropy of the system and butterfly velocities of the chaotic systems are ex-tracted. The results indicate that OTOC provides a faithful reflection of the information scrambling and chaotic behavior of quantum many-body systems.



Measuring the OTOC functions can reveal how quantum entanglement and information scrambles across all of the degrees of freedom in a system. This work here represents a first and encouraging step towards further experimentally observing OTOCs on large-sized quantum systems. The pre-sent method can be readily translated to other controllable systems.

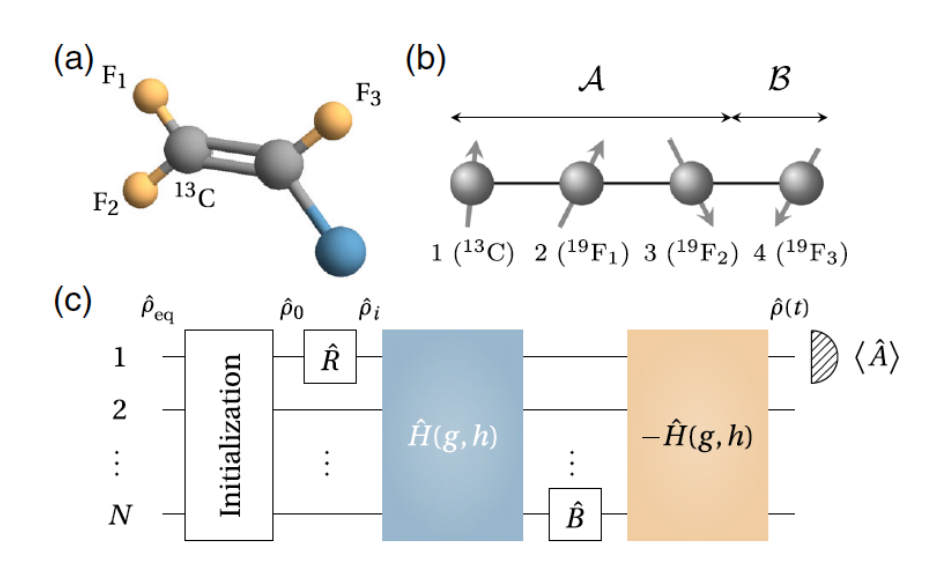


Fig. 2. Illustration of the physical system, the Ising model and the experimental scheme. (a) The structure of the C2F3I molecule used for the NMR simulation. (b) The four sites Ising spin chain, A and B label dividing the entire system into two subsystems in the later discussion of entanglement entropy. (c) Quantum circuit for measur-ing the OTOC for general N-site Ising.

#### References

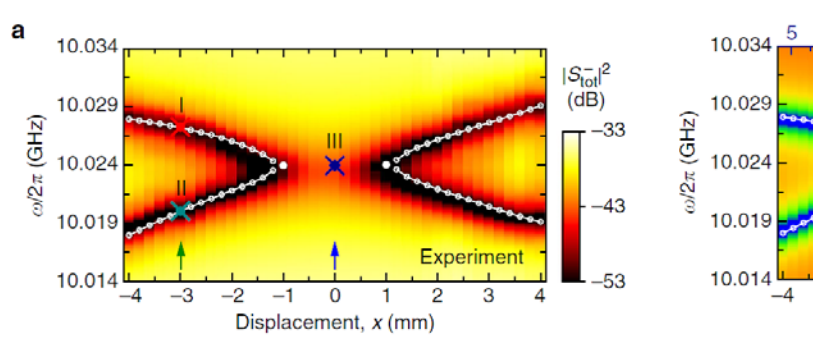
- [1] S. H. Shenker and D. Stanford, J. High Energy Phys. 03 067 (2014).
- [2] Wouter Buijsman, Vladimir Gritsev, Rudolf Sprik, Phys. Rev. Lett. 118, 080601 (2017).
- [3] P. Hosur, X.-L. Qi, D. A. Roberts, and B. Yoshida, J. High Energy Phys. 02 004 (2016).
- [4] A. Kitaev, in Proceedings of the Fundamental Physics Prize Symposium, Vol. 10 (2014).

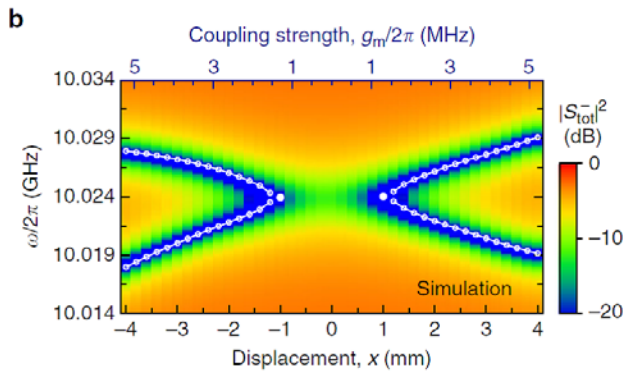
### OBSERVATION OF THE EXCEPTIONAL POINT IN CAVITY MAGNON-POLARITONS

Controlling light-matter interactions has persistently been pursued and is now actively explored. Understanding these interactions is not only of fundamental importance but also of interest for various applications. Recently, there has been an increasing number of studies on collective excitations of ferromagnetic spin system (i.e., magnons) coupled to microwave photons in a cavity (see, e.g., [1]–[5]). Owing to the strong coupling between magnons and cavity photons, a new type of bosonic quasiparticles called cavity magnon-polaritons can be created. While the damping rate of magnons is fixed, by

engineering the ports of cavity for inputting microwave photons and the related decay rates, the system of cavity photons coupled to magnons can be described by a non-Hermitian Hamiltonian. The hallmark of a non-Hermitian system is the existence of a singularity in its eigenvalues and eigenfunctions at some particular points in the parameter space of the system. This singularity is called the exceptional point.

**Fig. 1.** Observation of the exceptional point in cavity magnon–polaritons. (a) Measured total output spectrum vs. the displacement x of the YIG sphere in the cavity. (b) Calculated total output spectrum corresponding to the measured results in (a). Corresponding coupling strength is indicated according to the relation  $g_m/2\pi=1.3|x|$ .





Very recently, Zhang et al. at the CSRC [6] have experimentally demonstrated that the non-Hermiticity dramatically modifies the mode hybridization and spectral degeneracies in cavity magnon-polaritons. In their experiment, they engineered the dissipations of magnons and photons to produce an effective non-Hermitian PT-symmetric Hamiltonian. By tuning the magnon-photon coupling, they observed the polaritonic coherent perfect absorption and demonstrated the phase transition at the exceptional point. Thus, cavity magnonpolaritons with non-Hermitian nature are explored and achieved in this experiment. It paves the way to explore the non-Hermitian physics of the cavity magnon-polaritons.

#### References

[1] H. Huebl, C. W. Zollitsch, J. Lotze, F. Hocke, M. Greifenstein, A. Marx, R. Gross, and S. T. B. Goennenwein, Phys. Rev. Lett. 111, 127003 (2013).

[2] Y. Tabuchi, S. Ishino, T. Ishikawa, R. Yamazaki, K. Usami, and Y. Nakamura, Phys. Rev. Lett. 113, 083603 (2014).

[3] X. Zhang, C. L. Zou, L. Jiang, and H. X. Tang, Phys. Rev. Lett. 113, 156401 (2014).

[4] D. Zhang, X. M. Wang, T. F. Li, X. Q. Luo, W. Wu, F. Nori, and J. Q. You, NPJ Quantum Inf. 1, 15014 (2015).

[5] L. Bai, M. Harder, Y. P. Chen, X. Fan, J. Q. Xiao, and C. M. Hu, Phys. Rev. Lett. 114, 227201 (2015).

[6] D. Zhang, X. Q. Luo, Y. P. Wang, T. F. Li, and J. Q. You, Nature Commun. 8, 1368 (2017).

### OPTICAL LEVITATION OF NANODIAMONDS 21 BY DOUGHNUT BEAMS IN VACUUM

By trapping, detecting and manipulating nano- and micro-particles<sup>1</sup>, optical tweezers are widely used in biophysics, colloidal sciences, chemistry, microfluidic dynamics, and fundamental physics2. Because of the wide applicability and high tunablity of the optically levitated systems, several schemes were proposed to realize the ground-state cooling of the mechanical motion, to search for non-Newtonian gravity and to detect gravitational wave. Particularly, it brings about more interesting phenomena and novel applications when the trapped particles have internal degrees of freedom (such as spins or electric dipoles) and enter the quantum regime.

Optically levitated nanodiamonds with nitrogen-vacancy (NV) centers are one of the most promising candidates for implementing a spin-optomechanical hybrid system<sup>3,4</sup>. In principle, this system can have both long spin coherence time and high quality factor of mechanical oscillation in vacuum. The electron spins of NV centers were shown to have long spin coherence time (in the order of  $10^2 \, \mu s$ ) even in nanodiamonds of diameter about 20 nm. When trapped in high-vacuum, the dielectric particles are predicted to have ultra-high quality factor Q larger than  $10^{10}$ . Researchers have trapped diamond particles and observed the signal from NV centers in liquid, in air and very recently in vacuum with pressure down to  $100 \, Pa$ . Realizing high quality mechanical oscillation requires trapping the particles in high vacuum (e.g.,  $10^{-6} \, Pa$ ) to get  $Q \sim 10^{10}$ . However, the high-vacuum condition

usually causes the thermal damage problem, and experimentally trapping a nanodiamond in high vacuum is still very challenging. Nanodiamonds will absorb energy from the trapping laser beams due to the intrinsic defects and the inevitable imperfections or graphitization on diamond surface. The absorbed energy can hardly be dissipated in a high-vacuum environment, and the nanodiamonds will be quickly heated up significantly, which is unfavorable to the defect centers, or even burns out the diamond particles.

It is proposed here to solve the thermal damage problem by trapping a composite particle (a nanodiamond core coated with a less absorptive silica shell) at the center of strongly focused doughnut-shaped laser beams, as shown in Fig. 1. Systematical study on the trapping stability, heat absorption, and oscillation frequency concludes that the azimuthally polarized Gaussian beam and the linearly polarized Laguerre-Gaussian beam  $LG_{03}$  are the optimal choices. The respective oscillation frequency and quality factor got are shown in Fig. 2. With our proposal,

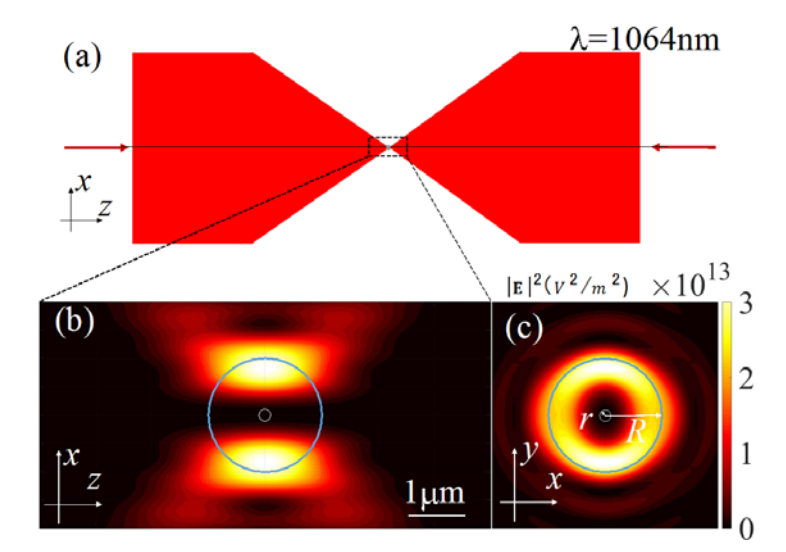


Fig. 1. (a) The schematic illustration of the system. A nanodiamond coated with a silica shell is levitated in an optical trap formed by two incoherent strongly-focused counter-propagating beams. (b) (c) Front view and side view of the intensity distribution of the two focused linearly polarized LG<sub>03</sub> incident beams in the focal region. The circles indicate the composite particle with the core radius r = 100nm and the shell radius  $R = 1\mu m$ .

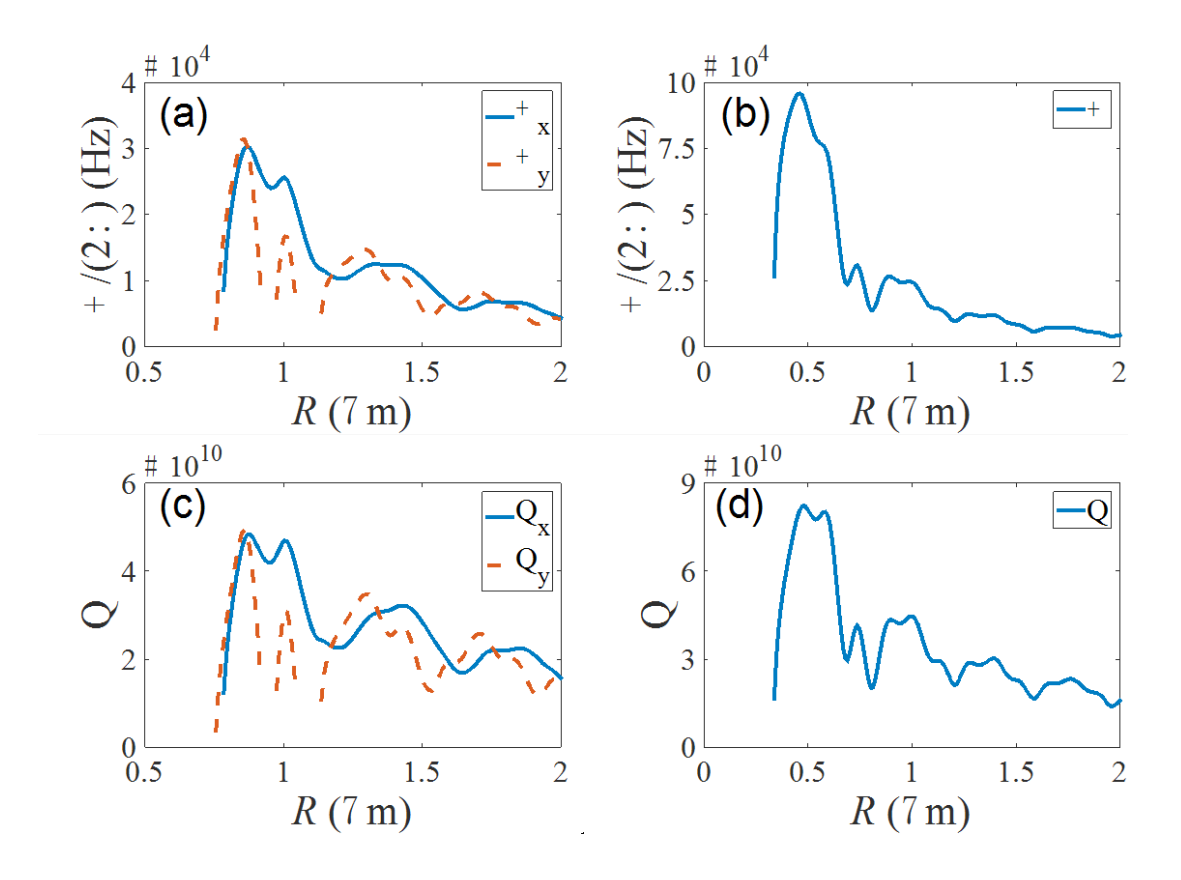


Fig. 2. The oscillation frequency  $\Omega/(2\pi)$  of the coreshell particle in dual-beam optical tweezers with (a) linearly polarized LG03 beams and (b) azimuthally polarized beams. (c) and (d) The mechanical quality factor Q under pressure  $10^{-6}$  Pa corresponding to cases (a) and (b), respectively. In all cases, the incident beams with power P1 = P2 = 50 mW are focused by lens with NA = 0.95.

particles with strong absorption coefficients can be trapped without obvious heating and, thus, the spin-optomechanical system based on levitated nanodiamonds are made possible in high vacuum with the present experimental techniques.

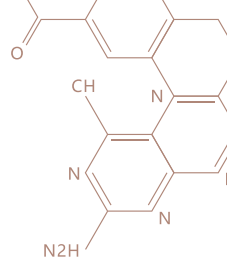
This work is supported by NKBRP (973 Program) 2014CB848700, NSFC No. 11374032 and NSAF U1530401, 2014011008-1, 2014021004 and NSFC through 11404201, 11674204.

For more information, please see the paper: "Optical levitation of nanodiamonds by doughnut beams in vacuum", *Laser Photonics Rev.*, 1600284 (2017). DOI: 10.1002/lpor.201600284.

#### References

- [1] D. G. Grier, Nature 424, 810 (2003).
- [2] T. Li, S. Kheifets, D. Medellin, and M. G. Raizen, Science 328,1673 (2010).
- [3] Z.-q. Yin, A. A. Geraci, and T. Li, Int. J. Mod. Phys. B 27, 1330018 (2013).
- [4] N. Zhao and Z.-q. Yin, Phys. Rev. A 90, 042118 (2014).





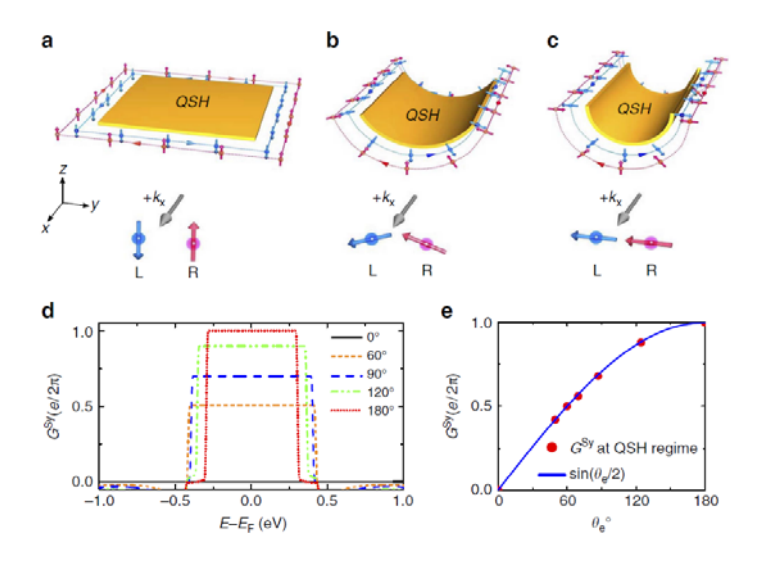
#### A UNIVERSAL RULE FOR CONTROLLING SPIN CURRENTS IN QUANTUM SPIN HALL SYSTEMS

A long-standing interest in spintronics is generating and transporting spin current (SC) in condensed matter systems. The discovery of pure spin current (PSC), for example, spin Hall current, that is decoupled from charge current (CC) has opened up exciting opportunities for spin transport, because it is expected that the transport of PSC has much smaller energy dissipation compared with that of conventional SC generated by ferromagnetic materials. Quantum spin Hall (QSH) system can exhibit exotic spin transport properties, especially, a transverse edge PSC of QSH effect can be generated under a four-terminal device setting. However, spin conservation mandates that there is no net SC under a two-terminal device setting in a QSH system. Although discovering new mechanism to control the SC and/or transverse PSC in a QSH system is of great importance for spintronics, its development is still at its infancy.

Recently, Prof. Bing Huang's group in CSRC in collaboration with Feng Liu's group in the University of Utah proposed a new concept of bending strain engineering to tune the spin transport properties of current in a quantum spin Hall system by control of its bending curvature. This concept of bending strain engineering of spins via topological nanomechanical architecture affords a promising route towards the realization of topological nanomechanospintronics.

#### References

[1] B. Huang, K. Jin, B. Cui, F. Zhai, J. Mei, and F. Liu, Nature Comm. 8, 15850 (2017).



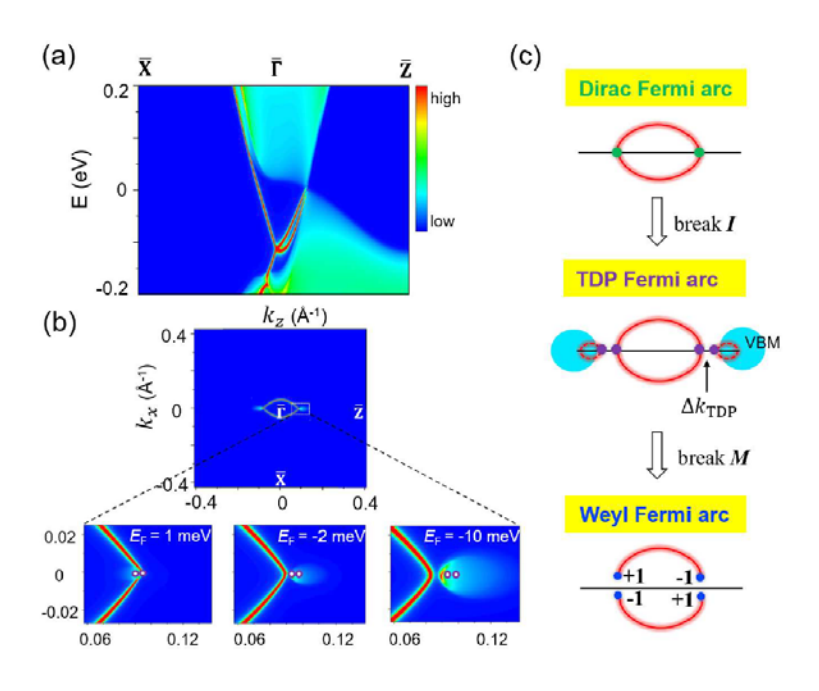
a quantum spin Hall system, as shown in Figure 1. They show that bending strain can be used to control the spin orientation of counterpropagating edge states of a quantum spin system to generate a non-zero spin current. This physics mechanism can be applied to effectively tune the spin current and pure spin current decoupled from charge

Fig. 1. (a)–(c) Schematic diagrams of spin current and charge current flowing along the edges as the bending angle increases from 0 (a) to 180 (c). A pair of edge states counter propagate along all four edges subject to TRS. The spins rotate adiabatically along the curved edges. The highlight of spin directions at the two opposite edges under the same charge current flow direction is shown in the bottom of (a)–(c). (d) Calculated spin conductance for the QSH ribbons with different bending angle in a two-terminal device setting. (e) The values of spin conductance in the QSH regime (plateau region) in (d) as a function of bending angle.

## PREDICTION OF IDEAL TOPOLOGICAL SEMIMETALS WITH TRIPLY DEGENERATE POINTS IN NACU3TE2 FAMILY

As topological phase extends from insulators to semimetals, new quasiparticles analogous to elementary particles in high-energy physics emerge in these topological materials. Interestingly, the band theory has shown that the crystal symmetries in solids allow for the existence of other types of topological quasiparticle excitations even without highenergy counterparts. Especially, the triply degenerate points (TDPs), formed by the crossing of a double-degenerate band and a nondegenerate band, can be recognized as an intermediate phase between Weyl (doubledegenerate) and Dirac (fourfold-degenerate) fermions. The TDP semimetals have been predicted to have some unique properties, e.g., Lifshitz transitions of Fermi surface, helical anomaly, large nonsaturating or negative magnetoresistance, and unconventional quantum Hall effects. One of the key problems for exploring the intrinsic properties of TDP fermions is the lack of ideal TDP semimetals, in which the TDPs around the Fermi level do not coexist with other quasiparticle bands. Therefore, it is of great importance to search for ideal host materials having only TDP fermions around Fermi level.

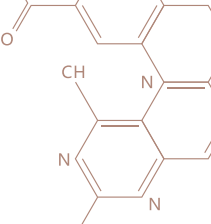
Recently, Bing Huang's group in CSRC disclose an effective approach to search for ideal TDP semimetals via selective band crossing between antibonding s and bonding p orbitals along a line in the momentum space with C3v symmetry. Applying this approach, they have successfully identified the NaCu3Te2 family of compounds to be ideal TDP semimetals, where two and only two pairs of TDPs are located around the Fermi level. Moreover, they demonstrate a fundamental mechanism to modulate energy splitting between a pair of TDPs, and illustrate the intrinsic features of TDP Fermi arcs in these ideal TDP semimetals, as shown in Figure 1.



**Fig. 1.** (a) Surface projected band and (b) Fermi surfaces with different EF for the (010) surface of a semi-infinite NaCu3Te2 system. Two circles in magnified Fermi surfaces denote the surface projections of two adjacent TDPs. (c) Evolution of Fermi arcs from Dirac to TDP to Weyl fermions.

#### References

- [1] D. G. Grier, Nature 424, 810 (2003).
- [2] T. Li, S. Kheifets, D. Medellin, and M. G. Raizen, Science 328,1673 (2010).
- [3] Z.-q. Yin, A. A. Geraci, and T. Li, Int. J. Mod. Phys. B 27, 1330018 (2013).
- [4] N. Zhao and Z.-q. Yin, Phys. Rev. A 90, 042118 (2014).



## SURFACE EVOLUTION OF A PT-PD-AU ELECTROCATALYST FOR STABLE OXYGEN REDUCTION

The exploration of new technologies for efficient energy management is attractive in order to reduce our dependence on environmentally unfriendly fossil fuels. Proton-exchange membrane fuel cells (PEMFCs) are thought to be an ideal solution for energy conversion because of their high efficiency, high reliability and low or zero carbon emissions1. Unfortunately, the sluggish reaction kinetics of the oxygen reduction reaction (ORR) at PEMFC cathodes and the poor durability of conventional ORR electrocatalysts have seriously hindered the development and commercial application of PEMFCs on a large scale1. As the most active metal electrocatalyst for ORR, Pt and Ptbased nanocatalysts have attracted substantial research interests over the past decade. The demonstrated approaches for achieving higher catalytic activities include exposing highly active lattice planes on their surfaces, alloying with other suitable metals to increase their intrinsic activity, and constructing hollow or core-shell1 structures to improve Pt utilization. Regarding improving catalyst durability, the addition of stabilizing elements and the optimization of crystallinity have been shown to be feasible.

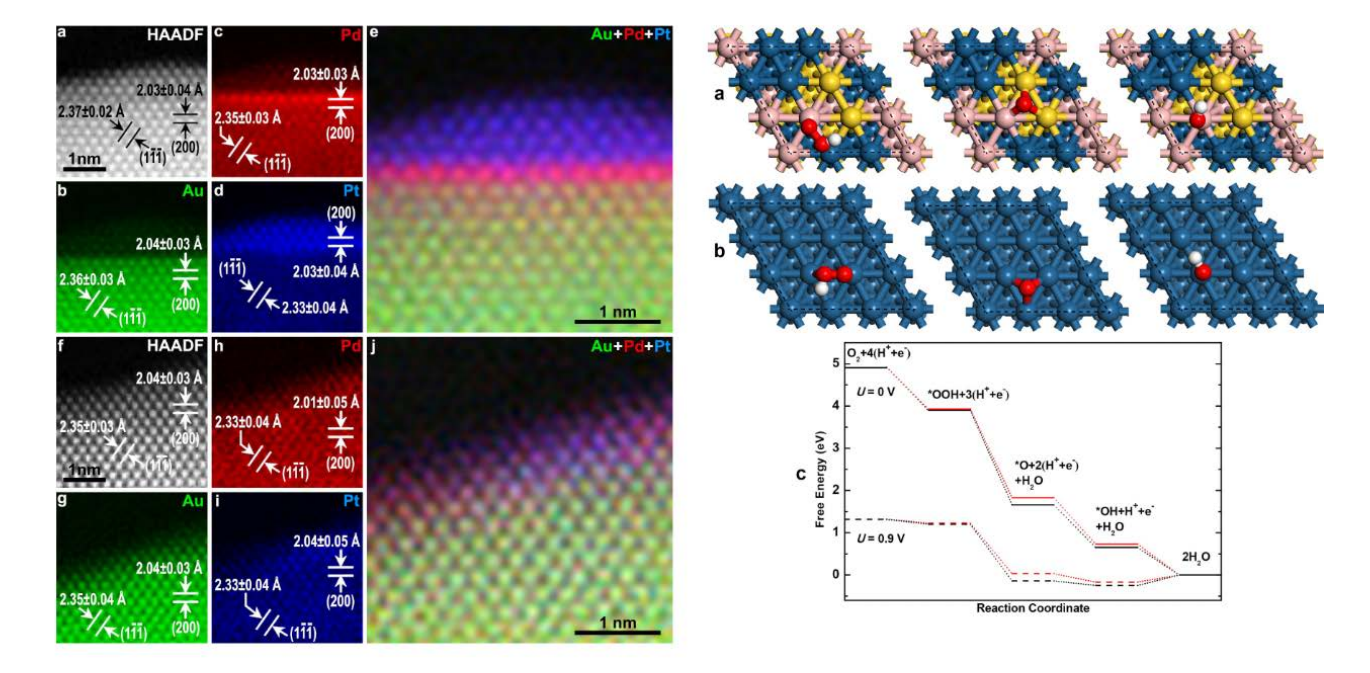
Recently, Dr. Li-Min Liu in CSRC worked with Dr. Yi Ding and Jun Luo's group at Tianjin University of Technology, designed an unsupported nanoporous catalyst with a sub-nanometer-thick PtPd shell on Au by theory and experiment, which demonstrates a high ORR activity (1.140 A mg<sub>Pt</sub><sup>-1</sup> at 0.9 V) and stability (1.471 A mg<sub>Pt</sub><sup>-1</sup> until 100,000 cycles). The DFT and experiment unveil the origin of the

activity change: the atomic-scale evolution of the shell from an initial PtPd alloy into a bilayer structure with a Pt-rich trimetallic surface and finally into a uniform and stable PtPdAu alloy. First-principles calculations further revealed that the surface atomic composition of the finally obtained PtPdAu decreases the free energy change of the final water formation from the \*OH on the catalyst surface and thereby enhances the ORR catalytic activity.

#### References

[1] Jian Li#, Hui-Ming Yin#, Xi-Bo Li#, Eiji Okunishi, Yong-Li Shen, Jia He, Zhen-Kun Tang, Wen-Xin Wang, Emrah Yucelen, Chao Li, Yue Gong, Lin Gu, Shu Miao, Li-Min Liu\*, Jun Luo\*, Yi Ding\*. Nature Energy 2017 DOI 10.1038/nenergy.2017.111.

**Fig. 1.** Left: Atomically-resolved elemental mapping of the surfaces of NPG-Pd-Pt<sub>10,000</sub> and NPG-Pd-Pt<sub>30,000</sub> electrocatalysts. **Right:** Calculated adsorption configurations of the intermediate species of ORR on the surfaces of the PtPdAu(111) and the pure Pt(111) models and the calculated free energy profiles of the ORR steps.



## BAND STRUCTURE ENGINEERING OF Cs<sub>2</sub>AgBiBr<sub>6</sub> PEROVSKITE THROUGH ORDER-DISORDERED TRANSITION

Given the low cost, suitable bandgap, high optical absorption and long carrier lifetime, the family of organic-inorganic perovskite halide A<sup>I</sup>B<sup>II</sup>X<sub>3</sub>, especially CH<sub>3</sub>NH<sub>3</sub>PbI<sub>3</sub>, has become the most investigated light-harvest material for solar cells in the last few years. Although solar cells based on CH3NH3PbI3 thin films have approached a high power conversion efficiency of more than 22%, two serious problems including toxicity of the water soluble Pb<sup>2+</sup> ions and thermodynamic instability of CH3NH3PbI3 in air against decomposition have presented major barriers to its commercial application. Cs<sub>2</sub>AgBiBr<sub>6</sub> was proposed as one of the inorganic, stable, and non-toxic replacement of CH<sub>3</sub>NH<sub>3</sub>PbI<sub>3</sub>. However, the wide indirect band gap of Cs<sub>2</sub>AgBiBr<sub>6</sub> suggests that its application in photovoltaics is limited.

Recently, Su-Huai Wei's group in CSRC [1-2] show that by introducing disorder to the cation occupancy of Ag and Bi in Cs2AgBiBr6 they could engineering the band structure of Cs<sub>2</sub>AgBiBr<sub>6</sub>. Using the Monte Carlo and the first principle calculation, they predicted that disordered Cs<sub>2</sub>AgBiBr<sub>6</sub> with the band structures changing from indirect band gap of 1.46 eV to pseudo-direct band gap of 0.44 eV could be synthesized by quenching from temperature beyond the phase transition temperature. Introducing n-type dopants such as Ba2+ and La3+ into the alloy can significantly reduce the energy difference and thus the transition temperature. Depending on the extent of disorder, the light absorption in the visible and the near infrared region for the disordered Cs2AgBiBr6 alloys could be considerably enhanced, which has broaden the application of the compound. This work shows that introducing cation disorder is a useful way for band structure engineering of the perovskite materials for various applications.

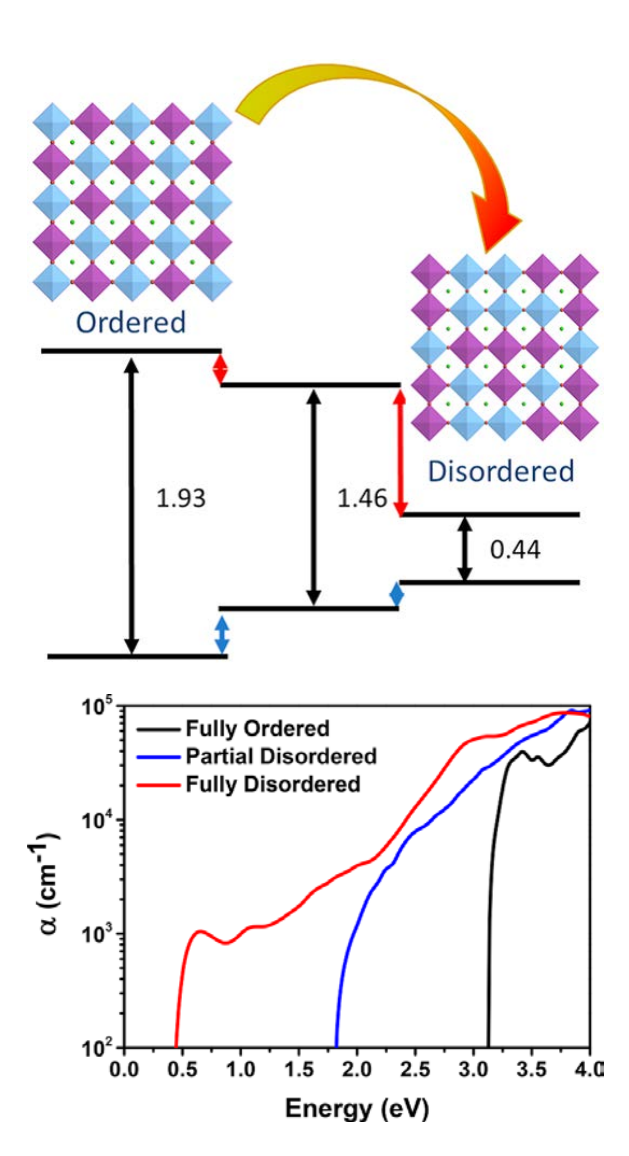
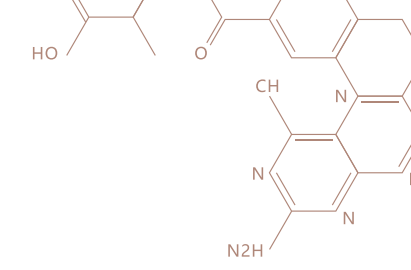


Fig. 1. The upper figure shows schematically the changes from the ordered double perovskite cell to the disordered perovskite cell and the corresponding changes of the band gap from ordered, partially disordered (at phase transition) to random atomic configurations. The lower figure shows the calculated optical absorption coefficients ( $\alpha$ ) of the fully ordered (black line), partial disordered (blue line), and fully disordered (red line)  $Cs_2AgBiBr_6$ .

#### References

- [1] J. Yang, P. Zhang, and S.-H. Wei\*, J. Phys. Chem. Lett. 9, 31 (2018).
- [2] P. Zhang, J. Yang, and S.-H. Wei\*, J. Mater. Chem. A (in press).

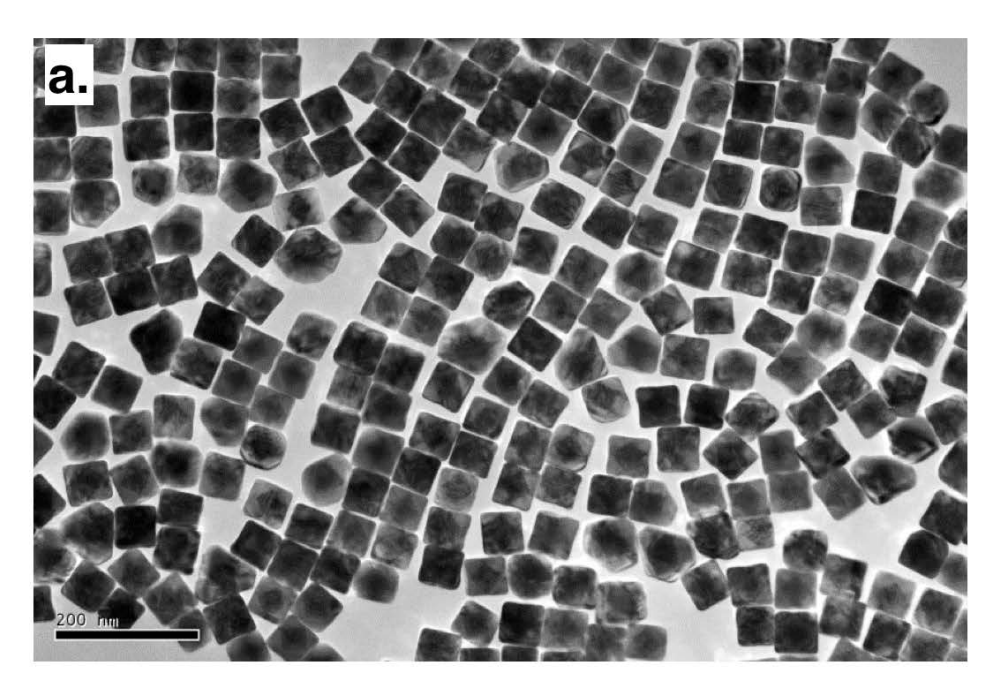


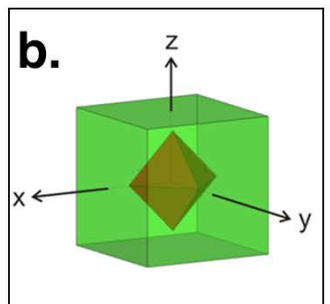
### A NEW ALGORITHM FOR XFEL SINGLE PARTICLE SCATTERING DATA ANALYSIS

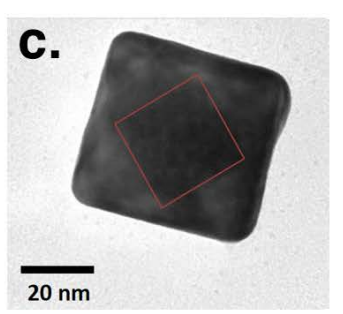
X-ray Free Electron Lasers (XFELs) generate ultrabright X-ray pulses with duration of 4-100 femtoseconds, possible to outrun X-ray radiation damage using the 'diffract-before-destroy' experimental approach. Using core-shell nanoparticles as model systems, we carried out a proof-ofprinciple experiment at LCLS, the first XFEL user facility (Figure 1 & 2). Over a million diffraction patterns were collected, and Haiguang Liu and coworkers analyzed about 54k patterns after initial screening. Because the synthetic nanoparticles have size variations, the pre-sorting based on particle sizes is necessary before merging the data to 3D fourier space. On the other hand, the size analysis from scattering patterns relies on correct orientation information. Using a reduced representation of the raw data, Haiguang Liu's group successfully recovered particle orientation and sorted out the particle sizes. The idea is to integrate the intensity information along the radial axis, the resulting 1D intensity profile at azimuth angles is less sensitive to the variations of particle sizes (Figure 3). The 1D profiles are then compared to the standard reference models to recover the particle orientation. The q-spacing (distance between speckles along scattering streaks) is then converted to particle size information. The recovered size distribution from XFEL data is very consistent with the data obtained using STEM experimental approach (Figure 4). This is the first time that the analysis of XFEL scattering data resulted from heterogeneous particles. The data description is summarized in the Scientific Data, and the new algorithm is published in the IUCrJ.

The experiment was carried out at LCLS in Stanford Linear Accelerator Center National Laboratories, by an international collaboration team under the leadership of Haiguang Liu, Brenda Hogue, Ilme Schlichting, and John Spence. The analysis work is mainly carried out by Ph.D student, Xuanxuan Li.

**Fig. 1.** The core-shell nanoparticles. (a) view under STEM; (b) schematic drawing of the particle, with gold core and palladium shell; (c) a closer view of a single particle.







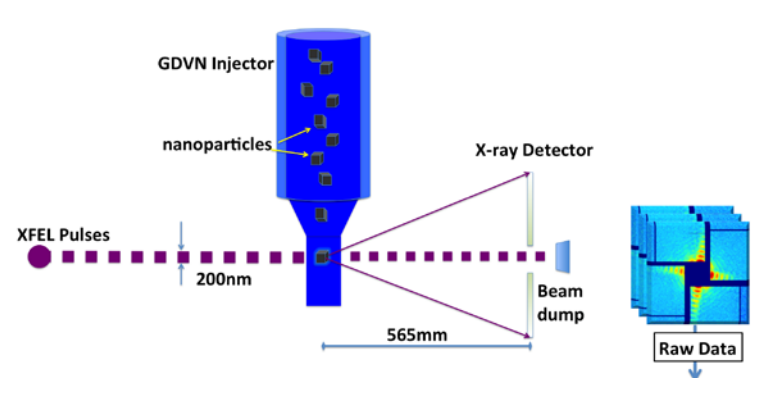


**Fig. 2.** Experimental setup at XFEL using diffract-before-destroy approach. Over 1 million raw images were collected at LCLS in SLAC national lab.

#### References

[1] Li Xuanxuan et al., Diffraction data of coreshell nanoparticles from an X-ray free electron laser, Scientific Data, 4:170048 (2017)
[2] Li Xuanxuan, John Spence, Brenda Hogue, Haiguang Liu. Merging single-shot XFEL diffraction data from inorganic nanoparticles: a new approach to size and orientation determination. IUCrJ, 4, 741-750 (2017)

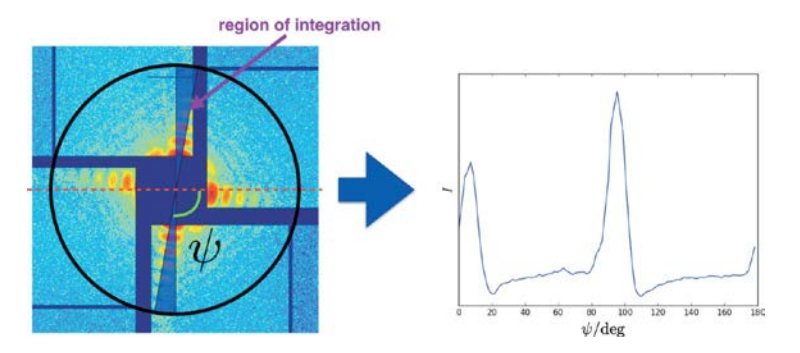
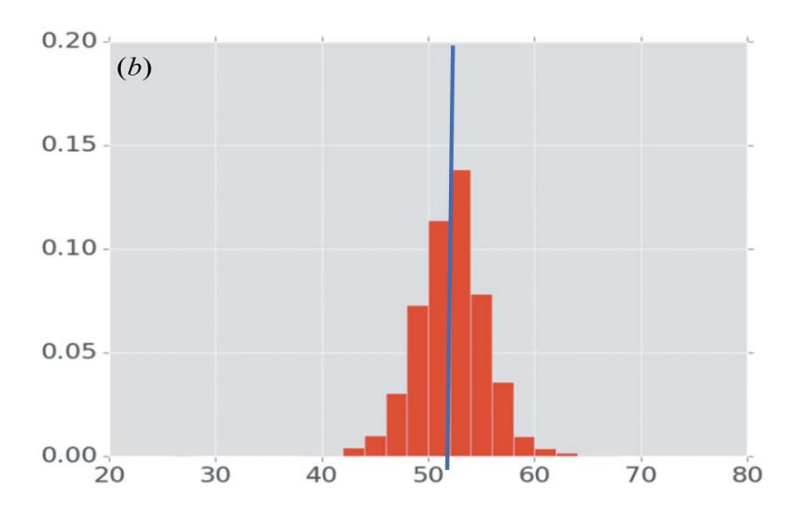


Fig. 3. Data reduction from 2D raw image to 1D intensity profile.



**Fig. 4.** The recovered particle size distribution and the average particle size (52nm) obtained from STEM.



## RATCHETING OF A VIRAL TRANSCRIPTION N2H PROTEIN MACHINE ALONG DNA WITHOUT BACKTRACKING

he RNA polymerases (RNAPs) play an essential role in gene expression as they transcribe information from DNA to RNA while synthesizing the RNA based on DNA. The viral RNAP from bacteriophage T7 is a prototypical single-subunit polymerase that is widely used in lab gene expression system as an efficient tool, yet rarely people understood underlying mechanisms well. T7 RNAP is indeed a smallest transcription machine, yet it is capable of working for all stages of transcription from initiation to elongation and to termination, without supports from any protein factor. It is in contrast with RNAPs from higher organisms, which constantly need assistances or regulations from a variety of protein factors. That being said, T7 RNAP sets a nice model system for physical investigations on transcription in a nutshell. In particular, the translocation mechanism of T7 RNAP on the transcribing DNA was controversial, and two basic working scenarios had been proposed, either as the thermally activated Brownian ratchet [1] or as the tightly coupled power-stroke engine [2].

To clarify the translocation mechanisms of T7 RNAP, Jin Yu's group in CSRC recently performed extensive all-atom molecular dynamics simulations accumulated to ten microseconds and constructed the Markov state model (MSM) to reveal substantial structural dynamics of the transcription machine on DNA [3] (see Fig 1). Notably, they demonstrated that T7 RNAP moves along DNA via Brownian alike paths, facilitated by essential structural elements such as O-helix and Y-helix from the fingers subdomain. Interestingly, they found that the synthesizing RNA strand and its pairing template DNA move in non-synchronized manner. They further discovered that the O-helix could rotate to open even prior to translocation, not only to facilitate the translocation, but also to resist backtracking. The finding thus explains a long-standing puzzle on T7 RNAP not being detected with

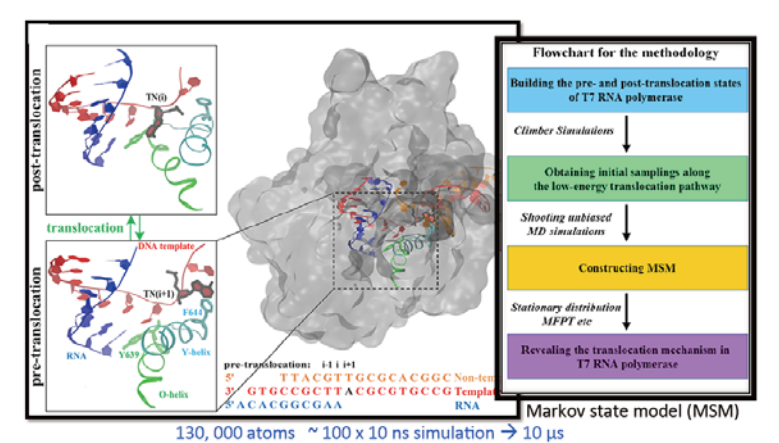
backtracking. Remarkably, they designed mutant T7 RNAPs via the O-helix to mimic structurally similar mitochondrial RNAPs for potential backtracking. Preliminary experimental tests from their experimental collaborator lab in PKU show survival of those mutants with more or less inhibited transcription activities, indicating the potential for backtracking. In summary, their work provides unprecedented detail and mechanistic insight into the translocation of a prototypical viral RNAP on DNA. The mechanism can be general for transcription machines with compact core structures. The rational re-design of the viral RNAP to acquire backtracking function preserved in other RNAP species also turns out to be highly promising.

#### References

[1] Thomen P, Lopez PJ, and Heslot F. Unravelling the mechanism of RNA-polymerase forward motion by using mechanical force. Phys. Rev. Lett. 94,128102 (2005)

[2] Yin YW and Steitz TA.The structural mechanism of translocation and helicase activity in T7 RNA polymerase. Cell 116, 393 (2004)

[3] Da LT<sup>+</sup>,E C<sup>+</sup>, Shuai Y, Wu S, Su XD, and Yu J. <u>T7 RNA polymerase translocation is facilitated by a helix opening on the fingers domain that may also prevent backtracking.</u> Nucl. Acids Res. 45, 7909 (2017) IF ~10.2



Step 1

Step 2

TN

Yeas

Pre-state

Post-state

**Fig. 1.** The structural views of the active site of T7 RNAP elongation complexes before (pre) and after (post) the translocation (*left*), the methodological chart (*middle*), and the translocation schematics obtained (*right*).

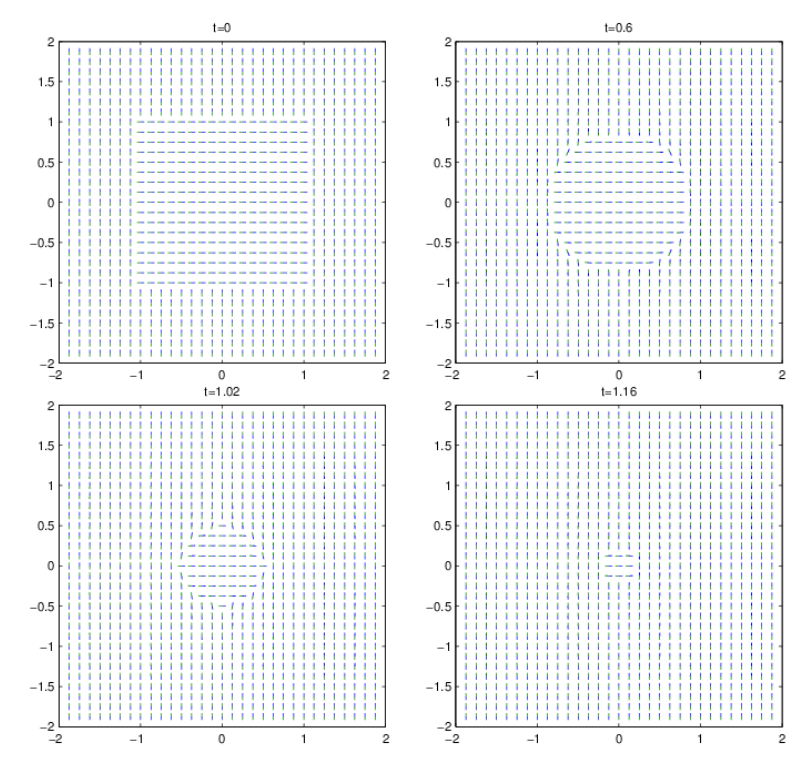
## A STABLE SCHEME FOR A 2D DYNAMICAL Q-TENSOR MODEL OF NEMATIC LIQUID CRYSTAL

Liquid crystals are intermediate states of matter between the commonly observed solid and liquid that have no or partial positional order but do exhibit an orientational order. The nematic phase is the simplest among all liquid crystal phases whose rod-like molecules have no translational order but possess a certain degree of long-range orientational order. The Landau-de Gennes theory[1] is a continuum theory to describe the nematic liquid crystals. In this framework, it is widely accepted that the local orientation and the degree of order for the liquid crystal molecules are characterized by a symmetric, traceless d  $\times$  d tensor called the Q-tensor in R<sup>d</sup> (d = 2,3). The dynamic Q-tensor model is a L<sup>2</sup> gradient flow generated by the liquid crystal free energy that contains a cubic term, which is physically relevant but makes the free energy unbounded from below, and for this reason, has been avoided in other numerical studies. The unboundedness of the energy brings significant difficulty in analyzing the model and designing numerical schemes [1]:

$$\partial_t Q^{ij} = \xi \Delta Q^{ij} + L_4 (2\partial_k (Q^{lk} \partial_l Q^{ij}) - \partial_i Q^{lk} \partial_j Q^{lk} + |\nabla Q|^2 \delta^{ij} / 2) - (a + \operatorname{tr}(Q^2))Q^{ij}$$

Recently, Yongyong Cai in CSRC in collaboration with Jie Shen in Purdue University and Xiang Xu in Old Dominion University, proposed an unconditionally stable numerical scheme to solve the 2D Q-tensor model for liquid crystal, and established its unique solvability and convergence[2]. The main difficulty in the analysis came from an unusual cubic term in the elastic energy, which made the free energy unbounded from below. By adding a stabilized term in the scheme, they were able to show that the norm of the numerical solution can be kept small which guaranteed the stability and the well-posedness. Numerical tests showed that the scheme is indeed first order accurate for a wide

Fig. 1. Orientation of 2D liquid crystal at different time with periodic boundary condition.





range of stabilizing constants, and produces physically consistent numerical simulations. The work provided essential ingredients for extensions to the 3D case, as well as the full dynamical model coupled with Navier-Stokes equations, which would lead to the better understanding of nematic liquid crystals.

#### References

[1] P.G. de Gennes and J. Prost, The physics of liquid crystals, Oxford Science Publications, Oxford, 1993.

[2] Y.Cai, J. Shen and X. Xu, Math. Models Methods Appl. Sci. 27, 1459 (2017).

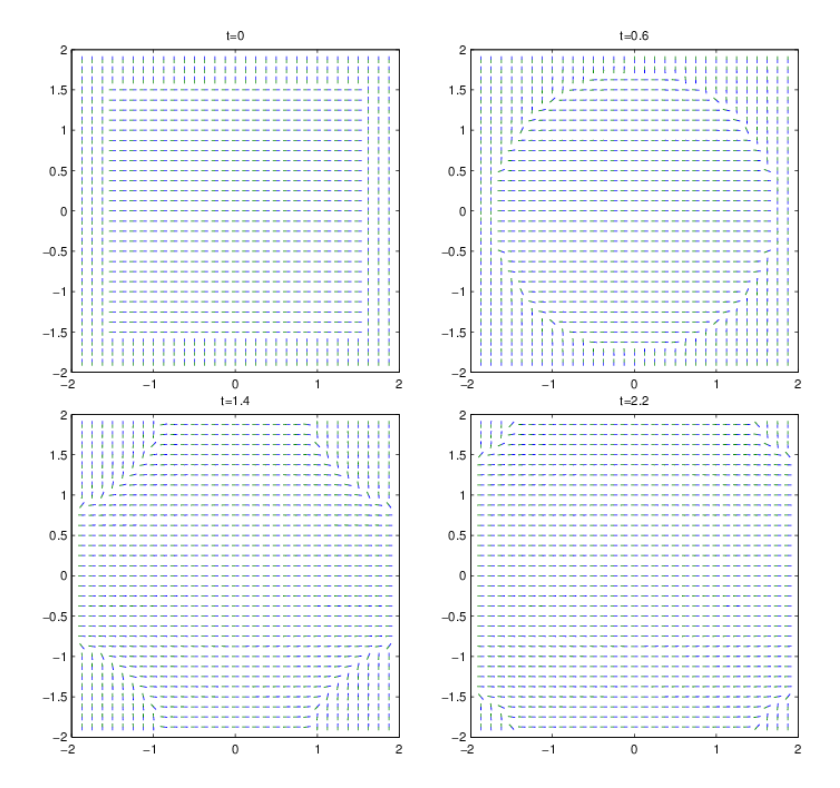


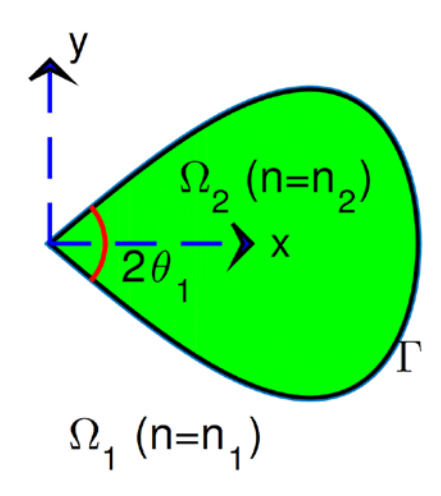
Fig. 2. Orientation of 2D liquid crystal at different time with different initial condition.

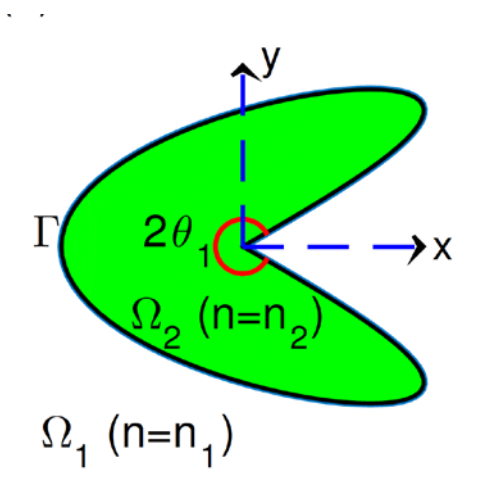
### CALCULATING CORNER SINGULARITIES BY BOUNDARY INTEGRAL EQUATIONS

Electromagnetic fields around metallic nanoparticles and in subwavelength apertures or slits of metallic films are often many orders of magnitude more intense than the incident wave. Strong near-fields of well-designed plasmonic structures have important applications in biological and chemical sensing, and can be used to enhance nonlinear optical effects, quantum optical effects, Raman scattering and other emission processes. The local field enhancement in plasmonic structures is the result of localized surface plasmon resonances, but geometric features such as corners and edges (see the geometric illustrations in Figures) also strongly influence the near-fields.

To analyze the local field enhancement phenomenon and to study the numerous applications, it is clearly important to calculate the near-fields accurately near sharp corners and edges where electromagnetic fields exhibit singularities and tend to infinity. For cylindrical structures, the singularity exponents of electromagnetic fields near sharp edges can be solved analytically, but in general the actual fields can only be calculated numerically.

Recently, CSRC postdoc Hualiang Shi, under the joint supervision of Professors Yayan Lu and Qiang Du used a boundary integral equation method to compute electromagnetic fields near sharp edges. They constructed the leading terms in asymptotic expansions based on numerical solutions. The numerically found singularity exponents agree well with the exact values in all the test cases presented in their work, indicating that the numerical solutions are accurate. Our integral equations are formulated for rescaled unknown functions to avoid unbounded field components, and are discretized with a graded mesh and properly chosen quadrature schemes.





#### References

Hualiang Shi, Ya Yan Lu, and Qiang Du, Calculating corner singularities by boundary integral equations, Journal of the Optical Society of America A, 34(6), pp. 961-966, (2017)

https://doi.org/10.1364/JOSAA.34.000961



## ERROR ANALYSIS OF A FINITE DIFFERENCE METHOD ON GRADED MESHES FOR A TIME-FRACTIONAL DIFFUSION EQUATION

The numerical solution of initial-boundary value problems with a fractional time derivative of order  $\alpha$ , where  $0 < \alpha < 1$ , has received much attention in the last few years. If  $\alpha = 1$ , then one has a standard parabolic partial differential equation, while  $0 < \alpha < 1$  means that the equation models an anomalous diffusion process (subdiffusion). Given smooth data, typical solutions of this problem are smooth in the spatial variable, and in the time variable for t > 0, but at the initial time t = 0 the solution has a weak singularity: it is continuous but its integer-order time derivatives blow up at tapproaches zero.

The figure shows a typical solution, and a cross-section of this solution along a line x=constant; clearly there is a singularity at t=0. But the vast majority of published analyses of numerical methods for this class of problem assume that the solution is a smooth function of both variables on all of the domain, i.e., they ignore the effect of the initial singularity. This global smoothness assumption limits severely the class of problems to which their theory can be applied; see [1].

The paper [2] is the first to give a finite difference analysis of a numerical method for these problems that is valid for problems that have a weak singularity at t = 0. In [2] one uses a uniform mesh in space and a special graded mesh in time (this mesh grading is often used in the solution of Volterra weakly integral equations, which are closely related to the fractional-derivative problem). A new discrete stability inequality is derived, showing how the solution at each time

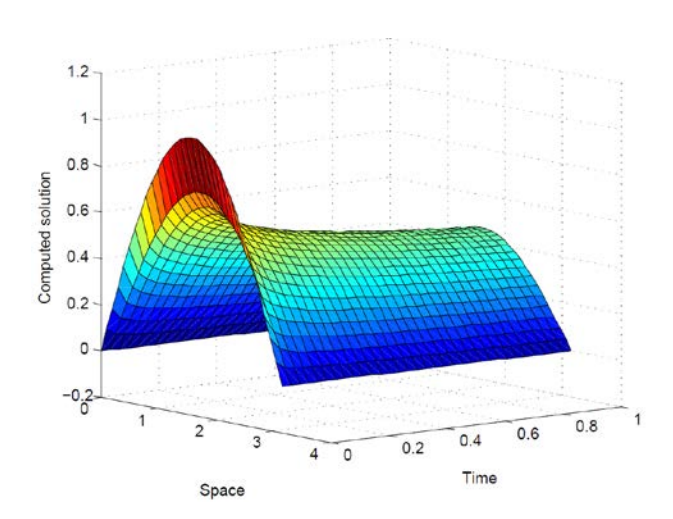
level depends on the data at earlier times; this is combined with a consistency error analysis to obtain a final convergence result in the discrete maximum norm that is sharp (as demonstrated by numerical experiments) and shows exactly how the error depends on the degree of mesh grading used. Consequently one can prescribe a priori an optimal mesh grading for the problem.

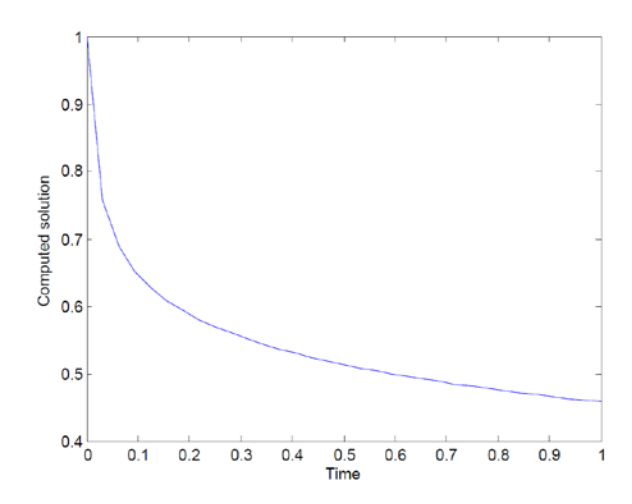
Reference [2] has attracted a great deal of attention in the fractional-derivative community: a copy of it on Researchgate has had more than 700 Reads.

#### References

[1] M.Stynes, Too much regularity may force too much uniqueness, Fract. Calc. Appl. Anal. 19 (2016), no.6, 1554–1562. DOI: https://doi.org/10.1515/fca-2016-0080

[2] M.Stynes, E.O'Riordan & J.L.Gracia, Error analysis of a finite difference method on graded meshes for a time-fractional diffusion equation, SIAM J. Numer. Anal. 55 (2017), 1057–1079. DOI: 10.1137/16M1082329







### NUMERICAL SOLUTION OF THE NONLOCAL DIFFUSION EQUATION ON THE REAL LINE

This paper is concerned with the numeral simulation of a nonlocal diffusion equation defined on the whole real axis. A challenging problem is how to construct artificial boundary conditions (ABCs) for these problems due to the nonlocality of the interaction. With the application of the Laplace transform in the spacial direction, rather than the classical temporal direction, a DtN-like mapping is obtained to be taken as an exact ABC for the nonlocal diffusion problem. In the practical numerical implementation, the nonlocal diffusion equation is first discretized in space to lead to a discrete nonlocal system on the whole real axis. After that, an exact ABC for the discrete nonlocal diffusion system is achieved on artificial boundary gridpoints. This exact ABC allowed one to reformulate the nonlocal system on the whole real axis into a finite nonlocal one on the truncated computational domain. So far, this is a pioneering work in the designing of exact ABCs for the nonlocal problems. The numerical examples were presented to verify the effectiveness of the approach in two parts. First, the schemes converge to the nonlocal problem by fixing horizon size  $\delta$  and taking  $h \rightarrow 0$ . Second, the numerical schemes are shown to converge to the correct local models when both  $\delta$  and  $h \rightarrow 0$ .

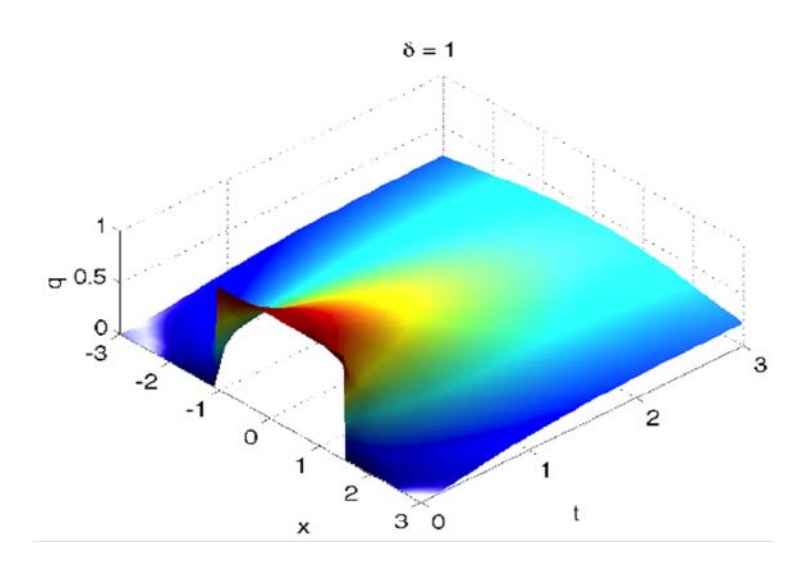


**Fig. 1.** The nonintegral kernel is used. One can see that our ABCs perfectly absorbed the heat flow which passes through the artificial boundary gridpoints, and do not generate any obvious approximation error.

#### References

[1] Chunxiong Zheng, Jiashun Hu, Qiang Du and J. Zhang. SIAM J. Sci. Comput. 2017. A3067-A3088.



## CH N

# FAST EVALUATION OF THE CAPUTO FRACTIONAL DERIVATIVE AND ITS APPLICATIONS TO FRACTIONAL DIFFUSION EQUATIONS

The computational operation and storage of numerically solving the time fractional PDEs are generally huge for the traditional direct methods since they require total O(MN) memory and  $O(MN^2)$  work, where N and M represent the total number of time steps and grid points in space, respectively. To overcome this difficulty, an efficient algorithm for the evaluation of the Caputo fractional derivative is presented. This algorithm is based on an efficient sum-of-exponentials (SOE) approximation for the Abel kernel over the interval [dt, T] with a uniform absolute errors. More importantly, the theoretical analysis is given to show that the number of exponentials P needed is of order P = $O(\log N)$  for T >> 1 or  $P = O(\log^2 N)$  for  $T \approx 1$  for fixed accuracy The resulting algorithm only requires only O(MP) storage and O(MNP) work when numerically solving the time fractional PDEs. Furthermore, the stability and error analysis of the new scheme is addressed, and several numerical examples are provided to demonstrate the performance of our scheme. For example, fast algorithm is applied to the nonlinear subdiffusion equation, Fig 1. shows the fast algorithm reduces the computational cost significantly.

#### References

[1] S. Jiang, J. Zhang, Q. Zhang and Z. Zhang, Commun. Comput. Phys., 21 (2017) 650-678.

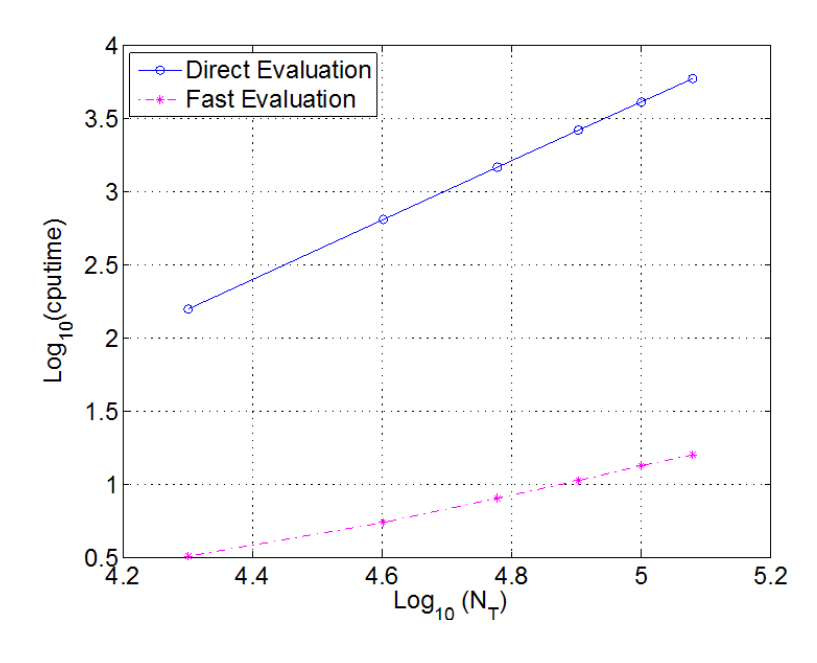


Fig. 1. The log-log (in base 10) plot of the CPU time (in seconds) versus the total number of time steps N.

# MATHEMATICAL AND NUMERICAL ANALYSIS OF DYNAMIC GINZBURG-LANDAU EQUATIONS IN NONCONVEX POLYGONS BASED ON HODGE DECOMPOSITION

Based on the Ginzburg-Landau theory of superconductivity, the macroscopic state of a superconductor is described by the complexvalued order parameter  $\psi$ , the real scalarvalued electric potential  $\phi$ , and the real vector-valued magnetic potential A. In the nondimensionalization form, the order parameter satisfies  $0 \le |\psi|^2 \le 1$ , where  $|\psi|^2 = 0$  corresponds to the normal state and  $|\psi|^2=1$  corresponds to the superconducting state, and  $0 < |\psi|^2 < 1$  represents an intermediate state between the normal and superconducting states. If the superconductor occupies a long cylinder in the x<sub>3</sub>-direction with a finite cross section and the external magnetic field is  $\mathbf{H}=(0,0,H)$ , then the order parameter  $\psi$  and the magnetic potential A=(A1,A2) are

governed by the TDGL(under gauge  $\phi = -\nabla \cdot \mathbf{A}$ ):

$$\eta \frac{\partial \psi}{\partial t} + (\frac{i}{\kappa} \nabla + \mathbf{A})^2 \psi + (|\psi|^2 - 1)\psi - i\eta \kappa \psi \nabla \cdot \mathbf{A} = 0, \tag{1a}$$

$$\frac{\partial \mathbf{A}}{\partial t} + \nabla \times (\nabla \times \mathbf{A}) - \nabla (\nabla \cdot \mathbf{A}) + \text{Re}[\psi^*(\frac{i}{\kappa} \nabla + \mathbf{A})\psi] = \nabla \times H.$$
 (1b)

If the computational domain  $\Omega$  contains reentrant corners, then the solution of (1) is often singular there, in particular,  $\mathbf{A}(t) \notin H^1(\Omega) \times H^1(\Omega)$  Hence solving (1) directly by the finite element method often yields spurious solutions. In addition, the singularity also makes it challenging to investigate the regularity of TDGL's solutions and convergence of numerical solutions.

To overcome this difficulty, Buyang Li from The Hong Kong Polytechnic University and Zhimin Zhang from CSRC reformulate the

$$\eta \frac{\partial \psi}{\partial t} + \left(\frac{i}{\kappa} \nabla + \mathbf{A}\right)^2 \psi + (|\psi|^2 - 1)\psi - i\eta \kappa \psi \nabla \cdot \mathbf{A} = 0, \quad (2a)$$

$$\Delta p = -\nabla \times \left( \operatorname{Re} \left[ \psi^* \left( \frac{i}{\kappa} \nabla + \mathbf{A} \right) \psi \right] \right), \tag{2b}$$

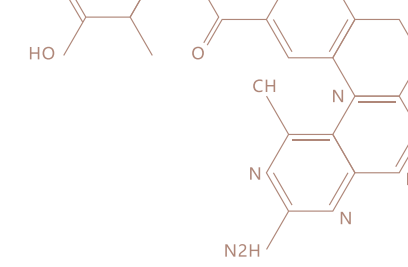
$$\Delta q = \nabla \cdot \left( \operatorname{Re} \left[ \psi^* \left( \frac{i}{\kappa} \nabla + \mathbf{A} \right) \psi \right] \right), \tag{2c}$$

$$\frac{\partial u}{\partial t} - \Delta u = H - p,\tag{2d}$$

$$\frac{\partial v}{\partial t} - \Delta v = -q. \tag{2e}$$



equations into an equivalent system of elliptic and parabolic equations (2) based on the Hodge decomposition. Let  $\mathbf{A} = \nabla \times u + \nabla v$  then we have Eq(2).



If  $H \in L^{\infty}((0,T); L^2) \cap L^2((0,T); H(curl))$ ,  $\psi_0 \in H^1$ ,  $\mathbf{A}_0 \in \mathbf{H}_n(curl, div)$  and  $|\psi_0| \le 1$  a.e. in  $\Omega$ , then the system (1) admits a unique weak solution. The reformulated system (2) also admits a unique solution, which coincides with the solution of (1).

Moreover, let xj, j = 1,..., m be the reentrant corners of the domain  $\Omega$ , then the solution has the decomposition

where  $\Psi \in L^2((0,T); H^2)$ ,  $\widetilde{u}, \widetilde{v} \in L^{\infty}((0,T); H^2)$ ,  $\Phi(r)$  is a given smooth cut-off function which equals 1 in a neighborhood of 0,  $\Theta_j(x)$  is the angle shown in Figure 1, and  $\alpha_j, \beta_j, \gamma_j \in L^2(0,T)$ .

$$\psi(x,t) = \Psi(x,t) + \sum_{j=1}^{m} \alpha_j(t) \Phi(|x-x_j|) |x-x_j|^{\pi/\omega_j} \cos(\pi\Theta_j(x)/\omega_j),$$
  
$$\mathbf{A} = \nabla \times u + \nabla v,$$

with

$$\begin{split} u(x,t) &= \widetilde{u}(x,t) + \sum_{j=1}^{m} \beta_j(t) \Phi(|x-x_j|) |x-x_j|^{\pi/\omega_j} \sin(\pi\Theta_j(x)/\omega_j), \\ v(x,t) &= \widetilde{v}(x,t) + \sum_{j=1}^{m} \gamma_j(t) \Phi(|x-x_j|) |x-x_j|^{\pi/\omega_j} \cos(\pi\Theta_j(x)/\omega_j), \end{split}$$

We solve (2) by the Lagrange finite element method by using the decoupled and linearized time-stepping scheme, with  $P_1 - P_1 - P_1 - P_1 - P_1 - P_1$  finite elements for discreted  $(\psi_h^n, p_h^n, q_h^n, u_h^n, v_h^n)$ , admits a unique solution when  $\tau < \eta/4$  and converges to the solution of (2), i.e.,

$$\max_{1 \le n \le N} (\left\| u^{n} - u_{h}^{n} \right\|_{H^{1}} + \left\| v^{n} - v_{h}^{n} \right\|_{H^{1}} + \left\| \mathbf{A}^{n} - \mathbf{A}_{h}^{n} \right\|_{L^{2}} + \left\| \psi^{n} - \psi_{h}^{n} \right\|_{L^{2}}) \le C(\tau + h^{\frac{\pi}{\omega} - \varepsilon})$$

where  $\Omega$  is the maximal interior angle of the domain  $\Omega$ ,  $\tau$  is an arbitrarily small constant, and C is a positive constant independent of  $\varepsilon$  and h.

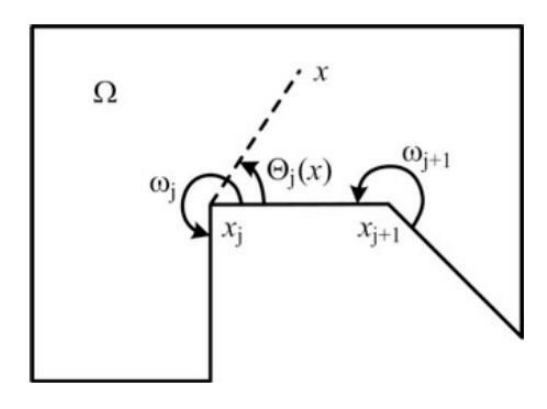


**Fig. 1.** Illustration of corner  $\mathcal{X}_j$ , in-terior angle  $\mathcal{O}_j$  and argument  $\Theta_i(x)$ .

#### References

B. Li and Z. Zhang: Mathematical and numerical analysis of time-dependent Ginzburg–Landau equations in nonconvex polygons based on Hodge decomposition. *Math. Comp.*, 86 (2017), pp. 1579–1608.

# HESSIAN RECOVERY FOR FINITE ELEMENT METHOD

Hessian matrix is particularly significant in adaptive mesh design, since it can indicate the direction where the function changes the most and guide us to construct anisotropic meshes to cope with the anisotropic properties of the solution of the underlying partial differential equation. It also plays an important role in finite element approximation of second order non-variational elliptic problems, some fully nonlinear equations and designing nonlocal finite element technique.

Consider the following variational problem: find

Fig. 1. An illustration of Hessian recovery at the point located on  $u_0$ .

An illustration:  $u_{11}$   $u_{10}$   $u_{1}$   $u_{1}$   $u_{1}$   $u_{1}$   $u_{2}$   $u_{3}$   $u_{4}$   $u_{5}$   $u_{15}$   $u_{16}$   $u_{17}$   $u_{18}$ 

 $u \in H^1(\Omega)$  such that

$$B(u,v) = \int_{\Omega} (D\nabla u + bu) \cdot \nabla v + cuv dx = f(v), \quad \forall v \in H^{1}(\Omega).$$
 (1)

Here D is  $2 \times 2$  a symmetric positive definite matrix, b is a vector, c is a number and  $f(\cdot)$  is a linear functional on  $H^1(\Omega)$ . All coefficient functions are smooth and the bilinear form  $B(\cdot,\cdot)$  satisfies the continuity condition.

For linear element function, their first order derivative are piecewise constant and the second are not well defined. Existing methods can not guarantee the convergence even on uniform meshes and it is very hard to generalize to higher order elements, so as to build a framework of analyzing Hessian recovery methods on general unstructured meshes.

Recently, Hailong Guo from University of California, Santa Barbara and Zhimin Zhang from CSRC, in collaboration with Ren Zhao from Wayne State University proposed an effective Hessian recovery strategy for the Lagrangian FEM of arbitrary order. They define  $T_h$  be a shape regular triangulation of a polygonal domain  $\widetilde{\Omega}$  with mesh size at most h and  $S_h$  be continuous finite element space of order k on  $T_h$ . Given  $u \in S_h$ , let  $G_h u \in S_h \times S_h$  be the recovered gradient using PPR. Rewrite  $G_h u$  as  $G_h u = (G_h^x u, G_h^y u)^T$ , in order to recover the Hessian matrix of u, gradient recovery operator  $G_h$  is applied to  $G_h^x u$  and  $G_h^y u$  one more time, respectively, and define the Hessian recovery operator  $H_h$  as follows

$$H_{h}u = (G_{h}(G_{h}^{x}u), G_{h}(G_{h}^{y}u)) = \begin{pmatrix} G_{h}^{x}(G_{h}^{x}u), G_{h}^{x}(G_{h}^{y}u) \\ G_{h}^{y}(G_{h}^{x}u), G_{h}^{y}(G_{h}^{y}u) \end{pmatrix}$$

The method preserves polynomials of degree k+1 on general unstructured meshes and superconvergences at a rate of O(h<sup>k</sup>) on mildly

$$(H_h^{xx}u)(z_0) = \frac{1}{36h^2}(-12u_0 + 2u_1 - 4u_2 - 4u_3 + 2u_4 - 4u_5 - 4u_6 + 4u_7 + 4u_8 + u_9 - 2u_{10} + u_{11} + 4u_{12} + 4u_{13} + 4u_{14} + u_{15} - 2u_{16} + u_{17} + 4u_{18}),$$

$$(H_h^{xy}u)(z_0) = \frac{1}{36h^2}(6u_0 - u_1 + 5u_2 - u_3 - u_4 + 5u_5 - u_6 - 2u_7 + u_8 + u_9 + u_{10} - 2u_{11} - 5u_{12} - 2u_{13} + u_{14} + u_{15} + u_{16} - 2u_{17} - 5u_{18}),$$

$$(H_h^{xx}u)(z_0) = \frac{1}{36h^2}(6u_0 - u_1 + 5u_2 - u_3 - u_4 + 5u_5 - u_6 - 2u_7 + u_8 + u_9 + u_{10} - 2u_{11} - 5u_{12} - 2u_{13} + u_{14} + u_{15} + u_{16} - 2u_{17} - 5u_{18}),$$

$$(H_h^{yy}u)(z_0) = \frac{1}{36h^2}(-12u_0 - 4u_1 - 4u_2 + 2u_3 - 4u_4 - 4u_5 + 2u_6 + u_7 - 2u_8 + u_9 + 4u_{10} + 4u_{11} + 4u_{12} + u_{13} - 2u_{14} + u_{15} + 4u_{16} + 4u_{17} + 4u_{18}),$$

structured meshes. In addition, it is proved to be ultraconvergent (two order higher) for translation invariant finite element space of any order.

#### Theorem 1(polynomial preserving property):

Let  $u \in W^{k+2}_{\infty}(K_z)$ ; then  $\|Hu - H_hu\|_{0,\infty,K_z} \le Ch^k |u|_{k+2,\infty,K_z}$ . If z is a node of translation invariant mesh and a mesh symmetric center of the involved nodes and  $u \in W^{k+3}_{\infty}(K_z)$ ; then  $|(Hu - H_hu)(z)| \le Ch^{k+1} |u|_{k+3,\infty,K_z}$ . Moreover, if  $u \in W^{k+4}_{\infty}(K_z)$  and k is an even number, then  $|(Hu - H_hu)(z)| \le Ch^{k+2} |u|_{k+4,\infty,K_z}$ .

#### Theorem 2(superconvergence on arbitrary meshes):

Suppose that the solution of (1) belongs to  $H^{k+2}(\Omega) \cap W_{\infty}^{k+1}(\Omega)$  for k=1,2,  $u_h$  be the finite element solution of (1) using  $S_h$  and  $T_h$  is a mildy unstructured mesh, then we have  $\|Hu - H_h u_h\|_{0,\Omega} \le Ch^k \|u\|_{k+2,\infty,\Omega}$ .

#### Theorem 3(ultraconvergence on translation invariant meshes):

Let all the coefficients in the bilinear operator  $B(\cdot,\cdot)$  be constant;  $\Omega_1 \subset\subset \Omega$  be separated by d=O(1); the finite element space  $S_h$ , which includes piecewise polynomials of degree k, be translation invariant in the directions required by the Hessian recovery operator  $H_h$  on  $u \in W^{k+3}_{\infty}(\Omega)$ . Then on any interior region  $\Omega_0 \subset\subset \Omega_1$ , we have  $\|Hu-H_hu_h\|_{0,\infty,\Omega_0} \leq C(\ln(1/h))^{\widetilde{r}} h^{k+1}\|_{k+3,\infty,\Omega}$ . (Here  $\widetilde{r}=1$  for linear element and  $\widetilde{r}=0$  for higher order element.)

#### References

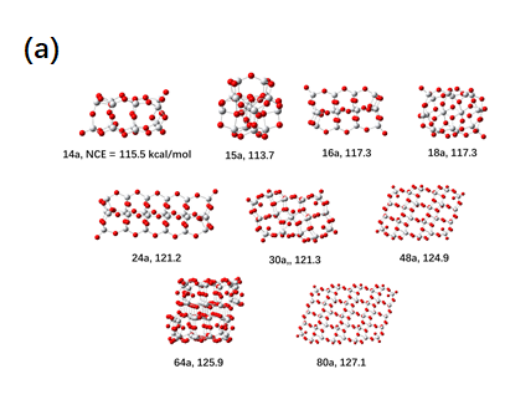
H. Guo, Z. Zhang, and R. Zhao, Hessian recovery for finite element methods. *Math. Comp.* 86(2017), No.306, 1671-1692.

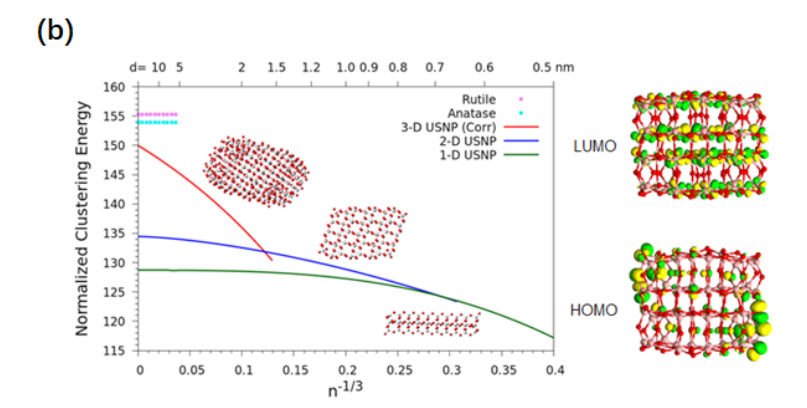
••••• 2017 ANNUAL REPORT RESEARCH HIGHLIGHTS

# MODELING THE FORMATION OF TIO<sub>2</sub> ULTRA-SMALL NANOPARTICLES

Titanium dioxide has been widely used as a heterogeneous photocatalyst for various photocatalytic oxidation and reduction reactions with many applications including water treatment and water splitting.<sup>[1]</sup> Further improvements in TiO<sub>2</sub>-based catalysts may impact solutions for major environmental and energy problems. Researchers have shown that the nanoparticle forms of TiO<sub>2</sub> exhibit better catalytic activities than does the bulk phase.<sup>[2]</sup> Recent studies also showed that the photoelectrochemical performance of TiO<sub>2</sub> nanoclusters is enhanced as the size of the nanocluster is reduced.<sup>[3]</sup> When

the particle size falls below 10 nm, the particles become the so-called ultra-small nanoparticles (USNPs) and display unique properties. [4][5] Despite that he properties of the solid, the surface, and nanoparticles of TiO<sub>2</sub> have been studied extensively, very little has been known about TiO2 USNPs. [6][7][8] It is important to predict the atomistic structures and the structure-property relationships for TiO<sub>2</sub> USNPs. An extensive range of low energy (TiO<sub>2</sub>)n clusters and USNPs (n up to 384) were predicted and validated by Chen and Dixon [9] using a novel bottom-up global optimization approach that is based on all-atom real-space calculations, and the structural evolution pathway from cluster to bulk nanoparticle was proposed (Fig. 1). This is a remarkable improvement over the previous studies on this research topic. Before this work, the largest (TiO<sub>2</sub>)n predicted was (TiO<sub>2</sub>)13 by Chen and Dixon. [10]

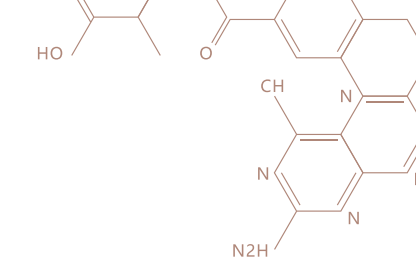




**Fig. 1.** (a) Selected global energy minima structures for (TiO<sub>2</sub>)n (b) Structural phase diagram for (TiO<sub>2</sub>)n USNPs.

To understand the structure-property relationships for the metal oxide cluster, USNP and bulk material, Chen and Dixon developed a novel fragment-based scheme (Fig. 2) [9] [11] to approximate the size-property relationships by the more computationally convenient fragment-property relationships. Surface energy densities were predicted for the surface fragments of the anatase-like USNPs using this new model. Based on the predicted surface energy densities and the partial density of states, the most catalytically active sites for the anatase-like 3-D USNPs were predicted to be the kink sites on Face-x surfaces consisting of an octahedral-Ti, the step (edge) sites between the Face-x and Face-y surfaces consisting of a square pyramidal-Ti (on Face-x), and the step sites consisting of trigonal bipyramidal Ti on the Face-y surfaces.





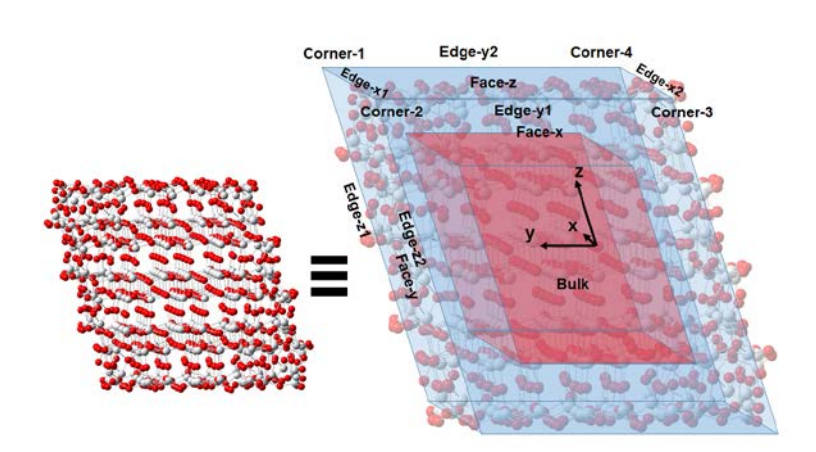


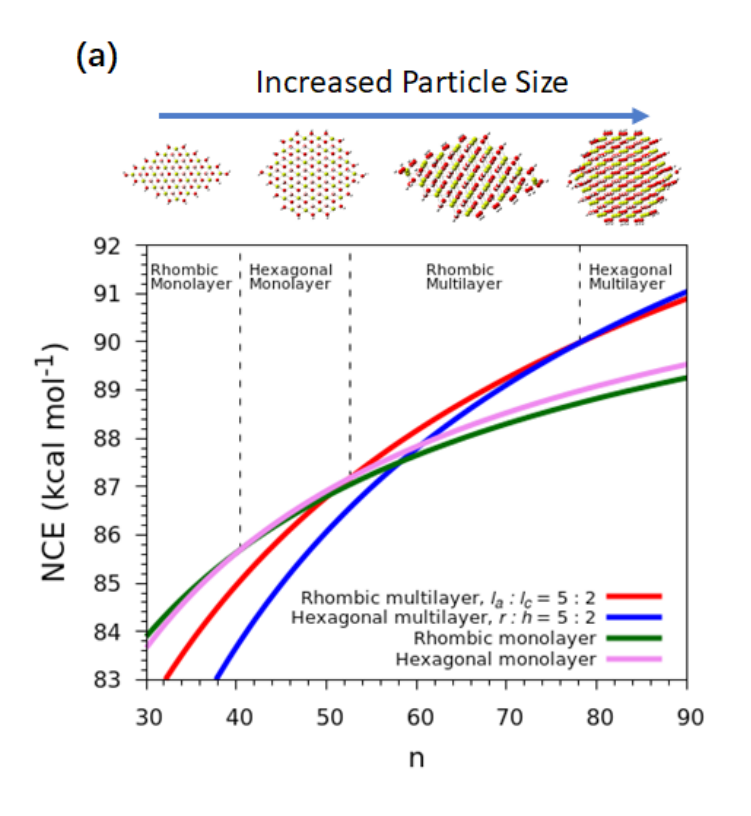
Fig. 1. Fragmentation of (TiO<sub>2</sub>)<sub>320</sub>.

Fragment Types	Surface Energy Density kcal/mol per TiO2
Corners 1-4	33.1
Edge-x1 + Edge-x2	24.5
Edge-y1 + Edge-y2	27.5
Edge-z1 + Edge-z2	24.8
Face-x	12.7
Face-y	16.2
Face-z	4.7
Bulk	0

**Table 1**. Surface energy densities for the anatase-like (TiO2)n USNP series.

In a follow-up work on the formation of brucite-related USNPs by Chen and Dixon, [11] the fragment-based energy decomposition model was further extended. The generated fragment-based thermodynamic parameters from the energy decomposition not only can be used to predict the stabilities of the fragment types, but also to predict a range of thermodynamics-related properties for the nanoparticle

series, including the structural phase diagram, ideal aspect ratio (morphology), and surface reactivities (Fig. 3). The fragment-based energy decomposition provides a "multum in parvo" way to compute the thermodynamic properties of large nanoparticles with CCSD(T)-level of high accuracy at a minimal computational cost. The high accuracy is achieved by choose appropriate DFT functional and basis set for energy calculations that produce energy landscape very close to the CCSD(T) results for the small clusters (of the benchmark set) and meanwhile produce the correct normalized dissociation energy at the thermodynamic limit.



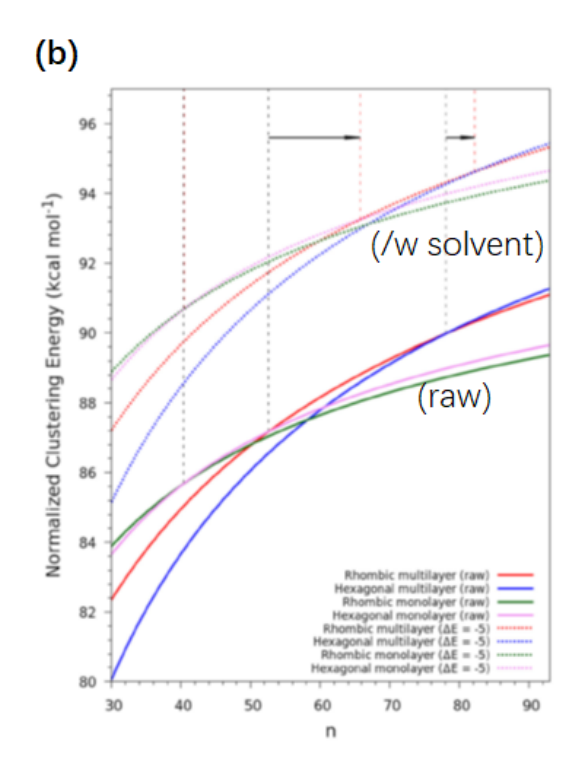


**Fig. 2.** (a) Structural phase diagram for brucite-related  $(Mg(OH)_2)_n$  USNPs. (b) Solvent effects on the structural phase diagram for  $(Mg(OH)_2)_n$  USNPs.

#### References

- [1] A. Fujishima, K. Honda, Nature, 1972, 238, 37-38.
- [2] H. Han, R. Ba, Ind. Eng. Chem. Res., 2009, 48, 2891-2898.
- [3] S. Srivastava, J. P. Thomas, Md. A. Rahman, M. Abd-Ellah, M. Mahapatra, D. Pradhan, N. F. Heinig, K. T. Leung, ACS Nano, 2014, 8, 11891-11898.
- [4] O. Regan, M. Grätzel, Nature, 1991, 353, 737-740.
- [5] M. R. Hoffmann, S. T. Martin, W. Choi, D. W. Bahnemann, Chem. Rev., 1995, 95, 69–96.
- [6] M. Amin, J. Tomko, J. J. Naddeo, R. Jimenez, D. M. Bubb, M. Steiner, J. Fitz-Gerald, S. M. O'Malley, Applied Surface Science, 2015, 348, 30-37.
- [7] Q. Wu, F. Huang, M. Zhao, J. Xu, J. Zhou, Y. Wang, Nano Energy, 2016, 24, 63-71.
- [8] N. Bayat, V. R. Lopes, J. Schölermann, L. D. Jensen, S. Cristobal, Biomaterials, 2015, 63, 1-13.
- [9] M. Chen, D. A. Dixon, Nanoscale, 2017, 9, 7143-7162.
- [10] M. Chen, D. A. Dixon, J. Chem. Theory Comput. 2013, 9, 3189-3200.
- [11] M. Chen, D. A. Dixon, J. Phys. Chem. C, 2017, 121, 21750-21762.



# HO O CH N

# MULTISCALE STUDY OF PLASMONIC SCATTERING AND LIGHT TRAPPING EFFECT IN SILICON NANOWIRE ARRAY SOLAR CELLS

Nanometallic structures that support surface plasmons provide new ways to confine light at deep-subwavelength scales. Plasmonics has emerged as a new technology with expanding applications in materials and device research. Experiments have demonstrated that the strong field localization of surface plasmons can effectively increase the optical path length and achieve light confinement in nanostructured solar cells. In this work, the effect of light scattering in nanowire array solar cells is studied by a multiscale approach combining classical electromagnetic (EM) and quantum mechanical simulations. A photovoltaic device is constructed by integrating a silicon nanowire array with a plasmonic silver nanosphere. (Figure 1) The light scatterings by plasmonic element and nanowire array are obtained via classical EM simulations, while current-voltage characteristics and optical properties of the nanowire cells are evaluated quantum mechanically.

**Fig. 2.** Current density per nanowire versus applied voltage of the photovoltaic devices with different numbers of surrounding nanowires under illumination of monochromatic light frequency of 3.4 eV.

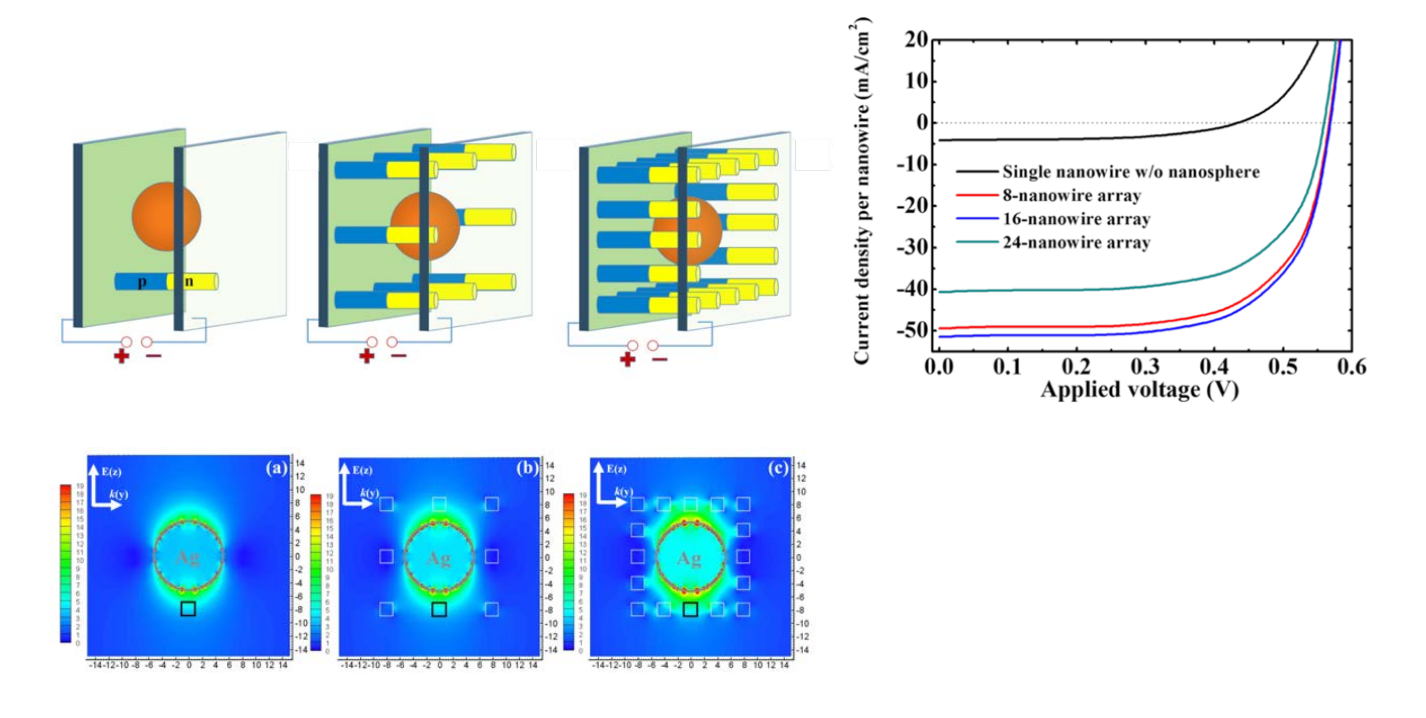


**Fig. 1.** Field enhancement distribution for (a) the single nanowire solar cell, (b) the 8-nanowire array solar cell, and (c) the 16-nanowire array solar cell. Squares represent the regions where the nanowire photoactive components are located.

In this work, ChiYung Yam's group in CSRC in collaboration with Lingyi Meng in Xiamen University applied a multiscale QM/EM method[1,2] to study the performance of plasmonic devices that contain vertically aligned silicon nanowire arrays and silver nano- spheres.

[3] Combining a classical EM description of plasmonic nanostructure and QM treatment of photoactive component, device performance and optical parameters of the nanowire array-based photovoltaic devices are determined. The light confinement effect due to nanowire array geometry and metallic nanoparticle is first obtained, and the actual device performance is then simulated quantum mechanically. The incorporation of metallic nanosphere leads to enhancement of light absorption in the device and results in dramatic improvement of PCE. The light trapping effect due to the nanowire array architecture was further investigated. Remarkably, it is shown that there exists an optimal nanowire number density in terms of optical confinement and solar cell PCE. To further improve the performance, plasmonic structures with different materials, shapes, sizes, and geometrical arrangements can be used for broadband plasmonic absorption. The present work demonstrates the multiscale QM/EM method as an efficient simulation tool for studying nanoscale optoelectronic devices. This is useful for understanding the mechanism of their energy conversion and helpful for improving the design of next- generation solar cells.

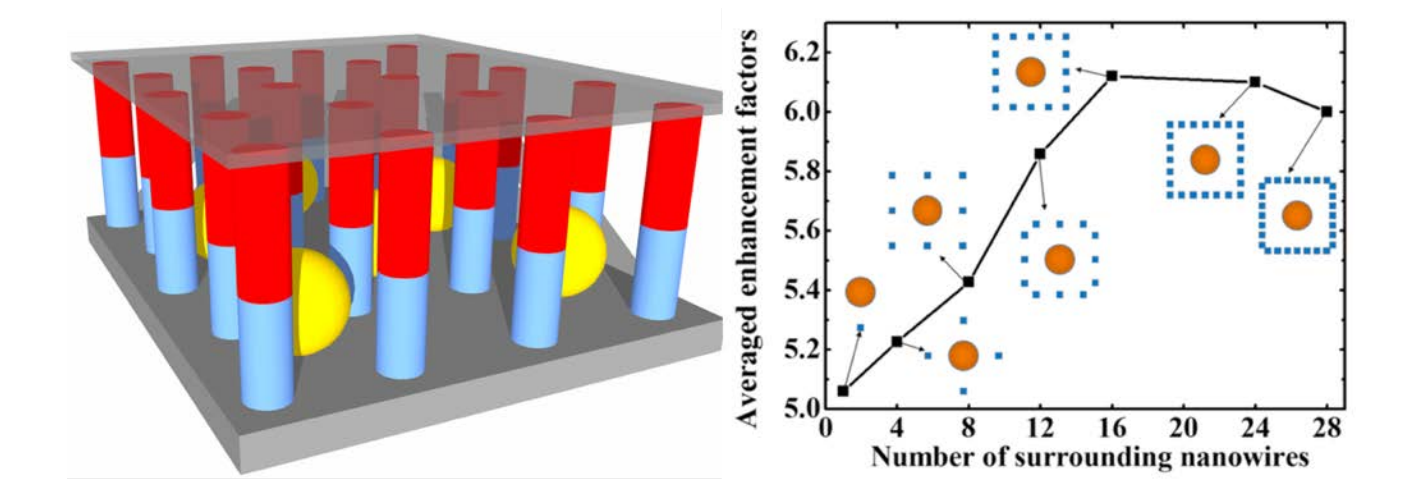
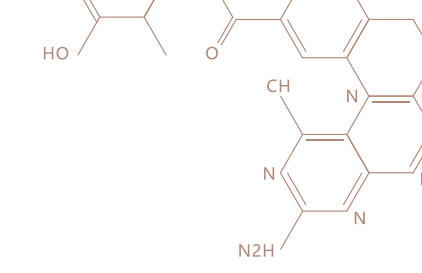


**Fig. 3.** Schematic diagram of silicon nanowire solar cells. (left) Averaged enhancement factors of nanowire solar cells marked in Figure 2 for devices with different nanowire densities. (right).

#### References

- [1] Lingyi Meng, ChiYung Yam, Yu Zhang, Rulin Wang and GuanHua Chen J. Phys. Chem. Lett. 6, 4410 (2015).
- [2] ChiYung Yam, Lingyi Meng, Yu Zhang and GuanHua Chen, Chem. Soc. Rev. 44, 1763 (2015).
- [3] Lingyi Meng, Yu Zhang and ChiYung Yam, J. Phys. Chem. Lett. 8, 571 (2017).





# 科研项目 PROJECTS

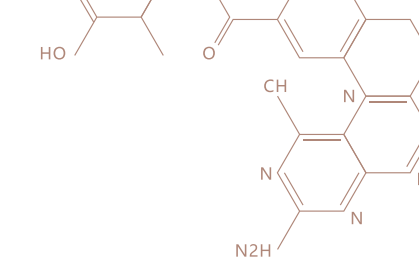
2017年中心承担中央组织部、科学技术部、国家基金委、博士后科学基金, 以及中物院等在研项目共92项,科研合同总经费已超过1.4亿元。2017年结题项目 26项,2018年新启动项目17项。

In the year 2017, the number of on-going projects in CSRC reaches 92 in total, which are supported respectively from the Ministry of Science and Technology of China, National Natural Science Foundation of China, China Postdoctoral Science Foundation and so on. The amount of funding reaches over 140 million Chinese Yuan. 26 projects have been completed in 2017 and 17 new projects will be started in 2018.

#### 在研的基金项目

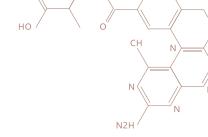
序号	项 目 负责人	职称	经费来源	项目类别	项目名称	起止时间
1	孙昌璞	教授	科学技术部	重大科学研究计划	固体量子计算的 器件物理基础	2014.01 - 2018.12
2	游建强	教 授	科学技术部	国家重点研发计划	高品质腔与固体量子态的耦 合及其量子调控	2016.07 - 2021.06
3	赵楠	特聘研究员	科学技术部	青年科学家 专题项目	自旋及其复合系统的量子操 纵与相干集成研究	2014.01 - 2018.12
4	魏苏淮	教 授	工业和信 息化部	国家重点研发计划	环境友好型高稳定性太阳能 电池的材料设计与器件研究	2016.07 - 2020.06
5	林海青	教授	国家自然科学 基金委员会	联合基金项目 中心项目	科学计算与物理 系统模拟研究	2015.02 - 2018.12
6	汤雷翰	教授	国家自然科学 基金委员会	联合基金项目 重点项目	复杂自适应物质的 跨尺度计算平台	2015.01 - 2018.12
7	张智民	教授	国家自然科学 基金委员会	重大研究计划 重点项目	强非线性偏微分方程基于梯 度重构的新型算法	2015.01 - 2018.12
8	王奇	教 授	国家自然科学 基金委员会	重大研究计划 重点项目	多相物质体系的计算建模算 法设计与数值分析	2017.01 - 2019.12

序号	项 目 负责人	职称	经费来源	项目类别	项目名称	起止时间
9	孙昌璞	教授	国家自然科学 基金委员会	重点项目	有限开放系统的量子相干效 应及其应用	2016.01 - 2020.12
10	魏苏淮	教 授	国家自然科学 基金委员会	重点项目	透明导电体的物理机理研究 与新材料设计	2017.01 - 2021.12
11	汤雷翰	教授	国家自然科学 基金委员会	重点项目	活性系统的热耗散及 长时动力学	2017.01 - 2021.12
12	张智民	教授	国家自然科学 基金委员会	面上项目	若干具有弱导数的新型计算 方法的梯度重构	2015.01 - 2018.12
13	王奇	教授	国家自然科学 基金委员会	面上项目	活性的、各向异性流体的数 学建模分析与计算	2016.01 - 2019.12
14	魏苏淮	教授	国家自然科学 基金委员会	面上项目	复杂半导体清洁能源材料 的理论研究	2017.01 - 2020.12
15	黄兵	特聘研究员	国家自然科学 基金委员会	面上项目	晶格匹配的层状合金做为新 型高效光源材料的理论探索	2016.01 - 2019.12
16	Stefano Chesi	特聘研究员	国家自然科学 基金委员会	面上项目	半导体纳米结构的 空穴自旋的相干性质	2016.01 - 2019.12
17	徐辛亮	特聘研究员	国家自然科学 基金委员会	面上项目	宏观热涨落体系的 非平衡态涨落定理	2016.01 - 2019.12
18	刘海广	特聘研究员	国家自然科学 基金委员会	面上项目	X射线自由电子激光在单分 子成像中的应用及相关计算 方法与理论研究	2016.01 - 2019.12
19	管鹏飞	特聘研究员	国家自然科学 基金委员会	面上项目	非晶合金中β-弛豫结构起源 的计算模拟研究	2016.01 - 2019.12
20	刘利民	特聘研究员	国家自然科学 基金委员会	面上项目	水溶液条件下光电催化材料 理论设计及其性能优化	2016.01 - 2019.12
21	胡广辉	特聘研究员	国家自然科学 基金委员会	面上项目	基于固定入射方向的反媒介 理论和算法研究	2017.01 - 2020.12
22	丁阳	特聘研究员	国家自然科学 基金委员会	面上项目	波状运动中的力矩规律在解 释生物驱动控制和设计机器 人柔性材料中的应用	2017.01 - 2020.12
23	张东波	特聘研究员	国家自然科学 基金委员会	面上项目	低维材料电子性质的应变调 控:自洽密度泛函紧束缚广 义布洛赫方法	2017.01 - 2020.12
24	任志勇	特聘研究员	国家自然科学 基金委员会	面上项目	纳米等离子体太阳能电池的 光学-电学相结合研究	2017.01 - 2020.12
25	周崇斌	特聘副 研究员	国家自然科学 基金委员会	面上项目	张量积投影态在变分蒙特卡 罗方法的理论及应用	2015.01 - 2018.12



序号	项 目 负责人	职称	经费来源	项目类别	项目名称	起止时间
26	Rubem Mondaini	特聘副 研究员	国家自然科学 基金委员会	面上项目	关联超流体中的 赝能隙相变研究	2017.01 - 2020.12
27	Mondaini Rubem	特聘副 研究员	国家自然科学 基金委员会	外国青年学者 基金项目	Many-body localization in full fermionic systems and its applications to quantum gases	2017.01 - 2018.12
28	BANDARU SATEESH	博士后	国家自然科学 基金委员会	外国青年学者 基金项目	Computational Modeling of Metal oxide Surface-Photo catalysts for Water Splitting reactions	2017.01 - 2018.12
29	曹外香	博士后	国家自然科学 基金委员会	青年科学基金项目	非线性双曲方程的间断有限 元超收敛分析和应用	2016.01 - 2018.12
30	李振华	博士后	国家自然科学 基金委员会	青年科学基金项目	密度矩阵级联方程在开放量 子体系中的应用研究	2016.01 - 2018.12
31	张书辉	博士后	国家自然科学 基金委员会	青年科学基金项目	二维材料中局域自旋间接耦 合的全电调控的理论研究	2016.01 - 2018.12
32	曹腾飞	博士后	国家自然科学 基金委员会	青年科学基金项目	黑磷 - 氮化硼杂化异质结光 催化特性的第一性原理研究	2016.01 - 2018.12
33	杜宇	博士后	国家自然科学 基金委员会	青年科学基金项目	求解高波数 Helmholtz 问题的PPR方法和弱有限元方法	2017.01 - 2019.12
34	胡自玉	工程师	国家自然科学 基金委员会	青年科学基金项目	二维材料的新型结构相和其 边缘态的量子调控的 理论研究	2017.01 - 2019.12
35	刘卯鑫	博士后	国家自然科学 基金委员会	青年科学基金项目	多量子比特与玻色场耦合系 统量子相变研究	2017.01 - 2019.12
36	李俊	博士后	国家自然科学 基金委员会	青年科学基金项目	核磁共振体系的量子控制模 型及其应用	2017.01 - 2019.12
37	尚宝双	博士后	国家自然科学 基金委员会	青年科学基金项目	金属玻璃塑性局域重组方向 敏感性研究	2017.01 - 2019.12
38	邓小龙	特聘研究员	中国工程物理 研究院	院长基金	陡峭界面可压缩多相流计算 流体力学方法发展与应用	2015.10 - 2018.09
39	赵兴举	博士后	中国博士后 科学基金	博士后创新人才 支持计划	半导体薄膜与衬底相互作用 下电子结构的原子级计算	2017.06 - 2019.05
40	曹外香	博士后	中国博士后 科学基金	特别资助	对流扩散方程的间断有限元 方法的超收敛分析和应用	2016.07 - 2018.06
41	王艺敏	博士后	中国博士后 科学基金	特别资助	超强和深度强耦合电路QED 系统的量子调控	2016.07 - 2018.06
42	唐振坤	博士后	中国博士后 科学基金	特别资助	高浓度电解质中锂离子反常超 快传输机理的第一原理研究	2016.07 - 2018.06
43	邵 慧	博士后	中国博士后 科学基金	特别资助	二维量子自旋系统的准粒子 激发和动力学性质的研究	2017.06 - 2019.05

序号	项 目 负责人	职称	经费来源	项目类别	项目名称	起止时间
44	周建伟	博士后	中国博士后 科学基金	特别资助	Cahn-Hilliard方程约束最优控制问题的谱(元)方法研究	2017.06 - 2019.05
45	邵 慧	博士后	中国博士后 科学基金	面上一等资助	随机数值解析延拓方法和量子 自旋系统动力学性质的研究	2016.11 - 2018.10
46	卞 磊	博士后	中国博士后 科学基金	面上二等资助	狄拉克方程的准确数值边界 条件的研究	2016.11 - 2018.10
47	时华良	博士后	中国博士后 科学基金	面上二等资助	金属纳米结构共振模的计算	2016.11 - 2018.10
48	苏春梅	博士后	中国博士后 科学基金	面上二等资助	Zakharov方程在亚音速极限 域下的数值方法及误差分析	2016.11 - 2018.10
49	熊伟	博士后	中国博士后 科学基金	面上二等资助	基于纳米机械振子的固态混 合量子器件的理论研究	2016.11 - 2018.10
50	袁 浩	博士后	中国博士后 科学基金	面上二等资助	新型耦合电路 QED系统中 光子的非平衡量子相	2016.11 - 2018.10
51	康 雷	博士后	中国博士后 科学基金	面上二等资助	狄拉克材料在太赫兹光电技 术上的应用	2016.11 - 2018.10
52	晋力京	博士后	中国博士后 科学基金	面上二等资助	多模光力学系统的非线性动 力学研究	2016.11 - 2018.10
53	张凯	博士后	中国博士后 科学基金	面上二等资助	超稳非晶态Sb2Se3薄膜的稳定性机制及其光学性能研究	2016.11 - 2018.10
54	李晓	博士后	中国博士后 科学基金	面上二等资助	非局部相场方程的能量稳定 且渐近相容的数值方法	2017.05 - 2019.04
55	卢键方	博士后	中国博士后 科学基金	面上二等资助	非局部扩散模型的间断有限 元模拟与分析	2017.05 - 2019.04
56	王 燕	博士后	中国博士后 科学基金	面上二等资助	弯曲基底上薄膜固态去湿问 题的数学模型与数值模拟	2017.05 - 2019.04
57	周建伟	博士后	中国博士后 科学基金	面上二等资助	基于广义Jacobi多项式谱元 方法的后验误差研究	2017.05 - 2019.04
58	秦伟	博士后	中国博士后 科学基金	面上二等资助	腔QED系统中基于耗散机制 实现基本量子门的研究	2017.05 - 2019.04
59	吴 威	博士后	中国博士后 科学基金	面上二等资助	量子耗散系统动力学的研究	2017.05 - 2019.04
60	胡麟	博士后	中国博士后 科学基金	面上二等资助	低维材料中缺陷诱发的载流子 非辐射性复合的新物理机制	2017.05 - 2019.04
61	李 季	博士后	中国博士后 科学基金	面上二等资助	相位恢复数值算法研究: 凸优化与低秩模型	2017.11 - 2019.10
62	董海霞	博士后	中国博士后 科学基金	面上二等资助	三维Stokes界面问题的高效 数值方法及其理论分析	2017.11 - 2019.10



序号	项 目 负责人	职称	经费来源	项目类别	项目名称	起止时间
63	王鹏德	博士后	中国博士后 科学基金	面上二等资助	两类非局部发展方程的保结 构数值方法	2017.11 - 2019.10
64	王建峰	博士后	中国博士后 科学基金	面上二等资助	设计并寻找理想的拓扑半金 属和拓扑超导材料	2017.11 - 2019.10
65	江 成	博士后	中国博士后 科学基金	面上二等资助	宇称 - 时间 - 对称的光力系 统中的非线性效应研究	2017.11 - 2019.10

#### 2018年新启动的基金项目

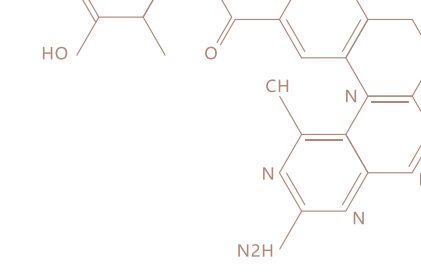
序号	项 目 负责人	职称	经费来源	项目类别	项目名称	起止时间
1	林海青	教授	国家自然科学 基金委员会	重点项目	海森堡模型和 Kitaev 模型的 元激发、激发谱和量子相变	2018.01 - 2022.12
2	庞国飞	博士后	国家自然科学 基金委员会	青年科学基金项目	分数阶导数对流-弥散方程 参数识别的多重精度高斯过 程回归算法	2018.01 - 2020.12
3	胡 麟	博士后	国家自然科学基金委员会	青年科学基金项目	非平衡态下二维宽带隙半导体中缺陷和掺杂性质的研究 和调控	2018.01 - 2020.12
4	袁少杰	博士后	国家自然科学 基金委员会	青年科学基金项目	超导量子比特的弱测量及其 量子力学时间对称性的研究	2018.01 - 2020.12
5	康 雷	博士后	国家自然科学 基金委员会	青年科学基金项目	典型狄拉克材料的非线性光 学性质的理论研究	2018.01 - 2020.12
6	张春芳	博士后	国家自然科学 基金委员会	青年科学基金项目	芳香烃超导材料制备中涉及 的化学反应的理论研究	2018.01 - 2020.12
7	吴 威	博士后	国家自然科学 基金委员会	青年科学基金项目	量子开放系统动力学的 数值研究	2018.01 - 2020.12
8	张闻钊	博士后	国家自然科学 基金委员会	青年科学基金项目	开放量子系统中光机械振子 辐射压冷却的理论研究	2018.01 - 2020.12
9	胡淑贤	特聘副 研究员	国家自然科学基金委员会	青年科学基金项目	含氮冠醚三价次锕系离子和 镧系离子配合物成键及电子 结构的理论研究	2018.01 - 2020.12
10	张继伟	特聘研究员	国家自然科学 基金委员会	面上项目	多尺度非局部模型的理论分 析和高效数值方法	2018.01 - 2021.12
11	蔡勇勇	特聘研究员	国家自然科学 基金委员会	面上项目	高振荡色散方程的多尺度计 算方法及分析	2018.01 - 2021.12



序号	项 目 负责人	职称	经费来源	项目类别	项目名称	起止时间
12	杨文	副教授	国家自然科学 基金委员会	面上项目	适用于连续模型的通用格林 函数方法及载流子局域输运 和干涉现象的理论研究	2018.01 - 2021.12
13	游建强	教授	国家自然科学基金委员会	面上项目	超越玻恩-马科夫近似的固 态量子比特系统的量子动力 学研究	2018.01 - 2021.12
14	高 翔	特聘副 研究员	国家自然科学 基金委员会	面上项目	低能电子-离子散射过程中 的 Breit 效应理论研究	2018.01 - 2021.12
15	李 勇	副教授	国家自然科学 基金委员会	面上项目	光力系统中光学非互易性传 输的理论研究	2018.01 - 2021.12
16	喻 进	特聘研究员	国家自然科学 基金委员会	面上项目	蛋白因子和分子机器在DNA 上的信号探测和信息识别	2018.01 - 2021.12
17	胡淑贤	特聘副 研究员	中国工程物理 研究院	院长基金	锕系化合物的多组态 量子化学研究	2018.01 - 2020.12

#### 2017年结题的基金项目

序号	项 目 负责人	职称	经费来源	项目类别	项目名称	起止时间
1	游建强	教授	国家自然科学 基金委员会	联合基金项目 重点项目	超导量子比特的优化与混合 量子器件的研究	2014.01 - 2017.12
2	朱诗尧	教 授	国家自然科学 基金委员会	联合基金项目 重点项目	人工微结构中宏观量子效应 的研究	2014.01 - 2017.12
3	李 勇	特聘研究员	国家自然科学 基金委员会	优秀青年科学 基金项目	量子光学	2015.01 - 2017.12
4	李增朝	博士后	国家自然科学 基金委员会	青年科学基金项目	基于马约拉纳束缚态的杂化 固态量子体系的量子动力学 研究	2015.01 - 2017.12
5	李睿	博士后	国家自然科学 基金委员会	青年科学基金项目	具有强自旋轨道耦合的半导 体量子点中单量子态的调控	2015.01 - 2017.12
6	王治海	博士后	国家自然科学 基金委员会	青年科学基金项目	耦合量子光学体系的 相干控制	2015.01 - 2017.12
7	赵楠	特聘研究员	国家自然科学 基金委员会	面上项目	基于金刚石"氮 - 空位"中 心的腔量子电动力学研究	2014.01 - 2017.12
8	Ahrens Sven	博士后	国家自然科学基金委员会	外国青年学者 基金项目	Investigation of the angular momentum conservation of light in photon-spin interactions	2017.01 - 2017.12



序	项 目	职称	经费来源	项目类别	项目名称	起止时间
号	负责人		红		<b>坝日石</b> 柳	佐江即间
9	Cadez Tilen	博士后	国家自然科学 基金委员会	外国青年学者 基金项目	Dynamical correlation functions of 1D correlated electron models	2017.01 - 2017.12
10	曹外香	博士后	中国博士后 科学基金	面上一等资助	高阶波动方程的局部间断有 限元超收敛研究	2015.05 - 2017.06
11	陈丽贞	工程师	中国博士后 科学基金	面上一等资助	不可压流体的非结构网格谱 元法并行计算	2015.11 - 2017.10
12	林恒福	博士后	中国博士后 科学基金	面上一等资助	磷烯的单双层侧向异质结特 性和磁各向异性的理论研究	2015.05 - 2017.04
13	彭 枫	博士后	中国博士后 科学基金	面上一等资助	高压下新型高氮含能 材料设计	2015.05 - 2017.04
14	王 达	博士后	中国博士后 科学基金	面上一等资助	磷烯的掺杂及其异质结构的 电化学性能研究	2015.05 - 2017.04
15	郑晓军	博士后	中国博士后 科学基金	面上一等资助	近邻库仑相互作用对FeSe中 磁性和超导电性的影响	2015.05 - 2017.04
16	苏山河	博士后	中国博士后 科学基金	面上二等资助	光驱动量子热机中的量子相 干效应及其应用研究	2015.11 - 2017.10
17	王艺敏	博士后	中国博士后 科学基金	面上二等资助	超强耦合系统和量子 Rabi 模型的几个问题研究	2015.11 - 2017.10
18	杨立平	博士后	中国博士后 科学基金	面上二等资助	强耦合自旋环境中中心自旋 退相干理论研究	2015.11 - 2017.10
19	张登科	博士后	中国博士后 科学基金	面上二等资助	基于磁振子的量子 变光转换器	2015.11 - 2017.10
20	杜宇	博士后	中国博士后 科学基金	面上二等资助	求解高波数亥姆霍兹问题的 数值方法的误差分析	2015.05 - 2017.04
21	龚跃政	博士后	中国博士后 科学基金	面上二等资助	保结构算法在多相流数值模 拟中的应用理论基础研究	2015.05 - 2017.04
22	张禧征	博士后	中国博士后 科学基金	面上二等资助	基于多体长程相互作用系统 的量子态调控与探测的研究	2015.05 - 2017.04
23	高飞	博士后	中国博士后 科学基金	面上二等资助	纳米尺度甲烷的活化与转化	2015.05 - 2017.04
24	王振华	博士后	中国博士后 科学基金	面上二等资助	单轴压力下石墨烯及类石墨 烯材料拓扑超导态的研究	2015.05 - 2017.04
25	宋文雄	博士后	中国博士后 科学基金	面上二等资助	Ge2Sb2Te5 相变存储材料的晶体相结构及其相变机理研究	2015.05 - 2017.04
26	符 凯	博士后	中国博士后 科学基金	面上二等资助	过冷流动沸腾的 传热机理研究	2015.05 - 2017.04



# 发表论文 TIONS

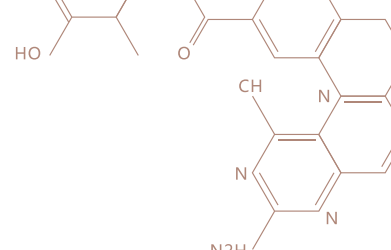
截至2017年底,中心合计发表论文约426篇 (被SCI收录408篇),其中包括第一单位及通讯作者第一单位发表论文213篇,其他合作论文213篇。在中心2017年发表的论文中,ESI高被引论文9篇,热点论文2篇。部分研究成果获得国际认可被著名期刊进行专门介绍或受邀撰写综述文章,部分发表文章被当期杂志作为封面文章或者亮点工作进行推介。

In the year 2017, CSRC published 426 papers (408 SCI-indexed papers). Among them, 213 papers had first or corresponding authors affiliated with CSRC, 9 are ESI Highly Cited Papers, 2 are ESI Hot Papers.

#### 物理系统模拟研究部

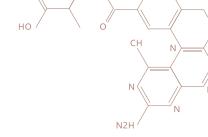
#### SIMULATION OF PHYSICAL SYSTEMS DIVISION

Dielectric nanoresonators for light manipulation; Yang, Zhong-Jian; Jiang, Ruibin; Zhuo, Xiaolu; Xie, Ya-Ming; 1 Wang, Jianfang; Lin, Hai-Qing; PHYSICS REPORTS-REVIEW SECTION OF PHYSICS LETTERS, 701 (2017) Structural and elastic properties of zinc-blende and wurtzite InN1-xBix alloys; Zhang, Min; Zhang, Chunfang; 2 Liang, Dan; Zhang, Ru; Lu, Pengfei; Wang, Shumin; JOURNAL OF ALLOYS AND COMPOUNDS, 708 (2017) Eigenstate thermalization in the two-dimensional transverse field Ising model. II. Off-diagonal matrix elements of 3 observables; Mondaini, Rubem; Rigol, Marcos; PHYSICAL REVIEW E, 96, 012157 (2017) Quantum-enhanced microscopy with binary-outcome photon counting; Jin, G. R.; Yang, W.; Sun, C. P.; 4 PHYSICAL REVIEW A, 95, 013835 (2017) Quantum many-body theory for electron spin decoherence in nanoscale nuclear spin baths; Yang, Wen; Ma, Wen-5 Long; Liu, Ren-Bao; REPORTS ON PROGRESS IN PHYSICS, 80, 016001 (2017) Fisher information of a squeezed-state interferometer with a finite photon-number resolution; Liu, P.; Wang, P.; 6 Yang, W.; Jin, G. R.; Sun, C. P.; PHYSICAL REVIEW A, 95, 023824 (2017) Effects of counter-rotating-wave terms on the non-Markovianity in quantum open systems; Wu, Wei; Liu, Maoxin; PHYSICAL REVIEW A, 96, 032125 (2017) Robustness of edge states in topological quantum dots against global electric field; Ou, Jin-Xian; Zhang, Shu-Hui; 8 Liu, Ding-Yang; Wang, Ping; Yang, Wen; JOURNAL OF APPLIED PHYSICS, 122, 034307 (2017)



	NO.
9	Focusing RKKY interaction by graphene P-N junction; Zhang, Shu-Hui; Zhu, Jia-Ji; Yang, Wen; Chang, Kai; 2D MATERIALS, 4, 035005 (2017)
10	Many-body self-localization in a translation-invariant Hamiltonian; Mondaini, Rubem; Cai, Zi; PHYSICAL REVIEW B, 96, 035153 (2017)
11	Nearly Deconfined Spinon Excitations in the Square-Lattice Spin-1/2 Heisenberg Antiferromagnet; Shao, Hui; Qin, Yan Qi; Capponi, Sylvain; Chesi, Stefano; Meng, Zi Yang; Sandvik, Anders W.; PHYSICAL REVIEW X, 7, 041072 (2017)
12	Quantum Zeno and anti-Zeno effects in quantum dissipative systems; Wu, Wei; Lin, Hai-Qing; PHYSICAL REVIEW A, 95, 042132 (2017)
13	Hyperhoneycomb boron nitride with anisotropic mechanical, electronic, and optical properties; Yu, Jin; Qu, Lihua; van Veen, Edo; Katsnelson, Mikhail I.; Yuan, Shengjun; PHYSICAL REVIEW MATERIALS, 1, 045001 (2017)
14	Structural and antiferromagnetic properties of Sm-doped chrysene; Wang, Xiao-Hui; Zhong, Guo-Hua; Han, Jia-Xing; Chen, Xiao-Jia; Lin, Hai-Qing; AIP ADVANCES, 7, 055707 (2017)
15	Frequency-renormalized multipolaron expansion for the quantum Rabi model; Cong, Lei; Sun, Xi-Mei; Liu, Maoxin; Ying, Zu-Jian; Luo, Hong-Gang; PHYSICAL REVIEW A, 95, 063803 (2017)
16	Magnetism, transport, and thermodynamics in two-dimensional half-filled Hubbard superlattices; Mondaini, Rubem; Paiva, Thereza; PHYSICAL REVIEW B, 95, 075142 (2017)
17	General Green's function formalism for layered systems: Wave function approach; Zhang, Shu-Hui; Yang, Wen; Chang, Kai; PHYSICAL REVIEW B, 95, 075421 (2017)
18	Pure dephasing of single Mn spin in semiconductor quantum dots; Liu, Dingyang; Lai, Wenxi; Yang, Wen; PHYSICAL REVIEW B, 96, 075443 (2017)
19	2 pi-flux loop semimetals; Li, Linhu; Chesi, Stefano; Yin, Chuanhao; Chen, Shu; PHYSICAL REVIEW B, 96, 081116 (2017)
20	The asymmetric quantum Rabi model in the polaron picture; Liu, Maoxin; Ying, Zu-Jian; An, Jun-Hong; Luo, Hong-Gang; Lin, Hai-Qin; JOURNAL OF PHYSICS A-MATHEMATICAL AND THEORETICAL, 50, 084003 (2017)
21	Confinement in the Bulk, Deconfinement on the Wall: Infrared Equivalence between Compactified QCD and Quantum Magnets; Sulejmanpasic, Tin; Shao, Hui; Sandvik, Anders W.; Unsal, Mithat; PHYSICAL REVIEW LETTERS, 119, 091601 (2017)
22	Optimization of STIRAP-based state transfer under dissipation; Ying-Dan Wang, Rong Zhang, Xiao-Bo Yan, Stefano Chesi; NEW JOURNAL OF PHYSICS, 19, 093016 (2017)
23	Thermal conductivity from phonon quasiparticles with subminimal mean free path in the MgSiO3 perovskite; Zhang, Dong-Bo; Allen, Philip B.; Sun, Tao; Wentzcovitch, Renata M.; PHYSICAL REVIEW B, 96, 100302 (2017)
24	Chiral topological insulating phases from three-dimensional nodal loop semimetals; Li, Linhu; Yin, Chuanhao; Chen, Shu; Araujo, Miguel A. N.; PHYSICAL REVIEW B, 95, 121107 (2017)

25	Dynamic localization of two electrons in AC-driven triple quantum dots and quantum dot shuttles; Qu, Jin-Xian; Duan, Su-Qing; Yang, Ning; CHINESE PHYSICS B, 26, 127308 (2017)
26	Dynamical localization and the effects of aperiodicity in Floquet systems; Cadez, Tilen; Mondaini, Rubem; Sacramento, Pedro D.; PHYSICAL REVIEW B, 96, 144301 (2017)
27	Premelting hcp to bcc Transition in Beryllium; Lu, Y.; Sun, T.; Zhang, Ping; Zhang, P.; Zhang, DB.; Wentzcovitch, R. M.; PHYSICAL REVIEW LETTERS, 118, 145702 (2017)
28	Charge transport in hybrid halide perovskites; Zhang, Mingliang; Zhang, Xu; Huang, Ling-Yi; Lin, Hai-Qing; Lu, Gang; PHYSICAL REVIEW B, 96, 195203 (2017)
29	Effective Zeeman splitting in bent lateral heterojunctions of graphene and hexagonal boron nitride: A new mechanism towards half-metallicity; Yue, Ling; Seifert, Gotthard; Chang, Kai; Zhang, Dong-Bo; PHYSICAL REVIEW B, 96, 201403 (2017)
30	Quantum criticality of spinons; He, Feng; Jiang, Yuzhu; Yu, Yi-Cong; Lin, HQ.; Guan, Xi-Wen; PHYSICAL REVIEW B, 96, 220401 (2017)
31	Universal Scaling and Critical Exponents of the Anisotropic Quantum Rabi Model; Liu, Maoxin; Chesi, Stefano; Ying, Zu-Jian; Chen, Xiaosong; Luo, Hong-Gang; Lin, Hai-Qing; PHYSICAL REVIEW LETTERS, 119, 220601 (2017)
32	Generalized Stoner criterion and versatile spin ordering in two-dimensional spin-orbit coupled electron systems; Liu, Weizhe Edward; Chesi, Stefano; Webb, David; Zulicke, U.; Winkler, R.; Joynt, Robert; Culcer, Dimitrie; PHYSICAL REVIEW B, 96, 235425 (2017)
33	Inhomogeneous strain-induced half-metallicity in bent zigzag graphene nanoribbons; Dong-Bo Zhang; Su-Huai Wei; NPJ COMPUTATIONAL MATERIALS, 3 (2017)
34	Effective Rheology of Two-Phase Flow in Three-Dimensional Porous Media: Experiment and Simulation; Sinha, Santanu; Bender, Andrew T.; Danczyk, Matthew; Keepseagle, Kayla; Prather, Cody A.; Bray, Joshua M.; Thrane, Linn W.; Seymour, Joseph D.; Codd, Sarah L.; Hansen, Alex; TRANSPORT IN POROUS MEDIA, 119 (2017)
35	A Monte Carlo Algorithm for Immiscible Two-Phase Flow in Porous Media; Savani, Isha; Sinha, Santanu; Hansen, Alex; Bedeaux, Dick; Kjelstrup, Signe; Vassvik, Morten; TRANSPORT IN POROUS MEDIA, 116 (2017)
36	Two-dimensional As1-XPX binary compounds: Highly tunable electronic structure and optical properties; Hu, Tao; Xu, Ben; Hong, Jisang; CURRENT APPLIED PHYSICS, 17 (2017)
37	Helium Shows New Chemistry Not Seen Anywhere Else; Botana, Jorge; Miao, Mao-Sheng; CHEM, 2 (2017)
38	Loschmidt Echo Revivals: Critical and Noncritical; Jafari, R.; Johannesson, Henrik; PHYSICAL REVIEW LETTERS, 118, 015701 (2017)



- Ensemble distribution for immiscible two-phase flow in porous media; Savani, Isha; Bedeaux, Dick; Kjelstrup, Signe; Vassvik, Morten; Sinha, Santanu; Hansen, Alex; PHYSICAL REVIEW E, 95, 023116 (2017)
- Linear Scaling of the Exciton Binding Energy versus the Band Gap of Two-Dimensional Materials; Zhang, Mingliang; Huang, Ling-Yi; Zhang, Xu; Lu, Gang; PHYSICAL REVIEW LETTERS, 118, 209701 (2017)

#### 量子物理与量子信息研究部

#### QUANTUM PHYSICS AND QUANTUM INFORMATION DIVISION

1	Simulation design and performance evaluation of a thermoelectric refrigerator with inhomogeneously-doped nanomaterials; Wang, Junyi; Wang, Yuan; Su, Shanhe; Chen, Jincan; ENERGY, 121 (2017)
2	Optical directional amplification in a three-mode optomechanical system; Li, Yong; Huang, Y. Y.; Zhang, X. Z.; Tian, Lin; OPTICS EXPRESS, 25 (2017)
3	Quantifying Spontaneously Symmetry Breaking of Quantum Many-Body Systems; Dong, Guo-Hui; Fang, Yi-Nan; Sun, Chang-Pu; COMMUNICATIONS IN THEORETICAL PHYSICS, 68 (2017)
4	Approaching Quantum-Limited Amplification with Large Gain Catalyzed by Optical Parametric Amplifier Medium; Zheng, Qiang; Li, Kai; COMMUNICATIONS IN THEORETICAL PHYSICS, 68 (2017)
5	Coherent-State Approach for Majorana Representation; Liu, Hao-Di; Fu, Li-Bin; Wang, Xiao-Guang; COMMUNICATIONS IN THEORETICAL PHYSICS, 67 (2017)
6	Single-photon-driven high-order sideband transitions in an ultrastrongly coupled circuit-quantum-electrodynamics system; Chen, Zhen; Wang, Yimin; Li, Tiefu; Tian, Lin; Qiu, Yueyin; Inomata, Kunihiro; Yoshihara, Fumiki; Han, Siyuan; Nori, Franco; Tsai, J. S.; You, J. Q.; PHYSICAL REVIEW A, 96, 012325 (2017)
7	Partially dark optical molecule via phase control; Wang, Z. H.; Xu, Xun-Wei; Li, Yong; PHYSICAL REVIEW A, 95, 013815 (2017)
8	Bistability and squeezing of the librational mode of an optically trapped nanoparticle; Xiao, Ke-Wen; Zhao, Nan; Yin, Zhang-qi; PHYSICAL REVIEW A, 96, 013837 (2017)
9	Quantum thermodynamic cycle with quantum phase transition; Ma, Yu-Han; Su, Shan-He; Sun, Chang-Pu; PHYSICAL REVIEW E, 96, 022143 (2017)
10	Measuring Out-of-Time-Order Correlators on a Nuclear Magnetic Resonance Quantum Simulator; Li, Jun; Fan, Ruihua; Wang, Hengyan; Ye, Bingtian; Zeng, Bei; Zhai, Hui; Peng, Xinhua; Du, Jiangfeng; PHYSICAL REVIEW X, 7, 031011 (2017)
11	Optimal design of measurement settings for quantum-state-tomography experiments; Li, Jun; Huang, Shilin; Luo, Zhihuang; Li, Keren; Lu, Dawei; Zeng, Bei; PHYSICAL REVIEW A, 96, 032307 (2017)

12	Electromagnetically induced transparency with superradiant and subradiant states; Feng, Wei; Wang, Da-Wei; Cai, Han; Zhu, Shi-Yao; Scully, Marlan O.; PHYSICAL REVIEW A, 95, 033845 (2017)
13	Spectroscopy and scattering: Analytical properties of scattering matrices in discrete and continuum regions; Zeng, De-Ling; Jin, Rui; Gu, Chun; Yue, Xian-Fang; Gao, Xiang; Li, Jia-Ming; PHYSICAL REVIEW A, 95, 042508 (2017)
14	Electron-spin filter and polarizer in a standing light wave; Ahrens, Sven; PHYSICAL REVIEW A, 96, 052132 (2017)
15	Spin in Compton scattering with pronounced polarization dynamics; Ahrens, Sven; Sun, Chang-Pu; PHYSICAL REVIEW A, 96, 063407 (2017)
16	Gyroscope with two-dimensional optomechanical mirror; Davuluri, Sankar; Li, Kai; Li, Yong; NEW JOURNAL OF PHYSICS, 19, 113004 (2017)
17	Analytical Property of Scattering Matrix: Spectroscopy Phenomena and Sharp Overlapping Autoionization Resonances; Jin, Rui; Han, Xiao-Ying; Gao, Xiang; Zeng, De-Ling; Li, Jia-Ming; SCIENTIFIC REPORTS, 7, 11589 (2017)
18	Learning time-dependent noise to reduce logical errors: real time error rate estimation in quantum error correction; Huo, Ming-Xia; Li, Ying; NEW JOURNAL OF PHYSICS, 19, 123032 (2017)
19	Observation of the exceptional point in cavity magnon-polaritons; Zhang, Dengke; Luo, Xiao-Qing; Wang, Yi-Pu; Li, Tie-Fu; You, J. Q.; NATURE COMMUNICATIONS, 8, 1368 (2017)
20	Hybrid Quantum-Classical Approach to Quantum Optimal Control; Li, Jun; Yang, Xiaodong; Peng, Xinhua; Sun, Chang-Pu; PHYSICAL REVIEW LETTERS, 118, 150503 (2017)
21	Floquet engineering of long-range p-wave superconductivity: Beyond the high-frequency limit; Li, Zeng-Zhao; Lam, Chi-Hang; You, J. Q.; PHYSICAL REVIEW B, 96, 155438 (2017)
22	Optical levitation of nanodiamonds by doughnut beams in vacuum; Zhou, Lei-Ming; Xiao, Ke-Wen; Chen, Jun; Zhao, Nan; LASER & PHOTONICS REVIEWS, 11, 1600284 (2017)
23	Quantum sensing of rotation velocity based on transverse field Ising model; Ma, Yu-Han; Sun, Chang-Pu; EUROPEAN PHYSICAL JOURNAL D, 71, 249 (2017)
24	Expedited Holonomic Quantum Computation via Net Zero-Energy-Cost Control in Decoherence-Free Subspace; Pyshkin, P. V.; Luo, Da-Wei; Jing, Jun; You, J. Q.; Wu, Lian-Ao; SCIENTIFIC REPORTS, 7, 44957 (2017)
25	Dark state with counter-rotating dissipative channels; Zhou, Zheng-Yang; Chen, Mi; Wu, Lian-Ao; Yu, Ting; You, J. Q.; SCIENTIFIC REPORTS, 7, 6254 (2017)
26	Nonadiabatic Holonomic Quantum Computation with Dressed-State Qubits; Xue, Zheng-Yuan; Gu, Feng-Lei; Hong, Zhuo-Ping; Yang, Zi-He; Zhang, Dan-Wei; Hu, Yong; You, J. Q.; PHYSICAL REVIEW APPLIED, 7, 054022 (2017)

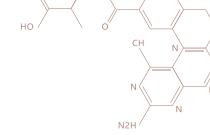
# HO CH N

### 材料与能源研究部 ———

#### MATERIALS AND ENERGY DIVISION

1	Microscopic mechanism of the tunable band gap in potassium-doped few-layer black phosphorus; Kim, Sun-Woo; Jung, Hyun; Kim, Hyun-Jung; Choi, Jin-Ho; Wei, Su-Huai; Cho, Jun-Hyung; PHYSICAL REVIEW B, 96, 75416 (2017)
2	Design of Lead-Free Inorganic Halide Perovskites for Solar Cells via Cation-Transmutation; Zhao, Xin-Gang; Yang, Ji-Hui; Fu, Yuhao; Yang, Dongwen; Xu, Qiaoling; Yu, Liping; Wei, Su-Huai; Zhang, Lijun; JOURNAL OF THE AMERICAN CHEMICAL SOCIETY, 139 (2017)
3	Boosting photoelectrochemical activities of heterostructured photoanodes through interfacial modulation of oxygen vacancies; An, Xiaoqiang; Zhang, Le; Wen, Bo; Gu, Zhenao; Liu, Li-Min; Qu, Jiuhui; Liu, Huijuan; NANO ENERGY, 35 (2017)
4	Origin of the high oxygen reduction reaction of nitrogen and sulfur co-doped MOF-derived nanocarbon electrocatalysts; Song, Zhongxin; Liu, Weiwei; Cheng, Niancai; Banis, Mohammad Norouzi; Li, Xia; Sun, Qian; Xiao, Biwei; Liu, Yulong; Lushington, Andrew; Li, Ruying; Liu, Limin; Sun, Xueliang; MATERIALS HORIZONS, 4 (2017)
5	Exploring Emerging Photovoltaic Materials Beyond Perovskite: The Case of Skutterudite; Yin, Yuan; Huang, Yang; Wu, Yelong; Chen, Guangde; Yin, Wan-Jian; Wei, Su-Huai; Gong, Xingao; CHEMISTRY OF MATERIALS, 29 (2017)
6	Intrinsic Defect Physics in Indium-based Lead-free Halide Double Perovskites; Xu, Jian; Liu, Jian-Bo; Liu, Bai-Xin; Huang, Bing; JOURNAL OF PHYSICAL CHEMISTRY LETTERS, 8 (2017)
7	First-Principles Study of Novel Two-Dimensional (C4H9NH3)(2)PbX4 Perovskites for Solar Cell Absorbers; Wang, Da; Wen, Bo; Zhu, Ya-Nan; Tong, Chuan-Jia; Tang, Zhen-Kun; Liu, Li-Min; JOURNAL OF PHYSICAL CHEMISTRY LETTERS, 8 (2017)
8	Pentavalent lanthanide nitride-oxides: NPrO and NPrO- complexes with N equivalent to Pr triple bonds; Hu, Shu-Xian; Jian, Jiwen; Su, Jing; Wu, Xuan; Li, Jun; Zhou, Mingfei; CHEMICAL SCIENCE, 8 (2017)
9	Atomic Sulfur Anchored on Silicene, Phosphorene, and Borophene for Excellent Cycle Performance of Li-S Batteries; Li, Fen; Zhao, Jijun; ACS APPLIED MATERIALS & INTERFACES, 9 (2017)
10	Enhanced Electrical and Optoelectronic Characteristics of Few-Layer Type-II SnSe/MoS2 van der Waals Heterojunctions; Yang, Shengxue; Wu, Minghui; Wang, Bin; Zhao, Li-Dong; Huang, Li; Jiang, Chengbao; Wei, Su-Huai; ACS APPLIED MATERIALS & INTERFACES, 9 (2017)
11	2D lateral heterostructures of monolayer and bilayer phosphorene; Lin, Heng-Fu; Liu, Li-Min; Zhao, Jijun; JOURNAL OF MATERIALS CHEMISTRY C, 5 (2017)
12	Understanding Size-Dependent Morphology Transition of Triangular MoS2 Nanoclusters: The Role of Metal Substrate and Sulfur Chemical Potential; Zhang, Peng; Kim, Yong-Hyun; JOURNAL OF PHYSICAL CHEMISTRY C, 121 (2017)
13	Formation of New Phases to Improve the Visible-Light Photocatalytic Activity of Tio(2) (B) Via Introducing Alien Elements; Li, Bai-Hai; Lin, Yun; Wang, Jian-Lin; Zhang, Xue; Wang, Yun-Rui; Jiang, Yu; Li, Ting-Shuai; Liu, Li-Min; Chen, Liang; Zhang, Wan-Li; Li, Yan-Rong; JOURNAL OF PHYSICAL CHEMISTRY C, 121 (2017)

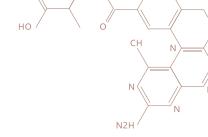
14	Earth-Abundant and Non-Toxic SiX (X = S, Se) Monolayers as Highly Efficient Thermoelectric Materials; Yang, Ji-Hui; Yuan, Qinghong; Deng, Huixiong; Wei, Su-Huai; Yakobson, Boris I.; JOURNAL OF PHYSICAL CHEMISTRY C, 121 (2017)
15	Tuning band gaps and optical absorption of BiOCl through doping and strain: insight form DFT calculations; Zhang, Le; Tang, Zhen-Kun; Lau, Woon-Ming; Yin, Wen-Jin; Hu, Shu-Xian; Liu, Li-Min; PHYSICAL CHEMISTRY CHEMICAL PHYSICS, 19 (2017)
16	Effect of water on the effective Goldschmidt tolerance factor and photoelectric conversion efficiency of organic-inorganic perovskite: insights from first-principles calculations; Tang, Zhen-Kun; Zhu, Ya-Nan; Xua, Zhi-Feng; Liu, Li-Min; PHYSICAL CHEMISTRY CHEMICAL PHYSICS, 19 (2017)
17	Influence of magnetic ordering and Jahn-Teller distortion on the lithiation process of LiMn2O4; Liu, Wei-Wei; Wang, Da; Wang, Zhifan; Deng, Jianguo; Lau, Woon-Ming; Zhang, Yanning; PHYSICAL CHEMISTRY CHEMICAL PHYSICS, 19 (2017)
18	Phase diagram and superconductivity of compressed zirconium hydrides; Li, Xiao-Feng; Hu, Zi-Yu; Huang, Bing; PHYSICAL CHEMISTRY CHEMICAL PHYSICS, 19 (2017)
19	Beyond the electrostatic model: the significant roles of orbital interaction and the dispersion effect in aqueous-pi systems; Zhao, Rundong; Zhang, Rui-Qin; PHYSICAL CHEMISTRY CHEMICAL PHYSICS, 19 (2017)
20	Synthesis, crystal structures, and electronic properties of one dimensional Ba9Sn3(Te1-xSex)(15)(x=0-1); Zhang, Jun; Su, Rui; Wang, Xiancheng; Li, Wenmin; Zhao, Jianfa; Deng, Zheng; Zhang, Sijia; Feng, Shaomin; Liu, Qingqing; Zhao, Huaizhou; Guan, Pengfei; Jin, Changqing; INORGANIC CHEMISTRY FRONTIERS, 4 (2017)
21	Crown ether complexes of actinyls: a computational assessment of AnO(2)(15-crown-5)(2+) (An = U, Np, Pu, Am, Cm); Hu, Shu-Xian; Li, Wan-Lu; Dong, Liang; Gibson, John K.; Li, Jun; DALTON TRANSACTIONS, 46 (2017)
22	Antimony Diffusion in CdTe; Colegrove, Eric; Harvey, Steven P.; Yang, Ji-Hui; Burst, James M.; Duenow, Joel N.; Albin, David S.; Wei, Su-Huai; Metzger, Wyatt K.; IEEE JOURNAL OF PHOTOVOLTAICS, 7 (2017)
23	Porous CoP nanosheet arrays grown on nickel foam as an excellent and stable catalyst for hydrogen evolution reaction; Guo, Pan; Wu, Yu-Xuan; Lau, Woon-Ming; Liu, Hao; Liu, Li-Min; INTERNATIONAL JOURNAL OF HYDROGEN ENERGY, 42 (2017)
24	CoS nanosheet arrays grown on nickel foam as an excellent OER catalyst; Guo, Pan; Wu, Yu-Xuan; Lau, Woon-Ming; Liu, Hao; Liu, Li-Min; JOURNAL OF ALLOYS AND COMPOUNDS, 723 (2017)
25	Structural evolution of FeH4 under high pressure; Li, Fei; Wang, Dashuai; Du, Henan; Zhou, Dan; Ma, Yanming; Liu, Yanhui; RSC ADVANCES, 7 (2017)
26	The distribution of excess carriers and their effects on water dissociation on rutile (110) surface; Wen, Bo; Zhang, Le; Wang, Da; Lang, Xiufeng; COMPUTATIONAL MATERIALS SCIENCE, 136 (2017)



	Periodic continuum solvation model integrated with first-principles calculations for solid surfaces; Yin, Wenjin;
27	Krack, Matthias; Li, Xibo; Chen, Lizhen; Liu, Limin; PROGRESS IN NATURAL SCIENCE-MATERIALS INTERNATIONAL, 27 (2017)
28	First Principles Calculations of Electronic Properties on M13Pt42 (M = Al, Ga, In, Mg, Ca, Sr); Ruan, Cheng-Ji; Han, Li-Hong; Chen, Xi; Li, Xue-Chao; Zhang, Chun-Fang; Lu, Peng-Fei; Guan, Peng-Fei; JOURNAL OF CLUSTER SCIENCE, 28 (2017)
29	Role of Methylammonium Orientation in Ion Diffusion and Current Voltage Hysteresis in the CH3NH3PbI3 Perovskite; Tong, Chuan-Jia; Geng, Wei; Prezhdo, Oleg V.; Liu, Li-Min; ACS ENERGY LETTERS, 2 (2017)
30	Gas sensing in 2D materials; Yang, Shengxue; Jiang, Chengbao; Wei, Su-Huai; APPLIED PHYSICS REVIEWS, 4, 021304 (2017)
31	Pressure effects on structure and dynamics of metallic glass-forming liquid; Hu, Yuan-Chao; Guan, Peng-Fei; Wang, Qing; Yang, Yong; Bai, Hai-Yang; Wang, Wei-Hua; JOURNAL OF CHEMICAL PHYSICS, 146, 024507 (2017)
32	Screening single-atom catalysts for methane activation: alpha-Al2O3(0001)-supported Ni; Gao, Fei; Gao, Shiwu; Meng, Sheng; PHYSICAL REVIEW MATERIALS, 1, 035801 (2017)
33	Carrier providers or killers: The case of Cu defects in CdTe; Yang, Ji-Hui; Metzger, Wyatt K.; Wei, Su-Huai; APPLIED PHYSICS LETTERS, 111, 042106 (2017)
34	Nonisovalent Si-III-V and Si-II-VI alloys: Covalent, ionic, and mixed phases; Kang, Joongoo; Park, Ji-Sang; Stradins, Pauls; Wei, Su-Huai; PHYSICAL REVIEW B, 96, 045203 (2017)
35	Tunneling lifetimes of electrons escaping from atoms under a static electric field; Zhao, Rundong; Sarwono, Yanoar Pribadi; Zhang, Rui-Qin; JOURNAL OF CHEMICAL PHYSICS, 147, 064109 (2017)
36	Creation of half-metallic f-orbital Dirac fermion with superlight elements in orbital-designed molecular lattice; Cui, Bin; Huang, Bing; Li, Chong; Zhang, Xiaoming; Jin, Kyung-Hwan; Zhang, Lizhi; Jiang, Wei; Liu, Desheng; Liu, Feng; PHYSICAL REVIEW B, 96, 085134 (2017)
37	Optical and fundamental band gaps disparity in transparent conducting oxides: new findings for the In2O3 and SnO2 systems; Sabino, Fernando P.; Oliveira, Luiz Nunes; Wei, Su-Huai; Da Silva, Juarez L. F.; JOURNAL OF PHYSICS-CONDENSED MATTER, 29, 085501 (2017)
38	Hydrogen Clathrate Structures in Rare Earth Hydrides at High Pressures: Possible Route to Room-Temperature Superconductivity; Peng, Feng; Sun, Ying; Pickard, Chris J.; Needs, Richard J.; Wu, Qiang; Ma, Yanming; PHYSICAL REVIEW LETTERS, 119, 107001 (2017)
39	Bonding reactivity descriptor from conceptual density functional theory and its applications to elucidate bonding formation; Zhou, Pan-Pan; Liu, Shubin; Ayers, Paul W.; Zhang, Rui-Qin; JOURNAL OF CHEMICAL PHYSICS, 147, 134303 (2017)
40	A Thermodynamic Model of Diameter- and Temperature-dependent Semiconductor Nanowire Growth; Li, Xinlei; Ni, Jun; Zhang, Ruiqin; SCIENTIFIC REPORTS, 7, 15029 (2017)



41	Bending strain engineering in quantum spin hall system for controlling spin currents; Huang, Bing; Jin, Kyung-Hwan; Cui, Bin; Zhai, Feng; Mei, Jiawei; Liu, Feng; NATURE COMMUNICATIONS, 8, 15850 (2017)
42	Substrate-Induced Synthesis of Nitrogen-Doped Holey Graphene Nanocapsules for Advanced Metal-Free Bifunctional Electrocatalysts; Zhang, Zheye; Cao, Tengfei; Liu, Shasha; Duan, Xianming; Liu, Li-Min; Wang, Shuai; Liu, Yunqi; PARTICLE & PARTICLE SYSTEMS CHARACTERIZATION, 34, 1600207 (2017)
43	Surface evolution of a Pt-Pd-Au electrocatalyst for stable oxygen reduction; Li, Jian; Yin, Hui-Ming; Li, Xi-Bo; Okunishi, Eiji; Shen, Yong-Li; He, Jia; Tang, Zhen-Kun; Wang, Wen-Xin; Yucelen, Emrah; Li, Chao; Gong, Yue; Gu, Lin; Miao, Shu; Liu, Li-Min; Luo, Jun; Ding, Yi; NATURE ENERGY, 2, 17111 (2017)
44	Understanding the maximum dynamical heterogeneity during the unfreezing process in metallic glasses; Wang, B.; Wang, L. J.; Wang, W. H.; Bai, H. Y.; Gao, X. Q.; Pan, M. X.; Guan, P. F.; JOURNAL OF APPLIED PHYSICS, 121, 175106 (2017)
45	Heterogeneity: the soul of metallic glasses; Guan Peng-Fei; Wang Bing; Wu Yi-Cheng; Zhang Shan; Shang Bao-Shuang; Hu Yuan-Chao; Su Rui; Liu Qi; ACTA PHYSICA SINICA, 66, 176112 (2017)
46	Controlling magnetic transition of monovacancy graphene by shear distortion; Gao, Fei; Gao, Shiwu; SCIENTIFIC REPORTS, 7, 1792 (2017)
47	New twinning route in face-centered cubic nanocrystalline metals; Wang, Lihua; Guan, Pengfei; Teng, Jiao; Liu, Pan; Chen, Dengke; Xie, Weiyu; Kong, Deli; Zhang, Shengbai; Zhu, Ting; Zhang, Ze; Ma, Evan; Chen, Mingwei; Han, Xiaodong; NATURE COMMUNICATIONS, 8, 2142 (2017)
48	Improved projected Green's function approach to electron tunneling lifetime calculations in quantum wells; Tao, Hong-Shuai; Zhao, Rundong; Sarwono, Yanoar Pribadi; Zhang, Rui-Qin; PHYSICAL REVIEW B, 96, 235428 (2017)
49	Self-assembly 2D zinc-phthalocyanine heterojunction: An ideal platform for high efficiency solar cell; Jiang, Xue; Jiang, Zhou; Zhao, Jijun; APPLIED PHYSICS LETTERS, 111, 253904 (2017)
50	Prediction of Ideal Topological Semimetals with Triply Degenerate Points in the NaCu3Te2 Family; Wang, Jianfeng; Sui, Xuelei; Shi, Wujun; Pan, Jinbo; Zhang, Shengbai; Liu, Feng; Wei, Su-Huai; Yan, Qimin; Huang, Bing; PHYSICAL REVIEW LETTERS, 119, 256402 (2017)
51	Effects of manganese doping on the structure evolution of small-sized boron clusters; Zhao, Lingquan; Qu, Xin; Wang, Yanchao; Lv, Jian; Zhang, Lijun; Hu, Ziyu; Gu, Guangrui; Ma, Yanming; JOURNAL OF PHYSICS-CONDENSED MATTER, 29, 265401 (2017)
52	Quasiparticle and optical properties of strained stanene and stanane; Lu, Pengfei; Wu, Liyuan; Yang, Chuanghua; Liang, Dan; Quhe, Ruge; Guan, Pengfei; Wang, Shumin; SCIENTIFIC REPORTS, 7, 3912 (2017)
53	Magnetism in the p-type Monolayer II-VI semiconductors SrS and SrSe; Lin, Heng-Fu; Lau, Woon-Ming; Zhao, Jijun; SCIENTIFIC REPORTS, 7, 45869 (2017)



54	Enhanced optical absorption via cation doping hybrid lead iodine perovskites; Tang, Zhen-Kun; Xu, Zhi-Feng; Zhang, Deng-Yu; Hu, Shu-Xian; Lau, Woon-Ming; Liu, Li-Min; SCIENTIFIC REPORTS, 7, 7843 (2017)
55	Direct observation of multiple rotational stacking faults coexisting in freestanding bilayer MoS2; Li, Zuocheng; Yan, Xingxu; Tang, Zhenkun; Huo, Ziyang; Li, Guoliang; Jiao, Liying; Liu, Li-Min; Zhang, Miao; Luo, Jun; Zhu, Jing; SCIENTIFIC REPORTS, 7, 8323 (2017)
56	Electronic and Optical Properties of Arsenene Under Uniaxial Strain; Xu, Wenqi; Lu, Pengfei; Wu, Liyuan; Yang, Chuanghua; Song, Yuxin; Guan, Pengfei; Han, Lihong; Wang, Shumin; IEEE JOURNAL OF SELECTED TOPICS IN QUANTUM ELECTRONICS, 23, 9000305 (2017)
57	Band Structure Engineering of Cs2AgBiBr6 Perovskite through Order-Disordered Transition: A First-Principle Study; Jingxiu Yang; Peng Zhang; Su-Huai Wei; JOURNAL OF PHYSICAL CHEMISTRY LETTERS, 9 (2017)
58	Intermolecular orbital interaction in $\pi$ systems; Rundong Zhao; Rui-Qin Zhang; MOLECULAR PHYSICS, (2017)

### 复杂系统研究部

#### **COMPLEX SYSTEMS DIVISION**

1	T7 RNA polymerase translocation is facilitated by a helix opening on the fingers domain that may also prevent backtracking; Da, Lin-Tai; E, Chao; Shuai, Yao; Wu, Shaogui; Su, Xiao-Dong; Yu, Jin; NUCLEIC ACIDS RESEARCH, 45 (2017)
2	Merging single-shot XFEL diffraction data from inorganic nanoparticles: a new approach to size and orientation determination; Li, Xuanxuan; Spence, John C. H.; Hogue, Brenda G.; Liu, Haiguang; IUCRJ, 4 (2017)
3	Deciphering Intrinsic Inter-subunit Couplings that Lead to Sequential Hydrolysis of F-1-ATPase Ring; Dai, Liqiang; Flechsig, Holger; Yu, Jin; BIOPHYSICAL JOURNAL, 113 (2017)
4	Nucleotide Selectivity at a Preinsertion Checkpoint of T7 RNA Polymerase Transcription Elongation; Chao, E.; Duan, Baogen; Yu, Jin; JOURNAL OF PHYSICAL CHEMISTRY B, 121 (2017)
5	7 x 7 RMSD matrix: A new method for quantitative comparison of the transmembrane domain structures in the G-protein coupled receptors; Wang, Ting; Wang, Yang; Tang, Leihan; Duan, Yong; Liu, Haiguang; JOURNAL OF STRUCTURAL BIOLOGY, 199 (2017)
6	Diffraction data of core-shell nanoparticles from an X-ray free electron laser; Li, Xuanxuan; Chiu, Chun-Ya; Wang, Hsiang-Ju; Kassemeyer, Stephan; Botha, Sabine; Shoeman, Robert L.; Lawrence, Robert M.; Kupitz, Christopher; Kirian, Richard; James, Daniel; Wang, Dingjie; Nelson, Garrett; Messerschmidt, Marc; Boutet, Sebastien; Williams, Garth J.; Hartmann, Elisabeth; Jafarpour, Aliakbar; Foucar, Lutz M.; Barty, Anton; Chapman, Henry; Liang, Mengning; Menzel, Andreas; Wang, Fenglin; Basu, Shibom; Fromme, Raimund; Doak, R. Bruce; Fromme, Petra; Weierstall, Uwe; Huang, Michael H.; Spence, John C. H.; Schlichting, Ilme; Hogue, Brenda G.; Liu, Haiguang; SCIENTIFIC DATA, 4, 170048 (2017)

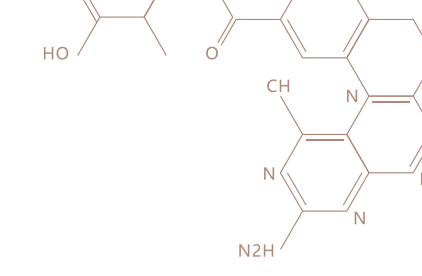


7	Dynamics of the excised base release in thymine DNA glycosylase during DNA repair process; Lin-Tai Dai; Yi Shi; Guodong Ning; Jin Yu; NUCLEIC ACIDS RESEARCH, (2017)
8	Protein crystal quality oriented disulfide bond engineering; Mengchen Pu; Zhijie Xu; Yao Peng; Yaguang Hou; Dongsheng Liu; Yang Wang; Haiguang Liu; Gaojie Song; Zhi-Jie Liu; PROTEIN&CELL, (2017)
9	Application of cryo-electron microscopy in structure biology: current status and future perspectives; Lanqing Huang; Haiguang Liu; PHYSICS, 2 (2017)
10	Determining Complex Structures using Docking Method with Single Particle Scattering Data; Wang, Hongxiao; Liu, Haiguang; FRONTIERS IN MOLECULAR BIOSCIENCES, 4 (2017)

### 应用与计算数学研究部

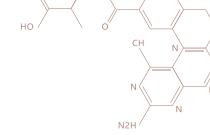
#### APPLIED AND COMPUTATIONAL MATHEMATICS DIVISION

1	Supercloseness of continuous interior penalty method for convection-diffusion problems with characteristic layers; Zhang, Jin; Stynes, Martin; COMPUTER METHODS IN APPLIED MECHANICS AND ENGINEERING, 319 (2017)
2	A novel linear second order unconditionally energy stable scheme for a hydrodynamic Q-tensor model of liquid crystals; Zhao, Jia; Yang, Xiaofeng; Gong, Yuezheng; Wang, Qi; COMPUTER METHODS IN APPLIED MECHANICS AND ENGINEERING, 318 (2017)
3	Structure-preserving Galerkin POD reduced-order modeling of Hamiltonian systems; Gong, Yuezheng; Wang, Qi; Wang, Zhu; COMPUTER METHODS IN APPLIED MECHANICS AND ENGINEERING, 315 (2017)
4	An energy stable algorithm for a quasi-incompressible hydrodynamic phase-field model of viscous fluid mixtures with variable densities and viscosities; Gong, Yuezheng; Zhao, Jia; Wang, Qi; COMPUTER PHYSICS COMMUNICATIONS, 219 (2017)
5	A stable scheme and its convergence analysis for a 2D dynamic Q-tensor model of nematic liquid crystals; Cai, Yongyong; Shen, Jie; Xu, Xiang; MATHEMATICAL MODELS & METHODS IN APPLIED SCIENCES, 27 (2017)
6	A conservative Fourier pseudo-spectral method for the nonlinear Schrodinger equation; Gong, Yuezheng; Wang, Qi; Wang, Yushun; Cai, Jiaxiang; JOURNAL OF COMPUTATIONAL PHYSICS, 328 (2017)
7	Preprocessing schemes for fractional-derivative problems to improve their convergence rates; Stynes, Martin; Luis Gracia, Jose; APPLIED MATHEMATICS LETTERS, 74 (2017)



	UNCONDITIONALLY CONVERGENT L1-GALERKIN FEMS FOR NONLINEAR TIME-FRACTIONAL
8	SCHRODINGER EQUATIONS; Li, Dongfang; Wang, Jilu; Zhang, Jiwei; SIAM JOURNAL ON SCIENTIFIC COMPUTING, 39 (2017)
9	NUMERICAL SOLUTION OF THE NONLOCAL DIFFUSION EQUATION ON THE REAL LINE; Zheng, Chunxiong; Hu, Jiashun; Du, Qiang; Zhang, Jiwei; SIAM JOURNAL ON SCIENTIFIC COMPUTING, 39 (2017)
10	EFFICIENT SPECTRAL AND SPECTRAL ELEMENT METHODS FOR EIGENVALUE PROBLEMS OF SCHRODINGER EQUATIONS WITH AN INVERSE SQUARE POTENTIAL; Li, Huiyuan; Zhang, Zhimin; SIAM JOURNAL ON SCIENTIFIC COMPUTING, 39 (2017)
11	Error estimates for time discretizations of Cahn-Hilliard and Allen-Cahn phase-field models for two-phase incompressible flows; Cai, Yongyong; Choi, Heejun; Shen, Jie; NUMERISCHE MATHEMATIK, 137 (2017)
12	Fast Evaluation of the Caputo Fractional Derivative and its Applications to Fractional Diffusion Equations: A Second-Order Scheme; Yan, Yonggui; Sun, Zhi-Zhong; Zhang, Jiwei; COMMUNICATIONS IN COMPUTATIONAL PHYSICS, 22 (2017)
13	A Numerical Analysis of the Weak Galerkin Method for the Helmholtz Equation with High Wave Number; Du, Yu; Zhang, Zhimin; COMMUNICATIONS IN COMPUTATIONAL PHYSICS, 22 (2017)
14	Fast Evaluation of the Caputo Fractional Derivative and its Applications to Fractional Diffusion Equations; Jiang, Shidong; Zhang, Jiwei; Zhang, Qian; Zhang, Zhimin; COMMUNICATIONS IN COMPUTATIONAL PHYSICS, 21 (2017)
15	Artificial Boundary Conditions for Nonlocal Heat Equations on Unbounded Domain; Zhang, Wei; Yang, Jiang; Zhang, Jiwei; Du, Qiang; COMMUNICATIONS IN COMPUTATIONAL PHYSICS, 21 (2017)
16	Optimal Superconvergence of Energy Conserving Local Discontinuous Galerkin Methods for Wave Equations; Cao, Waixiang; Li, Dongfang; Zhang, Zhimin; COMMUNICATIONS IN COMPUTATIONAL PHYSICS, 21 (2017)
17	Global existence and exponential stability for the compressible Navier-Stokes equations with discontinuous data; Kong, Huihui; Li, Hai-Liang; Liang, Chuangchuang; Zhang, Guojing; JOURNAL OF DIFFERENTIAL EQUATIONS, 263 (2017)
18	ERROR ANALYSIS OF A FINITE DIFFERENCE METHOD ON GRADED MESHES FOR A TIME-FRACTIONAL DIFFUSION EQUATION; Stynes, Martin; O'Riordan, Eugene; Luis Gracia, Jose; SIAM JOURNAL ON NUMERICAL ANALYSIS, 55 (2017)
19	CONVERGENCE OF A FAST EXPLICIT OPERATOR SPLITTING METHOD FOR THE EPITAXIAL GROWTH MODEL WITH SLOPE SELECTION; Li, Xiao; Qiao, Zhonghua; Zhang, Hui; SIAM JOURNAL ON NUMERICAL ANALYSIS, 55 (2017)
20	Two-Dimensional Elastic Scattering Coefficients and Enhancement of Nearly Elastic Cloaking; Abbas, Tasawar; Ammari, Habib; Hu, Guanghui; Wahab, Abdul; Ye, Jong Chul; JOURNAL OF ELASTICITY, 128 (2017)

21	Superconvergence of Immersed Finite Volume Methods for One-Dimensional Interface Problems; Cao, Waixiang; Zhang, Xu; Zhang, Zhimin; Zou, Qingsong; JOURNAL OF SCIENTIFIC COMPUTING, 73 (2017)
22	Superconvergence of Finite Element Approximations for the Fractional Diffusion-Wave Equation; Ren, Jincheng; Long, Xiaonian; Mao, Shipeng; Zhang, Jiwei; JOURNAL OF SCIENTIFIC COMPUTING, 72 (2017)
23	Numerical Methods and Comparison for the Dirac Equation in the Nonrelativistic Limit Regime; Bao, Weizhu; Cai, Yongyong; Jia, Xiaowei; Tang, Qinglin; JOURNAL OF SCIENTIFIC COMPUTING, 71 (2017)
24	Superconvergent Two-Grid Methods for Elliptic Eigenvalue Problems; Guo, Hailong; Zhang, Zhimin; Zhao, Ren; JOURNAL OF SCIENTIFIC COMPUTING, 70 (2017)
25	UNIFORM ERROR BOUNDS OF A FINITE DIFFERENCE METHOD FOR THE ZAKHAROV SYSTEM IN THE SUBSONIC LIMIT REGIME VIA AN ASYMPTOTIC CONSISTENT FORMULATION; Bao, Weizhu; Su, Chunmei; MULTISCALE MODELING & SIMULATION, 15 (2017)
26	SUPERCONVERGENCE OF DISCONTINUOUS GALERKIN METHODS FOR 1-D LINEAR HYPERBOLIC EQUATIONS WITH DEGENERATE VARIABLE COEFFICIENTS; Cao, Waixiang; Shu, Chi-Wang; Zhang, Zhimin; ESAIM-MATHEMATICAL MODELLING AND NUMERICAL ANALYSIS-MODELISATION MATHEMATIQUE ET ANALYSE NUMERIQUE, 51 (2017)
27	SUPERCONVERGENCE OF DISCONTINUOUS GALERKIN METHODS BASED ON UPWIND-BIASED FLUXES FOR 1D LINEAR HYPERBOLIC EQUATIONS; Cao, Waixiang; Li, Dongfang; Yang, Yang; Zhang, Zhimin; ESAIM-MATHEMATICAL MODELLING AND NUMERICAL ANALYSIS-MODELISATION MATHEMATIQUE ET ANALYSE NUMERIQUE, 51 (2017)
28	A C-0 linear finite element method for two fourth-order eigenvalue problems; Chen, Hongtao; Guo, Hailong; Zhang, Zhimin; Zou, Qingsong; IMA JOURNAL OF NUMERICAL ANALYSIS, 37 (2017)
29	Spectral Galerkin methods for a weakly singular Volterra integral equation of the second kind; Huang, Can; Stynes, Martin; IMA JOURNAL OF NUMERICAL ANALYSIS, 37 (2017)
30	STABLE EQUILIBRIA OF ANISOTROPIC PARTICLES ON SUBSTRATES: A GENERALIZED WINTERBOTTOM CONSTRUCTION; Bao, Weizhu; Jiang, Wei; Srolovitz, David J.; Wang, Yan; SIAM JOURNAL ON APPLIED MATHEMATICS, 77 (2017)
31	Calculating corner singularities by boundary integral equations; Shi, Hualiang; Lu, Ya Yan; Du, Qiang; JOURNAL OF THE OPTICAL SOCIETY OF AMERICA A-OPTICS IMAGE SCIENCE AND VISION, 34 (2017)
32	MATHEMATICAL AND NUMERICAL ANALYSIS OF THE TIME-DEPENDENT GINZBURG-LANDAU EQUATIONS IN NONCONVEX POLYGONS BASED ON HODGE DECOMPOSITION; Li, Buyang; Zhang, Zhimin; MATHEMATICS OF COMPUTATION, 86 (2017)
33	HESSIAN RECOVERY FOR FINITE ELEMENT METHODS; Guo, Hailong; Zhang, Zhimin; Zhao, Ren; MATHEMATICS OF COMPUTATION, 86 (2017)



34	2k SUPERCONVERGENCE OF Q(k) FINITE ELEMENTS BY ANISOTROPIC MESH APPROXIMATION IN WEIGHTED SOBOLEV SPACES; He, Wenming; Zhang, Zhimin; MATHEMATICS OF COMPUTATION, 86 (2017)	
35	Superconvergence of immersed finite element methods for interface problems; Cao, Waixiang; Zhang, Xu; Zhang, Zhimin; ADVANCES IN COMPUTATIONAL MATHEMATICS, 43 (2017)	
36	Analysis and numerical solution of a Riemann-Liouville fractional derivative two-point boundary value problem; Kopteva, Natalia; Stynes, Martin; ADVANCES IN COMPUTATIONAL MATHEMATICS, 43 (2017)	
37	Three-Dimensional Numerical Simulations of Biofilm Dynamics with Quorum Sensing in a Flow Cell; Zhao, Jia Wang, Qi; BULLETIN OF MATHEMATICAL BIOLOGY, 79 (2017)	
38	A Multiscale Mathematical Model of Tumour Invasive Growth; Peng, Lu; Trucu, Dumitru; Lin, Ping; Thompson Alastair; Chaplain, Mark A. J.; BULLETIN OF MATHEMATICAL BIOLOGY, 79 (2017)	
39	Superconvergence of the direct discontinuous Galerkin method for convection-diffusion equations; Cao, Waixiang; Liu, Hailiang; Zhang, Zhimin; NUMERICAL METHODS FOR PARTIAL DIFFERENTIAL EQUATIONS, 33 (2017)	
40	A HYBRIDIZABLE WEAK GALERKIN METHOD FOR THE HELMHOLTZ EQUATION WITH LARGE WAVE NUMBER: hp ANALYSIS; Wang, Jiangxing; Zhang, Zhimin; INTERNATIONAL JOURNAL OF NUMERICAL ANALYSIS AND MODELING, 14 (2017)	
41	A SECOND-ORDER CONVEX SPLITTING SCHEME FOR A CAHN-HILLIARD EQUATION WITH VARIABLE INTERFACIAL PARAMETERS; Li, Xiao; Qiao, Zhonghua; Zhang, Hui; JOURNAL OF COMPUTATIONAL MATHEMATICS, 35 (2017)	
42	STABILITY ANALYSIS FOR NONLINEAR SCHRODINGER EQUATIONS WITH NONLINEAR ABSORBING BOUNDARY CONDITIONS; Zhang, Jiwei; Xu, Zhenli; Wu, Xiaonan; Wang, Desheng; JOURNAL OF COMPUTATIONAL MATHEMATICS, 35 (2017)	
43	Blowup of Volterra Integro-Differential Equations and Applications to Semi-Linear Volterra Diffusion Equations; Yang, Zhanwen; Tang, Tao; Zhang, Jiwei; NUMERICAL MATHEMATICS-THEORY METHODS AND APPLICATIONS, 10 (2017)	
44	Nonconforming Finite Element Methods for Wave Propagation in Metamaterials; Yao, Changhui; Wang, Lixiu; NUMERICAL MATHEMATICS-THEORY METHODS AND APPLICATIONS, 10 (2017)	
45	Numerical Solution of the Time-Fractional Sub-Diffusion Equation on an Unbounded Domain in Two-Dimensional Space; Li, Hongwei; Wu, Xiaonan; Zhang, Jiwei; EAST ASIAN JOURNAL ON APPLIED MATHEMATICS, 7 (2017)	
46	High-Order Local Artificial Boundary Conditions for the Fractional Diffusion Equation on One-Dimensional Unbounded Domain; Zhang, Wei; Li, Can; Wu, Xiaonan; Zhang, Jiwei; JOURNAL OF MATHEMATICAL STUDY, 50 (2017)	
47	An Efficient Spectral-Galerkin Approximation and Error Analysis for Maxwell Transmission Eigenvalue Problems in Spherical Geometries; Jing An; Zhimin Zhang; JOURNAL OF SCIENTIFIC COMPUTING, 10 (2017)	

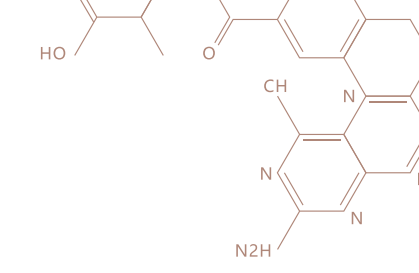


48	A C0 Linear Finite Element Method for Biharmonic Problems; Hailong Guo, Zhimin Zhang, Qingsong Zou; JOURNAL OF SCIENTIFIC COMPUTING, (2017)
49	Error estimates of a finite difference method for the Klein-Gordon-Zakharov system in the subsonic limit regime; Chunmei Su; Wenfan Yi; IMA JOURNAL OF NUMERICAL ANALYSIS, (2017)
50	Numerical solution to a liearized time fractional KDV equation on unbounded domains; Qian Zhang; Jiwei Zhang; Shidong Jiang; Zhimin Zhang; MATHEMATICS OF COMPUTATION, 87 (2017)
51	A discontinuous Galerkin method for stochastic Cahn-Hilliard equations; Chen Li; Ruibin Qin; Ju Ming; Zhongming Wang; COMPUTERS & MATHEMATICS WITH APPLICATIONS, (2017)
52	On global convergence of gradient descent algorithms for generalized phase retrieval problem; Ji Li; Zhou Tie; Chao Wang; JOURNAL OF COMPUTATIONAL AND APPLIED MATHEMATICS, 329 (2017)
53	A fully discrete direct discontinuous Galerkin method for the fractional diffusion-wave equation; Chaobao Huang; Na An; Xijun Yu; APPLICABLE ANALYSIS , (2017)

### 力学研究部

#### **MECHANICS DIVISION**

1	Real-time start of combustion detection based on cylinder pressure signals for compression ignition engines; Fang, Cheng; Ouyang, Minggao; Yang, Fuyuan; APPLIED THERMAL ENGINEERING, 114 (2017)	
2	High order spectral difference lattice Boltzmann method for incompressible hydrodynamics; Li, Weidong; JOURNAL OF COMPUTATIONAL PHYSICS, 345 (2017)	
3	Single-node second-order boundary schemes for the lattice Boltzmann method; Zhao, Weifeng; Yong, Wen-An; JOURNAL OF COMPUTATIONAL PHYSICS, 329 (2017)	
4	Transition of torque pattern in undulatory locomotion due to wave number variation; Ding, Y.; Ming, T. Y.; Goldman, D., I; INTEGRATIVE AND COMPARATIVE BIOLOGY, 57 (2017)	
5	STABILITY ANALYSIS OF A CLASS OF GLOBALLY HYPERBOLIC MOMENT SYSTEM; Zhao, Weifeng; Yong, Wen-An; Luo, Li-Shi; COMMUNICATIONS IN MATHEMATICAL SCIENCES, 15 (2017)	
6	A Sharp Interface Method for Compressible Multi-Phase Flows Based on the Cut Cell and Ghost Fluid Methods; Bai, Xiao; Deng, Xiaolong; ADVANCES IN APPLIED MATHEMATICS AND MECHANICS, 9 (2017)	
7	Propulsion via flexible flapping in granular media; Peng, Zhiwei; Ding, Yang; Pietrzyk, Kyle; Elfring, Gwynn J.; Pak, On Shun; PHYSICAL REVIEW E, 96, 012907 (2017)	
8	Variational approach to powder-binder separation in Poiseuille and Couette flows; Oh, Youngmin; Park, Dong Yong; Park, Seong Jin; Fontelos, Marco Antonio; Hwang, Hyung Ju; PHYSICS OF FLUIDS, 29, 033102 (2017)	



9	Maxwell iteration for the lattice Boltzmann method with diffusive scaling; Zhao, Weifeng; Yong, Wen-An; PHYSICAL REVIEW E, 95, 033311 (2017)
10	Simulating the Linearly Elastic Solid-Solid Interaction with a Cut Cell Method; Tao, Liang; Deng, Xiao-Long; INTERNATIONAL JOURNAL OF COMPUTATIONAL METHODS, 14, 1750072 (2017)
11	Hydrodynamics of larval fish quick turning: A computational study; Jialei Song; Yong Zhong; Haoxiang Luo; Yang Ding; Ruxu Du; PROCEEDINGS OF THE INSTITUTION OF MECHANICAL ENGINEERS PART C-JOURNAL OF MECHANICAL ENGINEERING SCIENCE, , I-9 (2017)
12	A comparative study of the single-mode Richtmyer–Meshkov instability; X Bai; XL Deng; L Jiang; SHOCK WAVES, (2017)

### 计算方法研究部

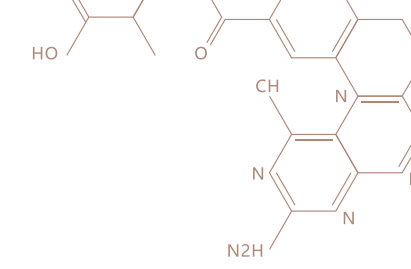
#### **ALGORITHMS DIVISION**

1	Multiscale Study of Plasmonic Scattering and Light Trapping Effect in Silicon Nanowire Array Solar Cells; Meng, Lingyi; Zhang, Yu; Yam, ChiYung; JOURNAL OF PHYSICAL CHEMISTRY LETTERS, 8 (2017)
2	Modeling the formation of TiO2 ultra-small nanoparticles; Chen, Mingyang; Dixon, David A.; NANOSCALE, 9 (2017)
3	Structures and Stabilities of (CaO)(n) Nanoclusters; Chen, Mingyang; Thanthiriwatte, K. Sahan; Dixon, David A.; JOURNAL OF PHYSICAL CHEMISTRY C, 121 (2017)
4	Structure and Stability of Hydrolysis Reaction Products of MgO Nanoparticles Leading to the Formation of Brucite; Chen, Mingyang; Dixon, David A.; JOURNAL OF PHYSICAL CHEMISTRY C, 121 (2017)
5	Enhanced Photovoltaic Properties Induced by Ferroelectric Domain Structures in Organometallic Halide Perovskites; Bi, Fuzhen; Markov, Stanislav; Wang, Rulin; Kwok, YanHo; Zhou, Weijun; Liu, Limin; Zheng, Xiao; Chen, GuanHua; Yam, ChiYung; JOURNAL OF PHYSICAL CHEMISTRY C, 121 (2017)
6	Discovering variable fractional orders of advection-dispersion equations from field data using multi-fidelity Bayesian optimization; Pang, Guofei; Perdikaris, Paris; Cai, Wei; Karniadakis, George Em; JOURNAL OF COMPUTATIONAL PHYSICS, 348 (2017)
7	Direct Solvers for the Biharmonic Eigenvalue Problems Using Legendre Polynomials; Chen, Lizhen; An, Jing; Zhuang, Qingqu; JOURNAL OF SCIENTIFIC COMPUTING, 70 (2017)
8	Rational design and first-principles studies of phenothiazine-based dyes for dye-sensitised solar cells; Govindarajan, Saranya; Gao, Shiwu; Cai, Wei; Yam, ChiYung; MOLECULAR PHYSICS, 115 (2017)



9	New ultra-incompressible phases of NbB4 predicted from first principles; Li, Xiao-Feng; Han, Li-Gang; Hou, Yunshan; Yan, Haiyan; Hu, Zi-Yu; Zhang, Sheng-Li; PHYSICS LETTERS A, 381 (2017)	
10	Legendre-Galerkin spectral-element method for the biharmonic equations and its applications; Zhuang, Qingqu; Chen, Lizhen; COMPUTERS & MATHEMATICS WITH APPLICATIONS, 74 (2017)	
11	Au-Ge MEAM potential fitted to the binary phase diagram; Wang, Yanming; Santana, Adriano; Cai, Wei; MODELLING AND SIMULATION IN MATERIALS SCIENCE AND ENGINEERING, 25, 025004 (2017)	
12	Exploring Promising Catalysts for Chemical Hydrogen Storage in Ammonia Borane: A Density Functional Theory Study; Bandaru, Sateesh; English, Niall J.; Phillips, Andrew D.; MacElroy, J. M. Don; CATALYSTS, 7, 140 (2017)	
13	A mixed Legendre-Galerkin spectral method for the buckling problem of simply supported Kirchhoff plates; Cao, Junying; Wang, Ziqiang; Cao, Waixiang; Chen, Lizhen; BOUNDARY VALUE PROBLEMS, , 34 (2017)	
14	Approximate DFT-Based Methods for Generating Diabatic States and Calculating Electronic Couplings: Models of Two and More States; Chou-Hsun Yang; ChiYung Yam; Haobin Wang; PHYSICAL CHEMISTRY CHEMICAL PHYSICS, (2017)	





84 - 85 |

### 学术活动

### 中心主办、合办的学术会议

#### **WORKSHOPS & CONFERENCES (2017)**

时间 Date	会议名称 Title
2017.02.11 - 12	材料建模与计算机模拟中的若干问题:概念、理论与方法 Workshop on Material Modeling and Computer Simulation: Concepts, Theories and Methods
2017.05.24 - 26	The 5th International Workshop on Frontiers in Quantum Physics and Quantum Information 第五届量子物理与量子信息前沿研讨会
2017.05.19 - 20	Workshop on Numerical Methods for Fractional-derivative Problems: Singularities and Fast Algorithms 分数阶微分方程的数值方法:奇异性和快速算法
2017.06.07 - 14	Focus Activity on Mathematical and Computational methods for Quantum and Kinetic Problems 量子与动力学理论中的数学问题与计算方法
2017.07.15 - 16	CSRC Workshop on DNA Chromosome Structure and Dynamics DNA染色体结构与动力研讨会
2017.08.07 - 11	CSRC Summer School on Applied Inverse Problems 应用反问题暑期班
2017.08.16 - 18	2017年全国半导体能源材料与技术博士后学术论坛 2017 Postdoctoral Academic National Forum: Semiconductor Energy Materials and Technology
2017.09.15	CSRC Symposium on Active Matter and Related Topics 活性物质研讨会
2017.12.04 - 09	Workshop on the Rabi Model, Strong Light-Matter Interactions and Other Quantum Phenomena in CQED Platforms 腔量子电动力学中的理论模型及实验培训会议
2017.12.13 - 12.16	第三届中物院计算材料学与计算化学论坛 The 3rd CAEP Computational Materials and Computational Chemistry Forum

### 培训班(2017)

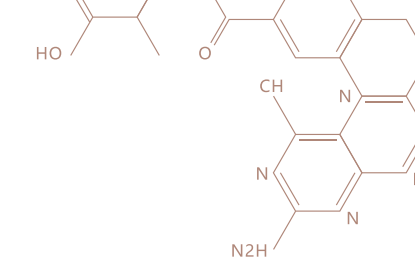
#### **TUTORIALS (2017)**

时间 Date	会议名称 Title
2017.05.08 - 12	多相物质界面问题的数值处理方法培训班
2017.05.22 - 23	量子开放系统理论与计算方法
2017.06.05 - 09	湍流: 理论, 实验, 模型与数值模拟培训班
2017.06.19 - 22	Workshop on Stochastic Computing and Uncertainty Quantification (UQ)
2017.07.10 - 14	AI深度学习及应用暑期班
2017.09.17 - 22	基于跨尺度高通量计算的新材料探索与设计
2017.12.04 - 09	腔量子电动力学中的理论模型及实验培训会议

#### 如需了解更多会议详情,请浏览:

For more details about Workshops & Conferences in CSRC, please visit: http://www.csrc.ac.cn/events/WorkshopsConferences/















#### 第三届中物院计算材料学与计算化学论坛



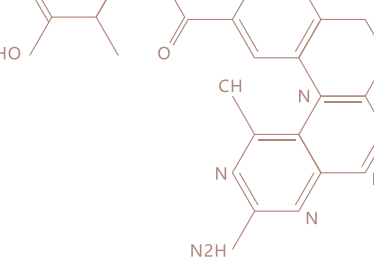
#### 基于跨尺度高通量计算的新材料探索与设计高级研修班











#### 前沿讲座

#### **CSRC COLLOQUIUM ON SCIENTIFIC FRONTIERS**

#### 2017年共6期(总61期)



高鸿钧 (Hong-Jun Gao)

2017-2-16

#### 纳米量子结构的构筑及其物性调控

中科院物理研究所 & 中国科学院大学 Institute of Physics & University of Chinese Academy of Sciences



2017-5-24

Basic Features of Virtual Element Methods

Istituto Universitario di Studi Superiori (IUSS) of Pavia, Italy



2017-9-13

Simulating, Emulating, Anticipating Condensed Matter Experiments: A Theorist's Dream

SISSA, and ICTP, Trieste, Italy



#### 2017-11-16

Bioinspired Molecular Electronics, Corrosion, and Water Splitting at Wayne State University

Department of Chemistry, Wayne State University, USA



Luiz Davidovich

#### 2017-12-11

Emergence of the Classical World from Quantum Mechanics: Schrödinger Cats, Entanglement, and Decoherence

Federal University of Rio de Janeiro, Brazil



2017-12-14

Perforations, Curvature and Thermal Fluctuations in Free-Standing Graphene

Harvard University, USA

David R. Nelson

#### 专题报告

#### **CSRC SEMINAR**

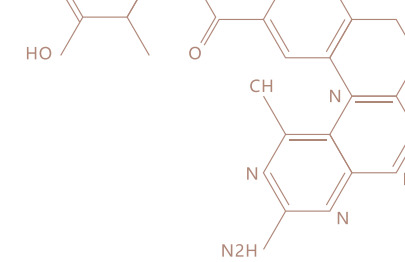
中心积极邀请国内外相关领域重要学者举行专题报告,活跃学术氛围,激发学术思维。2017年中心共举办专题讲座90期(总648期),报告人来自国内、香港、台湾、美国、英国、法国、德国、澳大利亚、新加坡、加拿大、瑞士、西班牙、葡萄牙、荷兰、挪威、新西兰、日本等著名高校及科研单位。

CSRC invites national and overseas leading researchers to give academic seminars. In 2017, CSRC has already held 90 seminars.

#### 如需了解更多报告信息,请浏览:

For more details about Seminars in CSRC, please visit: http://www.csrc.ac.cn/events/seminars/





### 合作交流

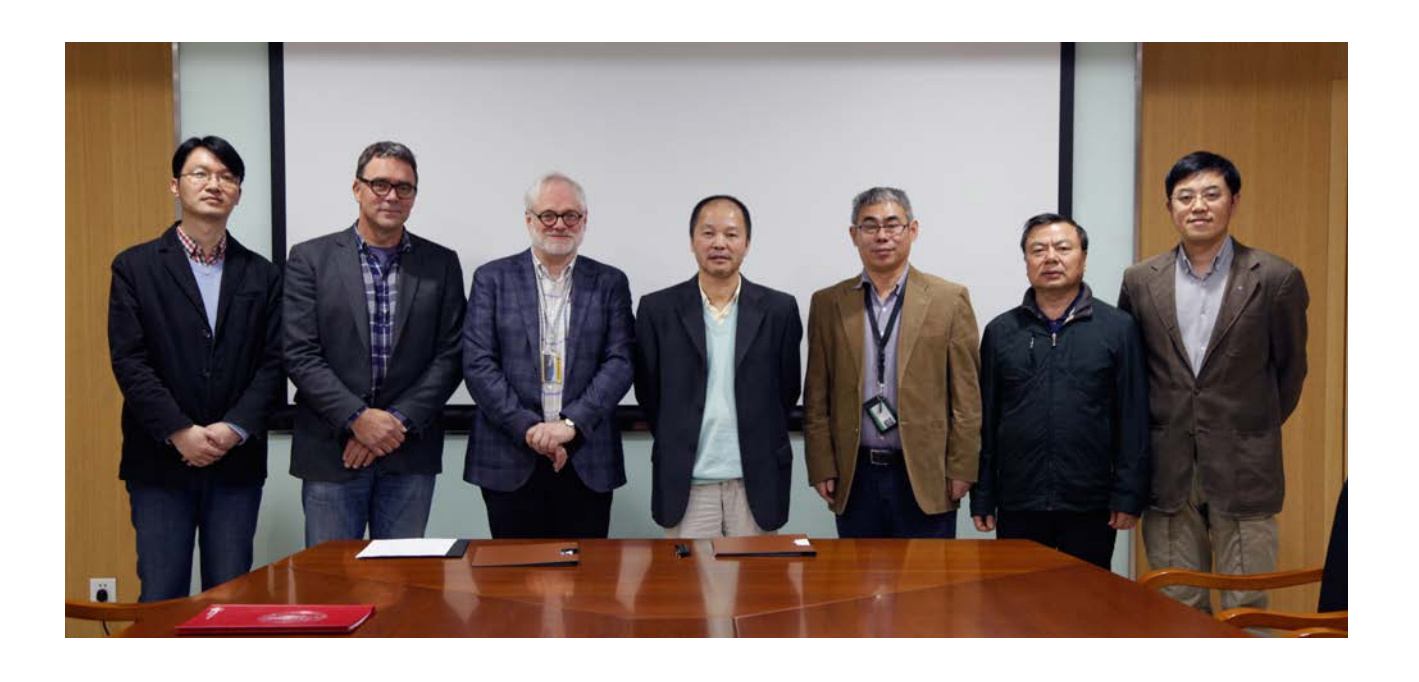
# LABOR-ATIONS

北京计算科学研究中心非常重视与科研机构及高校的合作,在积极组织承办国内外学术会议之时,也鼓励 科研人员与国内外其他科研机构之间的互访交流,扩展学术视野和扩大学术影响。目前已与国际数所科研机构 签署了合作协议,为打造中心作为国际一流的开展计算科学及相关学科交叉研究的综合平台而不断努力。

2017年11月,中心分别与挪威科技大学及挪威奥斯陆大学正式签订了合作备忘录。双方拟在教育和科研方面展开深入的交流与合作,互相借鉴双方的优势学科领域和教学优势,在合作项目、合办学术活动、同享资源、人员互访、合招博士后等具体方面携手合作。

To facilitate scientific interactions between CSRC scientists and scientists elsewhere, CSRC has developed partnerships with several universities and research institutions around the world. Besides engaging in long-term scientific collaborations, CSRC staff also host conferences, workshops, and seminars with collaborators. Through these activities, CSRC is working towards extending the frontier in computational science research and improving its competitive edge and prestige.

On November 2017, two new Memorandums of Understanding were signed among Beijing Computational Science Research Center (CSRC) and Norwegian University of Science and Technology (NTNU), University of Oslo (UIO) respectively. All parties agreed to explore possibilities for cooperation in education and research, in the forms of exchange of research personnel, educational program for graduate students and post-doctoral fellows and so on.







#### 国际合作伙伴

#### INTERNATIONAL PARTNERSHIP

- Norwegian University of Science and Technology, Norway 挪威科技大学
- University of Oslo, Norway 挪威奥斯陆大学
- Institute for Quantum Computing, University of Waterloo, Canada 加拿大滑铁卢大学
- University of Warwick, UK 英国华威大学
- The Hong Kong University of Science and Technology, China 香港科技大学
- Commissariat à l'énergie atomique et aux énergies alternatives, France 法国原子能与可替代能源委员会
- Department of Physics, the Chinese University of Hong Kong, China 香港中文大学
- Department of Physics, National Taiwan Normal University, China 国立台湾师范大学
- Center for Simulational Physics, The University of Georgia, USA 美国乔治亚大学
- RIkagaku KENkyusho/Institute of Physical and Chemical Research, Japan 日本理化学研究所
- Hearne Institute for Theoretical Physics, Louisiana State University, USA 美国路易斯安那州立大学
- College of Sciences, Old Dominion University, USA 美国奥多明尼昂大学
- Korea Institute for Advanced Study, South Korea 韩国高等科学院



























## 学术访问

中心在加强与科研机构及高校的合作交流,积极组织承办国内外学术会议之余,也鼓励科研人员与国内外 其他科研机构之间的互访交流。成立至今,中心接待了来自20多个国家和地区的访问学者超过2500余人次,中 心科研人员外出参加学术交流活动超过1500余人次。其中,2017年中心来访学者超过了350人次,中心人员外 出学术交流200余人次。

中心欢迎国内外各机构相关专业的科研人员和教师,以访问学者和客座研究人员的形式来访,进行短期或长期合作研究。中心也与同行们一起举办学术活动如会议、讲习班等。在中心访问期间,中心将提供一定的生活和住房补贴。



2017 香港浸会大学代表团访问中心 07.04 The HKBU Delegation Visited CSRC

Since its establishment, more than 2500 visiting scholars from over 20 countries and regions have visited CSRC. CSRC faculty members went out for academic eschange for more than 1500 times. During the year 2017, CSRC has hosted over 350 visiting scholars.

CSRC warmly welcomes scientists around the world to visit for collaboration and exchange. CSRC frequently hosts academic activities such as conferences, workshops, and seminars together with its counterparts. Living allowance and housing subsidies are provided during visitor's stay at CSRC.

# CSRCH 科研大楼 BUILDING



【 中关村软件园一二期鸟瞰图 】

**ZPark** 



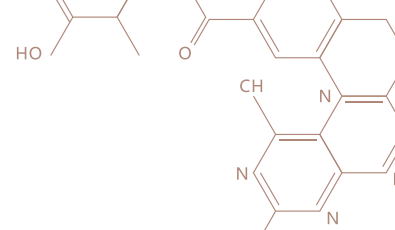












— Gym

N2H /









〖健身房〗○-







### 天河二号-计科中心集群系统 Cluster Tianhe2-JK

The CSRC is equipped with the state of art high performance computing facilities, which include a dedicated in-house 14,000+ core cluster TianHe2-JK in addition to many smaller clusters.

For more details about CSRC Computing, please visit: http://www.csrc. ac.cn/en/facility/cmpt/

